THESIS FOR THE DEGREE OF DOCTOR OF PHILOSOPHY

Steel converter slag as an oxygen carrier

FREDRIK HILDOR

Department of Chemistry and Chemical Engineering

CHALMERS UNIVERSITY OF TECHNOLOGY

Gothenburg, Sweden 2023

Steel converter slag as an oxygen carrier
FREDRIK HILDOR
ISBN 978-91-7905-790-9

Doktorsavhandlingar vid Chalmers tekniska högskola
Ny serie nr 5256
ISSN 0346-718X

Department of Chemistry and Chemical Engineering
Chalmers University of Technology
SE-412 96 Gothenburg
Sweden
Telephone + 46 (0)31-772 1000

Cover:
Scanning Electron Microscopy (SEM) image of particles of steel converter slag, which is also called LD slag. Surrounding the SEM image are illustrations of the different research areas covered in this thesis.

Chalmers Digitaltryck
Gothenburg, Sweden 2023

Steel converter slag as an oxygen carrier

FREDRIK HILDOR
Division of Energy and Materials
Department of Chemistry and Chemical Engineering
Chalmers University of Technology

Abstract

Thermal conversion of fuels can be used to produce heat and power in addition to chemicals. In order to be aligned with climate targets, it is necessary that such systems do not emit carbon dioxide to the atmosphere. Carbon capture and storage (CCS) can be used together with fuel conversion systems to prevent CO_2 from entering the atmosphere. If CCS is used together with biomass-based fuels, it is possible to achieve a net-flow of carbon dioxide out of the atmosphere, so called negative emissions.

Chemical looping technologies for combustion (CLC) and gasification (CLG) are technologies which can be used for heat, power and chemical production with no or low penalties for carbon capture. In any chemical looping applications, a functional oxygen carrier is essential. The oxygen carrier is normally a metal oxide based material that can transport oxygen from one reactor to another. However, when fuel is introduced into the system, ash can react with the oxygen carrier and decrease its operational lifespan, especially reactive ash from biomass and low-grade fuels. Therefore, there is growing interest in low-cost oxygen carriers that can contribute to making the process economically feasible. Low-cost oxygen carriers can be obtained from ores or as byproducts of the steel industry. Of particular interest is steel converter slag, which is also known as Linz-Donawitz (LD) slag. LD slag is generated in significant amounts, contains sufficient amount of iron oxide (that can act as an oxygen carrier) and available at a low cost.

This work presents a comprehensive overview of the chemistry and behavior of LD slag when it is implemented as an oxygen carrier in chemical-looping applications. The material has been investigated in laboratory reactors, in addition to pilot and semi-industrial units, and LD slags interactions with different fuel components, ash, alkali salts, sulfur and tars have been investigated.

It is concluded from this work that LD slag can be viable as material for both CLC and CLG processes with biomass. In contrast to other bed materials, such as silica sand or the commonly investigated iron-based oxygen carrier ilmenite, the slag has limited reactivity with reactive alkali components. This results in more alkali being available in the gas phase, which is beneficial for tar cracking and for the gasification rate of the solid char. The high content of calcium in the LD slag is also favorable in terms of gasification and ash interactions. Calcium oxide catalyzes both the water-gas shift reaction and is catalytic towards tar cracking. A high level of calcium also increases the melting points of both the K-Ca-P and K-Ca-Si matrixes. However, the structural integrity of the material is lower compared to, for example, ilmenite, resulting in more fines being generated during the process. Overall, LD slag is a potential oxygen carrier that is suitable for chemical-looping processes that utilize low-grade fuels.

Keywords: Steel converter slag, LD slag, Oxygen carrier, Chemical looping, Oxygen carrier aided combustion, Biomass

List of Publications

This thesis is based on the experimental work presented in the following papers, which are referred to in the text according to their Roman numerals.

Paper I
Hildor, F., Mattisson, T., Leion, H., Linderholm, C., & Rydén, M. (2019).
Steel converter slag as an oxygen carrier in a 12 MWth CFB boiler–Ash interaction and material evolution.
International Journal of Greenhouse Gas Control, 88, 321-331.

Paper II
Hildor, F., Leion, H., Linderholm, C. & Mattisson, T. (2020).
Steel converter slag as an oxygen carrier for chemical-looping gasification.
Fuel Processing Technology,210, 106576.

Paper III
Hildor, F., Leion, H. & Mattisson, T. (2022)
Steel Converter Slag as an Oxygen Carrier—Interaction with Sulfur Dioxide
Energies 2022, 15(16), 5922

Paper IV
Hildor, F., Soleimanisalim, A. H., Seemann, M., Mattisson, T. & Leion, H., (2022)
Tar characteristics generated from a 10 kWth chemical-looping biomass gasifier using steel converter slag as an oxygen carrier
Fuel, Volume 331, Part 1, 1 January 2023, 125770

Paper V
Hildor, F., Mattisson, T., Linderholm, C & Leion, H. (2023)
Metal impregnation on steel converter slag as an oxygen carrier
Accepted - Greenhouse Gases: Science and Technology

Paper VI
Hildor, F., Yilmaz, D., & Leion, H. (2023)
Interaction behavior of sand-diluted and mixed Fe-based oxygen carriers with potassium salts
Fuel, Volume 339, 127372

Paper VII
Hildor, F., Leion, H. & Linderholm, C
Effect of weathering on steel converter slag used as an oxygen carrier
Manuscript

Contribution report:

Paper I: Principal author, involved in experimental work at the semi-industrial boiler, responsible for experimental work in the laboratory scale, data evaluation and writing.

Paper II: Principal author, responsible for experimental work, data evaluation and writing.

Paper III: Principal author, responsible for experimental work, data evaluation and writing.

Paper IV: Principal author, involved in experimental work, responsible for tar-data evaluation and writing.

Paper V: Principal author, responsible for experimental work, data evaluation and writing.

Paper VI: Principal author, supervision of experimental work, responsible of data evaluation and writing.

Paper VII: Principal author, responsible for experimental work, data evaluation and writing.

Related peer-reviewed papers not included in this thesis

Leion, H., Frick, V., & Hildor, F. (2018).
Experimental Method and Setup for Laboratory Fluidized Bed Reactor Testing.
Energies, 11(10), 2505.

Mattison, T., Hildor, F., Li, Y., & Linderholm, C. (2019).
Negative emissions of carbon dioxide through chemical-looping combustion (CLC) and gasification (CLG) using oxygen carriers based on manganese and iron.
Mitigation and Adaptation Strategies for Global Change, 1-21.

Störner, F., Hildor, F., Leion, H., Zevenhoven, M., Hupa, L. & Rydén, M. (2020).
Potassium Ash Interactions with Oxygen Carriers Steel Converter Slag and Iron Mill Scale in Chemical-Looping Combustion of Biomass—Experimental Evaluation Using Model Compounds
Energy & Fuels, *34*(2), 2304-2314.

Hildor, F., Zevenhoven, M., Brink, A., Hupa, L. & Leion, H. (2020)
Understanding the interaction of potassium salts with an ilmenite oxygen carrier under dry and wet conditions
ACS Omega, 5(36), 22966-22977.

Attah M., Hildor F., Yilmaz D., Leion H. (2021)
Vanadium Recovery from Steel Converter Slag Utilized as an Oxygen Carrier in Oxygen Carrier Aided Combustion (OCAC)
Cleaner Production, Vol. 293 art. no. 126159

Andersson V., Soleimani Salim A.H., Kong X., Hildor F., Leion H., Mattisson T., Pettersson J.B.C. (2021)
Alkali-wall interactions in a laboratory-scale reactor for chemical looping combustion studies
Fuel Processing Technology, Vol. 217, art. no. 106828

Acknowledgments

My deepest gratitude goes to my supervisors Henrik Leion, Tobias Mattisson and Carl-Johan Linderholm. It has been a joy working with you all and thank you for all the help, discussions, and contributions to the work. Tobias, thank you for all the important discussions on the higher levels of research and thermodynamics. Carl-Johan, thank you for your support and guidance in the labs at Energy Technology. A special thanks to Henrik, without whom I would not have dared to start this journey.

The Swedish Research Council (VR), the Swedish Energy Agency and ÅForsk are acknowledged for financially supporting this work. Thanks to this financial support, I have been able to dedicate myself to my experimental work and have been able to attend conferences to present my results and gain new knowledge.

I have been privileged to have valued colleagues at two different divisions at Chalmers: Energy and Materials at the Department of Chemistry and Chemical Engineering and Energy Technology at the Department of Space, Earth and Environment. I have appreciated all the help, as well as the tips and tricks that I have received from you all. I have also enjoyed all the discussions in this multicultural environment at *fika* sessions, lunches, meetings and when we cross paths in the labs and the corridors. It is clear that it is the supporting colleagues who make the working place such a good place to be.

I am also grateful for the support of my family: my wife and son, my parents and brothers, in all aspects of life. Thank you for your support, advice, babysitting and your cheering me on along the way. In particular, I want to thank my wonderful wife Amanda for her support and for the adventure that we are sharing.

Fredrik Hildor, February 2023

Table of Contents

“Pollution is nothing but the resources we are not harvesting. We allow them to disperse because we’ve been ignorant of their value.” **- Buckminster Fuller**

Introduction

The Glasgow Climate Pact (2021) and Paris Agreement (2015) both address the global commitment to limit global warming [1,2]. The goal is to limit global warming to 1.5°C above the preindustrial levels, and one of the key measures to achieve this is to limit global greenhouse gas emissions (GHGs). Of the GHGs, carbon dioxide (CO_2) is the largest contributor to global warming, due to the large volume of cumulative emissions, as well as the long residence times of such emissions in the atmosphere. CO_2 emissions are known to be correlated to global warming not by yearly emissions, but by cumulative emissions to the atmosphere [3].

To decrease the levels of CO_2 emissions, increased energy and material efficiencies, as well as the development of carbon-neutral technologies are essential. However, the shift towards a carbon-neutral Society is not something that can be achieved overnight. Emissions of CO_2 are likely to continue for several decades before net-zero emissions are achieved. Nevertheless, since it is the global cumulative CO_2 emissions that affect global warming, it is also possible, and will even be necessary, to extract CO_2 from the atmosphere in order to restrict the total cumulative emissions to a sustainable level [4]. To address the issue of CO_2 extraction from the atmosphere, the Intergovernmental Panel on Climate Change (IPCC) has published a special report focusing on one of the opportunities for CO_2 reduction: Carbon Capture and Storage (CCS) [5]. CCS entails carbon being captured from a source and then stored in a secure way so that the carbon is not released to the atmosphere, for example below ground in aquifers or depleted oil/gas wells. Depending on the source of the carbon, CCS can reduce the emissions of CO_2 from humans to almost zero and may even yield net negative emissions. Negative emissions are obtained if CO_2 is extracted directly or indirectly from the air and is permanently stored in the process. An alternative strategy for negative emissions is to capture the CO_2 generated from the combustion of biofuels for power and/or heat generation. This approach is commonly called Bio-Energy with Carbon Capture and Storage (BECCS) [6]. Negative emissions of any kind could have great importance in a future in which carbon emissions are limited. Negative emissions can also be a way to restore the global CO_2 concentration in the atmosphere to a sustainable level [5–7]. According to the majority of the scenarios suggested by IPCC to achieve the 1.5°C target, capturing CO_2 via technological inventions is necessary [4].

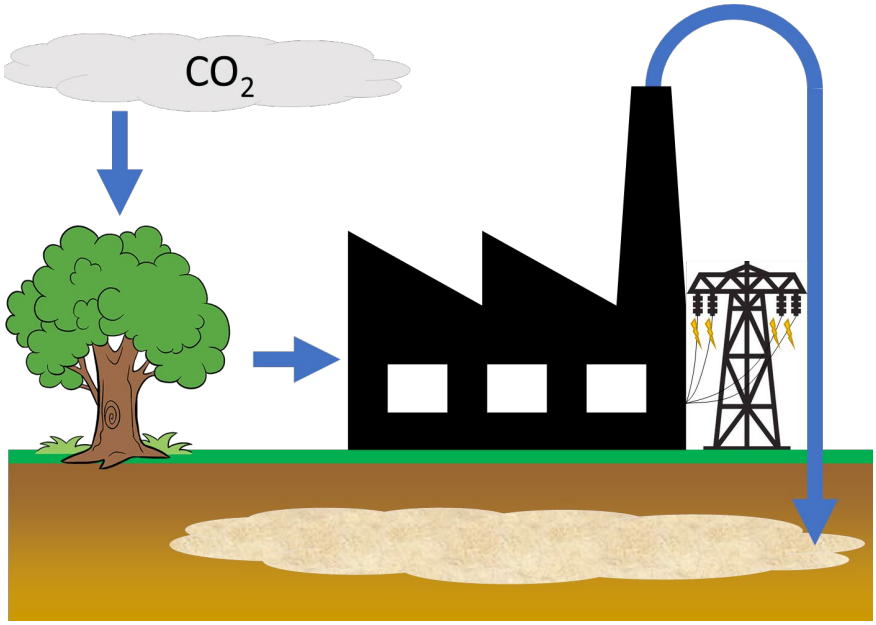

Figure 1. Illustration of the carbon flow in Bio-Energy with Carbon Capture and Storage (BECCS).

BECCS, as illustrated for electricity production in Figure 1, can be achieved using various methods for the thermal conversion of biomass. For power production using biomass, fluidized bed boilers are considered favorable because of their fuel flexibility. Traditionally, silica sand has been used as a bed material for heat transport. It is also possible to change the bed material to an active bed material, which in addition transports oxygen, a so-called 'oxygen carrier'. An oxygen carrier is commonly a metal oxide that can be reduced and oxidized under conditions relevant for thermal conversion. If an oxygen carrier is applied in a conventional fluidized bed boiler this is called Oxygen Carrier-Aided Combustion (OCAC) [8]. However, the conversion of the fuel can also be divided into two different reactors, where the oxygen carrier transports oxygen from one reactor to the other. This means that the conversion of the fuel to mainly CO_2 and H_2O can be conducted without any dilution with nitrogen, making it suitable for CCS. This two-reactor layout, which aims for the full conversion of fuel to CO_2 and H_2O, is called Chemical-Looping Combustion (CLC). Vital to both OCAC and chemical looping applications is the oxygen carrier [9–11]. The oxygen carrier selected for each of these processes should preferably be durable, reactive, sustainable and cheap [12]. Therefore, in the last few years, different ores and iron-containing industrial byproducts have studied intensely as potential oxygen carriers [13].

This thesis investigates the use of steel converter slag in applications designed to provide more-efficient thermochemical processes for biomass conversion, which can promote efficient carbon capture. This slag, which is also known as Linz-Donawitz (LD) slag, is a byproduct of the steel manufacturing process and is available in significant amounts at limited cost, due to the low demand for this material for other applications. LD slag was investigated in the seven papers included in this thesis. The scope of the work can be divided into three areas of investigation, as illustrated in Figure 2: Ash interaction, Reactivity, and Operation. **Paper I** investigates the ash interactions of LD slag particles, which have been used in the Chalmers 12-MW Circulating Fluidized Bed (CFB) boiler. **Paper II** delves deeper into the reactivity of LD slag towards solid fuels. **Paper III** investigates the interactions of sulfur with LD slag and how this element affects the reactivity of LD slag particles. **Paper IV** evaluates the behaviors of tar species during pilot plant Chemical-Looping Gasification (CLG) operations using LD slag as an oxygen carrier. **Paper V** explores the effects of adding small amounts of reactive elements to the slag, so as to increase the reactivity of the material. **Paper VI** examines the interactions of LD slag with the common and problematic ash element potassium, in presence of the other bed materials silica sand and ilmenite. **Paper VII** investigates the effect of outdoor storage of pre-treated LD slag particles, as well as how the material weathers and how this affects its reactivity.

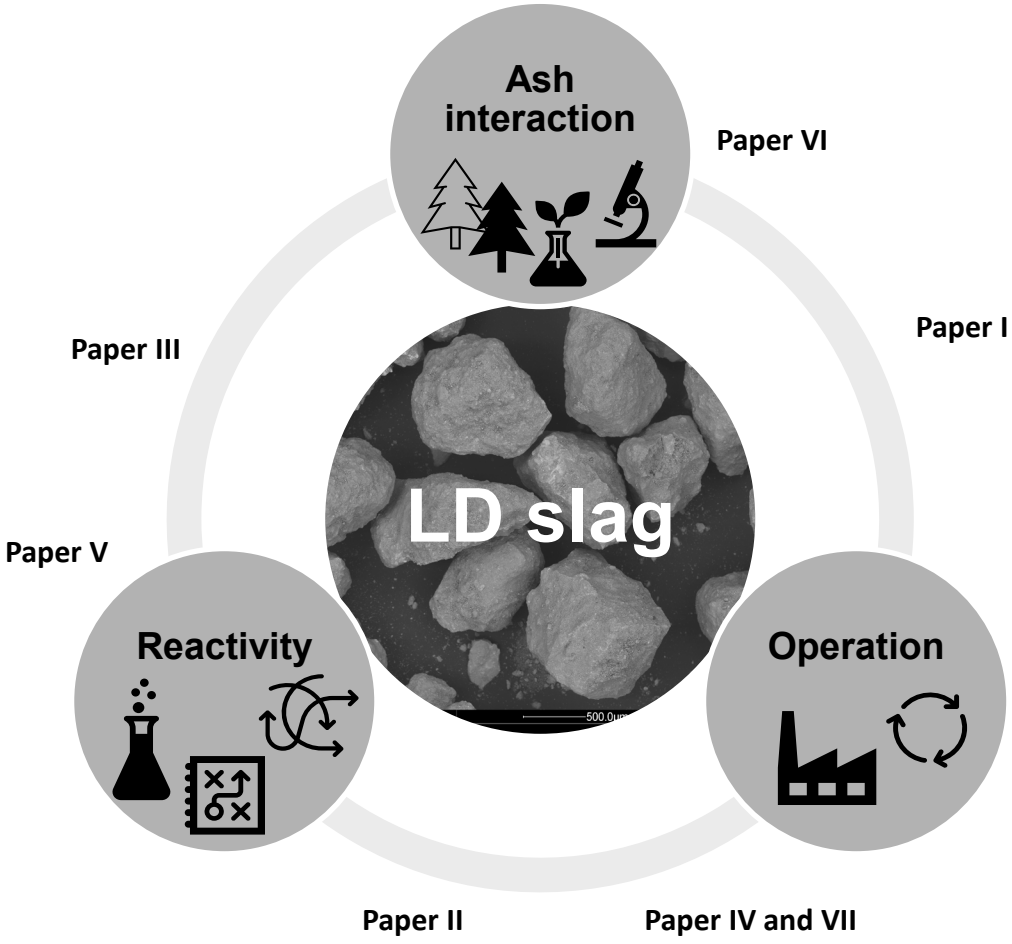

Figure 2. Illustration of the main research areas in focus in this work.

Chapter 1

1. Carbon capture and the roles of oxygen carriers

Capturing CO_2 from flue gases in a commercial biofuel power plant to obtain BECCS requires a large amount of energy since the CO_2 level in the flue gas is relatively low, approximately 15%. Several different technologies are available to achieve BECCS from power plants and they are normally divided into three categories: i) post-combustion; ii) pre-combustion; and iii) oxyfuel combustion [5].

In post-combustion, CO_2 in the flue gas is separated from the other gases through a separation step, for example in an amine scrubbing unit. This is an energy-intensive operation that requires a large amount of heat to regenerate the amine. However, it is a relatively simple and well-established process that can be retrofitted to a power plant [5]. SaskPower's Boundary Dam plant in Canada and NRG's Petra Nova plant in the US are two full-scale power plants for coal combustion that have applied this technology for carbon capture [14].

In pre-combustion with solid fuel, the fuel is first gasified to generate a syngas that contains mainly CO and H_2. The gas mixture is then converted further in a water-gas shift reactor where CO is converted with steam to produce CO_2 and more H_2. Thereafter, the CO_2 is separated from the H_2 and transported to storage. The H_2 can be utilized as a carbon-free fuel in, for example, power plants or fuel cells where the only emission is water [5].

Oxyfuel combustion utilizes pure oxygen and recirculated flue gas for combustion, resulting in the flue gases not being mixed with the nitrogen from the air. Pure oxygen is obtained through the use of an air separation unit [5]. This is the technique that was used previously by Vattenfall in the oxyfuel test facility at Schwarze Pumpe power station in Germany [15].

However, all of these technologies require gas-gas separation, which is very energy-intensive and costly due to the work needed to separate the gases. Another technology for power production suitable for carbon sequestration that has emerged in recent decades is CLC. CLC avoids energy-intensive gas separation owing to the intelligent layout of the combustion system [7,16]. A chemical-looping system normally consists of two interconnected fluidized beds: an air reactor, and a fuel reactor. Between these two beds, oxygen carrier particles are circulating. This oxygen carrier – a metal oxide – transports oxygen and heat from the air reactor, which is fluidized with air, to the fuel reactor where the oxygen from the oxygen carrier is used to convert the fuel. In this way, the flue gases from the fuel reactor are not diluted with nitrogen from the air. Depending on the amount of oxygen transported by the oxygen carrier, full conversion of the fuel to CO_2 and H_2O can be achieved, in CLC. However, limiting the oxygen transport will result in partial conversion of the fuel, which can be used in downstream processes; this is called Chemical-Looping Gasification (CLG) [5,17]. In Figure 3, these two designs are graphically described.

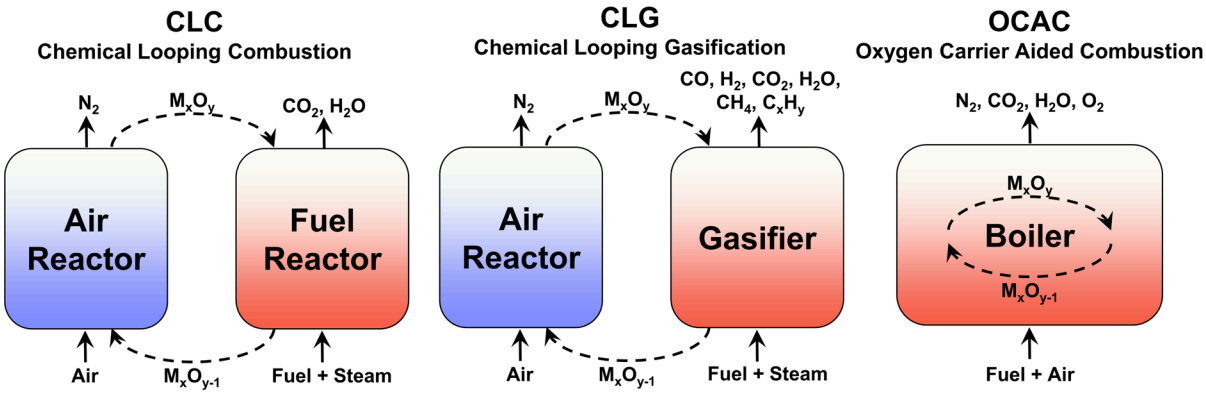

Figure 3. Schematic overview of CLC, CLG and OCAC

Besides CLC and CLG, oxygen carriers can be utilized directly in conventional fluidized beds. This is called Oxygen Carrier Aided Combustion (OCAC), which is also visualized in Figure 3. This is not a method for direct CO_2 separation, but rather a method to create an oxygen buffer in the fluidized bed, which may confer benefits with respect to combustion efficiency and emissions [8].

1.1 Chemical-Looping Combustion

Comparing different separation techniques for fuel conversion, CLC emerges as one of the most-energy-efficient tools to sequester CO_2. Here, the oxygen carrier provides heat and oxidizes the fuel by providing oxygen to generate ideally only CO_2 and water, as schematically illustrated in Figure 3. Since the flue gas from the CLC fuel reactor comprises of almost pure CO_2, no energy-consuming gas separation is needed and the capture cost of CO_2 is lower compared to other methods [5,17].

The heat of combustion in a CLC unit will be the same as for conventional combustion in air. The conversion of the fuel is separated into two steps according to reaction R1 and R2. Reaction R1 is always exothermic and occurs in the air reactor, where the oxygen carrier is oxidized. Reaction R2 is in most cases endothermic, depending on the fuel and oxygen carrier used, and occurs in the fuel reactor, where the fuel is converted into H_2O and CO_2 using the oxygen from the oxygen carrier. The metal in the oxygen carrier, M in R1 and R2, is not limited to any specific metal, as several different transition metals or metal oxide mixtures can be utilized as an oxygen carrier for this process. The combustion or conversion of fuel is, therefore, dependent upon both the choices of fuel and oxygen carrier.

$$M_xO_{y-1} + \frac{1}{2}O_2 \rightarrow M_xO_y \quad \{R1\}$$

$$(2n+m)M_xO_y + C_nH_{2m} \rightarrow (2n+m)M_xO_{y-1} + mH_2O + nCO_2 \quad \{R2\}$$

Applying solid fuel to CLC involves conversion of the fuel in several steps. The volatile matter will react with oxygen carriers when released during the pyrolysis of the fuel. The remaining char will, thereafter, undergo gasification forming gaseous matter according to the endothermic reactions R3 and R4, whose products can in turn react with the oxygen carrier [18,19]. Direct solid-solid interactions between oxygen carrier and char are not expected to occur to any great extent in a fluidized bed [20]. The gasification of char is affected by both temperature and the surrounding atmosphere where, for example, the presence of CO_2, O_2 and steam increases the overall gasification rate [18].

$$C_nH_m + nH_2O \rightarrow nCO + \left(n + \frac{m}{2}\right)H_2 \quad \{R3\}$$

$$C_nH_m + nCO_2 \rightarrow 2nCO + \left(\frac{m}{2}\right)H_2 \quad \{R4\}$$

Besides R2, which oxidizes the gaseous matter generated from the volatiles and gasified char, some oxygen carriers can also release oxygen as gas-phase O_2 (see R5). This phenomenon is called Chemical Looping with Oxygen Uncoupling (CLOU) [21]. The advantage associated with oxygen carriers having CLOU properties is that the O_2 released in the fuel reactor can react with the solid fuel according to exothermic R6 [18], thereby increasing the gasification rate. However, to have a significant CLOU effect, the oxygen release mediated by the oxygen carrier needs to be sufficiently high, and the equilibrium partial pressure of oxygen must be high enough to create a driving force towards gaseous oxygen. Nevertheless, only a few oxygen carriers have pronounced CLOU properties [17,21].

$$M_xO_y \rightarrow M_xO_{y-1} + \frac{1}{2}O_2 \quad \{R5\}$$

$$C + ½O_2 \rightarrow CO \quad \{R6\}$$

CLC can be used with essentially any fuel, and several studies have investigated CLC with gaseous and solid fuels, originating from both fossil sources and biomass [10,17]. However, several parameters set the solid fossil fuels and biomass fuels apart. Solid biomass fuels, compared for example with coal, have a lower energy density, higher content of volatiles, are more-variable in chemical composition, and have a very different ash composition [22,23]. Ash consists of the non-combustible and non-volatile elements of the fuel and depends on the source of the fuel. This ash can cause agglomeration and deactivation, both in conventional boilers with sand and in oxygen carrier applications. Some regeneration of the oxygen carrier bed will, therefore, be necessary for thermal solid fuel conversion processes. Therefore, it is essential to identify low-cost oxygen carriers that can be operated with different fuels in a technically feasible way, and ideally at a low cost [24–26].

1.2 Chemical-Looping Gasification

Limiting the oxygen provided via the oxygen carrier to the fuel provides the opportunity to gasify thermally the solid fuels to gaseous products, as in the CLG process. The general layout of the CLG process is depicted in Figure 3.

CLG using biomass as the fuel has been studied to a lesser extent than biomass CLC, both regarding scale and operational hours [27]. Continuous experiments with CLG have been performed in reactors using rice husk [28,29], as well as at a semi-industrial scale at the Chalmers 2–4-MW Dual Fluidized Bed (DFB) gasifier. In this semi-industrial gasifier, it has been shown that a mere bed material composition of12% ilmenite in silica sand decreased the tar generation by 50% [30]. CLG has also been achieved using a fuel with a high metal content in the same 2–4-MW DFB gasifier, and the effects of oxygen carriage have been studied [31]. Even though this was not an autothermal gasification unit, it was concluded that the heat balance over the system was strongly affected by the oxygen transport.

Modeling studies have shown that controlling an autothermal, large-scale CLG process is a complicated balancing act. This is because the oxygen carrier transports both oxygen and heat from the air reactor to the fuel reactor. Decreasing the oxygen transfer by decreasing the circulation decreases at the same time the heat transfer. Thus, decoupling these mechanisms would be beneficial [32,33]. Using an oxygen carrier with a low oxygen transport capacity could, therefore, be an advantage.

The layout of CLG is similar to that of the DFB gasifier used in the near-commercial-scale gasification plant GoBiGas, which had a production capacity of 20 MW of biomethane gas [34]. The main difference is that the bed material does not manifest any oxygen carrier properties in a DFB gasifier. This results in the need for partial combustion in the air reactor [35]. However, compared to the GoBiGas plant, which was designed to produce

CH_4 [35], a CLG plant would be more-favorable for the production of a syngas that contains mainly CO and H_2 [11].

The main principle of CLG with partial oxidation can also be applied to the reforming of gases such as methane. In that case, the process is called Chemical-Looping Reforming (CLR). CLR is a promising technology from the techno-economic point of view for hydrogen production from methane with carbon capture, producing so-called 'Blue Hydrogen' [36]. The principle of CLR can also be applied for tar removal downstream of a gasification process, assuming that a selective oxygen carrier can be identified [27].

1.3 Oxygen Carrier Aided Combustion

Oxygen carriers can also be utilized as bed materials in conventional fluidized bed boilers, simply by replacing all or parts of the bed inventory with oxygen-carrying material. This is the OCAC process. The principal task of the oxygen carrier in OCAC is the same as in CLC: to transport oxygen from oxygen-rich locations to fuel-rich locations. However, in OCAC, this is performed within the same bed. This increases the combustion efficiency within the bed and smoothens the temperature differences, resulting in lower emissions of NOx and CO [8].

OCAC has been applied at industrial scale and has been proven to reduce CO emissions by 80% and NOx emissions by 30%. This was achieved using a mixture of 40% ilmenite in a bed of silica sand in a 12-MW_{th} bubbling fluidized boiler [8]. OCAC has also been applied at larger scale, in a 115-MW_{th} power plant, where it was observed that the oxygen excess could be decreased and the boiler load increased to 123 MW_{th} as a result of using the oxygen carrier ilmenite as the bed material [37]. In summary, it has been shown that OCAC can lead to lower levels of emissions, increased fuel load in existing boilers, and a reduced need for excess oxygen. Combined with easy implementation, it is clear that OCAC is a highly promising technology for fuel conversion.

In itself, OCAC is not a technology that facilitates inherent CO_2 separation, as is the case for CLC and CLG. The flue gases are still a mixture of nitrogen, remaining excess oxygen, and combustion products. Nevertheless, OCAC can be favorable for facilities that intend to perform post-combustion CO_2 capture from a plant with a fluidized bed boiler. Considering post-combustion capture with, for example, an amine process [5], OCAC can increase the efficiency of the process because lower air-to-fuel ratios can be used, thereby increasing the CO_2 concentration in the flue gas [8,38]. Higher CO_2 concentrations in the flue gas decrease the minimum work requirement for gas separation, what makes the capture of CO_2 less-energy-consuming [39]. From another perspective, oxyfuel combustion in a fluidized bed system offers the possibility to retrofit current power plants without the energy penalty linked to CO_2 separation from the flue gas. Instead, oxygen needs to be produced or supplied to the process [40]. OCAC might also offer the possibility to reduce the amount of excess oxygen in the oxyfuel process and, thereby, decrease the cost of CO_2 capture.

1.4 Bed materials and oxygen carriers

Currently, sand is the bed material that is most often used in conventional fluidized bed boilers used for heat and power production. For the conversion of the fuel, sand is considered to be an inert material that transports heat to the reaction and improves the mixing in a boiler [41]. In contrast, oxygen carriers additionally transport oxygen to the fuel. Efficient oxygen carriers are key components of chemical-looping processes. The oxygen carrier is ideally a material that can be used and operated as a bed material in a fluidized bed at combustion temperatures without excessively rapid chemical and mechanical decay rates. Consequently, the important criteria for a suitable oxygen carrier [19,24,26,42] are as follows:

- Sufficient oxygen transport capacity to reduce the amount of oxygen carrier needed.
- High melting temperature to avoid sintering.
- Not environmentally harmful.
- Sufficient reactivity with both oxygen and the fuel.
- Relatively high mechanical strength at high temperatures, to avoid attrition and to increase the lifetime of the oxygen carrier.
- Available at a low cost. The cost for the oxygen carrier is especially important for solid fuel CLC due to the unavoidable losses of oxygen carrier in the fuel ash separation and the deactivation caused by the ash.

The most-intensively investigated oxygen carriers are oxides of transition metals for CLC, such as nickel, cobalt, copper, iron and manganese [43]. Nickel has been considered due to its excellent reactivity. However, besides being expensive and toxic, nickel has a thermodynamic constrain converting fuel to CO_2 and H_2O [42].

Copper is of interest as an oxygen carrier because it exerts significant oxygen release via its CLOU properties, and it has been used in larger continuous reactors [44,45]. However, copper-containing oxygen carriers have certain disadvantages, as they have been associated with issues related to agglomeration at higher temperatures [24,46] as well as being expensive compared to alternative materials [42].

Manganese oxide has also attracted interest as an oxygen carrier due to its comparably low price and its CLOU properties [17,21]. The thermodynamic properties of pure manganese oxide can be altered and improved through the use of mixed oxides that contain manganese oxide, together with elements such as iron, silicon, calcium, nickel, magnesium and copper [47]. To obtain mixed manganese oxide at a lower price, manganese ore has been investigated for solid fuel combustion, in which it is acknowledged that bed regeneration is needed to avoid ash accumulation. Manganese ores from different regions have been investigated in small-scale reactors [48,49], and have also been tested in Chalmers 12-MW_{th} CFB boiler [50].

Iron-based oxygen carriers have been studied in the forms of synthesized particles, ores and waste products that contain iron oxide. Iron-based oxygen carriers are assumed to be environmentally friendly compared to oxygen carriers that contain cobalt or nickel [51]. In addition, iron-based oxygen carriers have been studied using synthesized particles with iron present on several different support materials [24,51–53]. However, when operating with solid fuels, there is a need to utilize less-costly oxygen carriers, such as ores or waste materials [54]. Since iron is common in the industrial infrastructure, it is also present in different waste streams, and such materials, e.g., sewage sludge ash and slag, have been examined as oxygen carriers [55,56]. However, these types of materials are not "pure" and it needs to be considered what other compounds and elements are introduced into the thermal conversion process with the oxygen carrier, as these 'contaminants' may affect the overall process.

When utilizing a waste or a slag product as an oxygen carrier the metal content must be sufficiently high to enable adequate oxygen transport. However, if considering an oxygen transfer of only 1 wt.%, the oxygen transfer is not the limiting factor for thermal stability in a CLC unit. Instead, it is the heat transfer from the air reactor to the fuel reactor that is the critical factor. This is the case because energy is released in the air reactor (where oxidation occurs) and heat has to be transported to the fuel reactor (where endothermal reactions predominate) for the conversion of the fuel. Therefore, is it essential that a CLC reactor is designed so that enough material can be circulated between the two reactors to cover the energy balance [57].

Over the years, ilmenite has become a benchmark oxygen carrier that has been studied at different scales [8,37,54,56,58], and it has been used as a model material for the design of a 1,000-MW_{th} CLC plant [59]. Ilmenite is the name of a titanium-iron oxide mineral and also the dominant crystalline phase with the formula $FeTiO_3$. It is a relatively common mineral and is applied industrially to produce the TiO_2 used in e.g. pigments and sunscreen [60]. Ilmenite can be oxidized to form pseudobrookite and rutile with the chemical formula Fe_2TiO_5. This oxygen carrier has mainly been investigated for solid fuels, since it is an ore that can be obtained at a relatively low cost [61]. Today, it is also industrially used as an oxygen carrier in facilities that are implementing OCAC [13,37]. One of its characteristics is the binding of alkali into the titanium structure of the particles. Since the formed potassium titanate has a high melting point, boilers operated with ilmenite may experience less issues with agglomeration of the bed material [8,38,62].

In this work, ilmenite is used as a reference material in most of the papers, as it is also an iron-based oxygen carrier. Ilmenite has previously been evaluated in the same reactors as are used in the experimental work of this thesis. In the small laboratory scale batch fluidized bed reactor ilmenite was concluded to have a good conversion of CO and H_2 and less good conversion of CH_4 [61]. The same material has also been evaluated in the semi-industrial scale 12-MW_{th} CFB boiler at Chalmers with wood chips as fuel [63].

1.4.1 Steel converter slag (LD slag)

During year 2018, roughly 4.7 Mt of steel were produced in Sweden, and approximately 1,810 Mt of steel were produced worldwide [64]. Linked to this, several byproducts are produced during the conversion of iron ore into steel. The two largest side-streams are: blast furnace slag, with 175–300 kg/t of steel; and LD slag, with 85–200 kg/t of steel [65,66]. Of these two major byproducts, LD slag is of interest for usage as an oxygen carrier due to its higher iron content and good availability.

LD slag is a mixture of fluxes and contains the remaining impurities from the iron ore that was not removed in the blast furnace and which is not intended to be in the final steel product. The composition of LD slag is, therefore, dependent upon the origin of the iron ore. Some LD slag can be recirculated into the steel process, but due to the risk of phosphorus accumulation in the steel process, the potential for recirculation is limited [66]. Consequently, more than 300 kt of LD slag are produced annually in Sweden alone [50]. Generally, the elemental composition of LD slag is Ca (21%–43%), Fe (8%–27%) and Si (4%–9%), together with minor components such as Mg, Mn, Ti, Al, P and V [66–68]. These elements are present and stable in various different phases [68].

Due to the phosphorus content of LD slag, it can be used as a fertilizer. In Germany, slags have been used since 1880 as agricultural fertilizers, and adjustments to the manufacturing process have been monitored to meet standards and regulations [69]. However, in Sweden and some other regions of the world, the vanadium content of the slag is relatively high. Since there are concerns regarding the effects of vanadium on plant life [70], the usage of LD slag as a fertilizer has been avoided in the Nordic countries. The high vanadium content of LD slag is due to the higher vanadium content of the iron ore in the Nordic region [71]. Some efforts have been made to extract vanadium from the LD slag used as an oxygen carrier, but with limited success [72].

Due to its availability, limited industrial demand and iron content, LD slag has been considered as an potential oxygen carrier [56,73,74]. Besides the expected low cost of LD slag [50], there is also an environmental benefit associated with using a material that is an industrial byproduct and that is not utilized to a great extent today. In connection with the studies included in this thesis, LD slag has been operated as a bed material in the 12-MW_{th} CFB boiler at Chalmers University of Technology under OCAC conditions [50]. The findings from this operation, and from previous studies investigating LD slag, can be summarized as follows:

- LD slag can be utilized as an oxygen carrier and has similar reaction properties to other iron-based oxygen carriers [56,73].
- LD slag can be operated as a bed material in a CFB. It can be handled in a similar manner to sand, and there are no problems related to agglomeration [50].
- OCAC operation with only LD slag results in high CO emissions. The addition of ammonium sulfate or elementary sulfur decreases the CO emissions, suggesting that limited alkali absorption is the cause of the increased emissions [50].
- LD slag can be operated at full scale in combination with sand, yielding reasonably low CO emissions [50].

- NOx emissions may increase due to catalytic formation [74] and there are increased NOx emissions when using LD slag at a certain air-to-fuel ratio compared to using sand [50]. This is similar to other low-cost oxygen carriers such as ilmenite [8] and manganese ore [75], which have been used in the same boiler.

1.5 Ash interactions, agglomeration and corrosion

Solid fuel always contains inorganic material that forms ash during combustion. The compositions and phases of these inorganic materials depend on the origin of the fuel. Regardless of whether the fuel is of fossil or biomass origin, some of the inorganics in the fuel matrix have high boiling temperatures and will end up as solid ash. In fluidized bed combustion systems where a solid bed material is used, there are issues regarding how to separate the ash from the bed material. Therefore, regeneration of the bed is a commonly used method to avoid the accumulation of ash in the fluidized bed boiler [23].

The interaction of ash with the bed can result in the formation of products with low melting points, so-called 'melts'. Melts have a tendency to fuse particles to agglomerates in a fluidized bed, which can lead to defluidization. There are two main mechanisms for agglomeration. The first involves an ash component from the fuel reacting with the bed material to form a phase with a low melting temperature. An example of this is potassium in a silica sand bed. Thus, potassium reacts with the silica sand to form potassium silicate, which has a low melting point and can melt in the boiler. In the second mechanism, the ash is inert towards the bed material but forms phases with a low melting temperature. This ash melts and adheres to the surfaces of the particles, which leads to agglomeration. This second mechanism is, in principle, independent of the bed material. An example of this is the ash from rapeseed cake that is rich in potassium-calcium-phosphates with a low melting temperature [22,76]. The two mechanisms are illustrated in Figure 4.

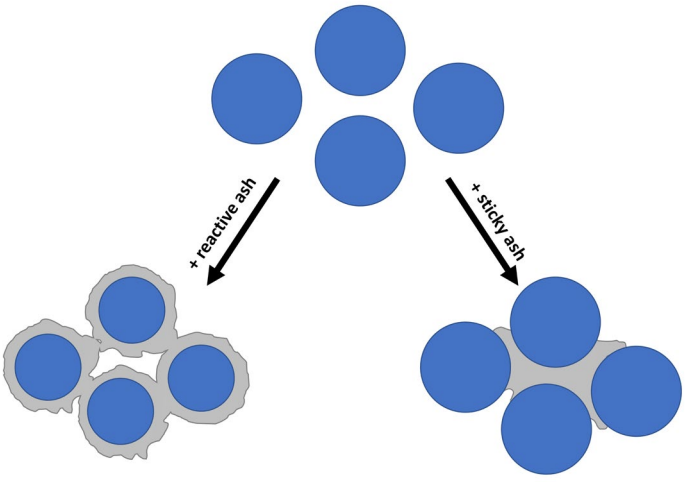

Figure 4. Illustration of the first and second agglomeration mechanisms based on [76]. *Left: The first mechanism – a reactive ash, e.g., reactive potassium reacts with silica sand bed material to form potassium silicate with a low melting temperature. Right: The second mechanism – a sticky ash melt, e.g., sticky ash from rapeseed that contains potassium–calcium–phosphates that can cause bed particles to adhere to each other.*

Since alkali decreases the melting temperature of silica sand in biomass combustion, regeneration of the bed also prevents excessive accumulation of reactive alkali, which can result in bed agglomeration. In general, compared to fossil fuels, biomass has higher contents of both alkali and phosphorus, both of which can promote agglomeration [76]. Moreover, these elements can interact with the bed material in combustion processes. Bed ash can also react with oxygen carriers to cause agglomeration or deactivation of the oxygen carrier in a chemical-looping application [77]. At the same time, alkali is known to increase the reactivity and char conversion rate for certain oxygen carriers [78,79]. The well-studied oxygen carrier ilmenite has the ability to react with potassium to form potassium titanates [62,80]. Potassium titanate has a comparably high melting temperature, resulting in ilmenite having a higher capacity to accumulate potassium than silica sand [81]. In other words, a fluidized bed that contains ilmenite is less-sensitive to alkali-mediated agglomeration and, therefore, less-prone to bed defluidization as compared to a bed of silica sand.

In addition to alkali and phosphorus, biomass contains large amounts of calcium. Calcium has been observed to accumulate on the surfaces of oxygen carriers such as ilmenite [82] and bed materials such as olivine [83] and feldspar [84]. In these studies, using different bed materials, calcium has been shown to migrate inwards to the particle interior to ion-exchange elements such as magnesium. Calcium has also been associated with increased melting temperature in silica-potassium-calcium mixtures. Potassium and silica are often the main contributors to agglomeration in fluidized bed boilers that employ silica sand [76].

Another important element in the fuel is sulfur. Sulfur is a common element in both biofuels and fossil fuels. In a conventional combustion process different forms of sulfur oxides, normally grouped as SOx are formed. SOx emissions from power plants contribute to acid rain and have negative impacts on human health. Desulfurization has since been performed and developed the middle of the last century, and today sulfur emissions regulations are well-established [85,86]. In the 1960s and 1970s, one of the most-intensively investigated method was the introduction of limestone into the furnace, which was found to be especially suitable for conventional fluidized bed boilers [85,87].

More recently, sulfur has come to be regarded to be more than just an issue for combustion processes. Corrosion of the superheaters in bio-fired power plants are related to alkali where especially potassium in combination with chlorine have been observed as a problem. Sulfur addition, either as an additive to the boiler or as a sulfur-rich fuel such as peat in co-combustion, represents a way to limit corrosion. An excess of sulfur in relation to potassium inhibits the formation of KCl, since the compound K_2SO_4 is thermodynamically more-favorable [22]. Sulfur recirculation from flue gas treatment in industrial-scale waste-to-energy power plants has also shown that the electricity output from a plant can be increased. This is also related to the decreased corrosion, which enables a higher surface temperature on the superheaters [88].

In chemical-looping applications, sulfur is not only oxidized to SO_2 or SO_3. From both the thermodynamic calculations [89,90] and experiments [90–93], it is clear that mainly H_2S is formed if the oxygen access is subject to under-stoichiometric conditions, as in CLG.

When over-stoichiometric conditions are used, as in CLC, mostly SO_2 is formed, as is the case for conventional combustion. These studies, that used ilmenite and copper-based oxygen carriers, it is also suggest that most of the sulfur will be released in the fuel reactor. However, a recent study of ilmenite and sulfur interaction under OCAC conditions suggests that in combination with biofuel ash, sulfur is also absorbed into the structure of ilmenite [94]. This could indicate that more sulfur is transported to the air reactor and released there, considering the lower vapor pressure of SO_2 and the higher reactor temperature in the air reactor.

1.6 Aim and scope of this thesis

This thesis aims to investigate the properties and potential of LD slag as an oxygen carrier for thermal conversion processes using biomass. LD slag is compared to other bed materials that are relevant for solid fuel combustion and gasification. To obtain a comprehensive understanding of the viability of LD slag, experiments are conducted at different scales and under different conditions. Reactivity tests are made in a small laboratory-scale, batch fluidized bed reactor using various fuels. The propensities to react with reactive ash species and other important components, such as sulfur and tar precursors, are investigated at small scale. Experiments in larger pilots and a semi-industrial unit using LD slag are also performed. Various physical and chemical characterization methods are employed throughout the experiments. Thus, a much better understanding of the viability of LD slag for chemical-looping processes is acquired. It is also expected that the studies will contribute to a better understanding of Fe-based oxygen carrier materials in general.

Chapter 2

2. Experimental

The papers included in this thesis are based on work that extends from laboratory scale to semi-industrial scale. Most of the experiments were conducted in a laboratory scale fluidized batch reactor. A pilot-scale, 10-kW circulating chemical looping reactor was used for testing LD slag under CLG conditions, and the focus of this work included in this thesis was on the tar formation. Material interactions were instigated using the bed material from the Chalmers semi-industrial, 12-MW_{th} CFB boiler. For all of these experiments, the same batch of LD slag has been used.

2.1 Bed materials

Although LD slag was the main bed material used in these studies, other bed materials were employed for comparison. These materials were chosen because they are commonly used in relevant applications [10,34,35]. Ilmenite is often used in CLC and could be considered to be a benchmark oxygen carrier. Olivine is used in indirect gasification and is known for its activity towards the conversion of tars. It also has some oxygen-carrying capacity [58,96]. Currently, silica sand is the standard bed material in fluidized bed boilers. The bed materials used in the studies of this thesis are listed in Table 1, together with their size distributions and bulk densities. As-received materials were heat-treated at 950°C for 24 h in a box furnace before being used in the batch fluidized bed reactor. This heat treatment was necessary to oxidize the particles, burn off organic components such as oil, and remove moisture and crystal-bound water.

Table 1. List of the bed materials investigated in this thesis. Bulk density was measured for the heat-treated particles.

Material	*Provider*	*Bulk density [kg/m³]*	*Size fraction [µm]*
LD slag	SSAB Merox AB (Sweden)	1400	150-400
Ilmenite	Titania A/S (Norway)	1800	100-300[26]
Olivine	Sibelco Nordic AB	1600	180-500
Sand	Merck	1300	180-250

The LD slag used in the different papers originates from the same batch of 28 t of LD slag that was delivered to Chalmers for use in the experiments carried out in the 12-MWth CFB boiler. The material was industrially sieved to a size of 150–400 µm with a yield of 20%-25% of the desired size, and heat treated prior to transport to Chalmers University of Technology [50]. Elemental analyses of the LD slag and the other bed materials are shown in Table 2.

Table 2. Elemental analyses of the studied bed materials, excluding oxygen. LD slag, olivine and sand were analyzed with ICP-SFMS, and ilmenite was analyzed with XRF. The balance is mainly oxygen. Values are given in wt.%.

Element	*LD slag*	*Ilmenite*	*Olivine*	*Sand*
Fe	17	36	5	0.36
Ti	0.78	28	-	0.04
Ca	32	0.22	-	0.05
Si	5.6	0.67	20	45
Mg	5.9	2.0	30	0.24
Mn	2.6	0.21	-	0.01
V	1.5	0.12	-	0
Al	0.76	0.17	0.24	0.22
Cr	0.33	0.06	0.21	0
Ni	0.002	0.03	0.25	0

2.1.1 Impregnation of LD slag

Wet impregnation, which is a method for adding chemical elements to a particle, is commonly used in catalyst production. A controlled amount of an element can be added to the structure of a particle by dissolving the active element, then wetting the particle with the solution, followed by drying. This allows the active element to precipitate on the surface of the particle. Wet impregnation was performed on LD slag to add Ni, Cu, Mn and Ce nitrates, which are elements that are known to act as reactive oxygen carriers [27,97–99] or that have catalytic properties [100]. Details of the impregnation technique are provided in **Paper V**.

2.2 Fuels

Both gaseous and solid fuels were used in these studies. Gases were provided by Linde (formerly AGA). For the oxidation reaction, bottled air was used in the laboratory batch reactor and air from the surroundings was used in the larger units. The reducing gases used were syngas (50% CO in H_2), CH_4, CO, N_2 saturated with C_6H_6, H_2 diluted in Ar, SO_2, CO_2, and a steam and gasification mixture (14% CH_4, 14.9% CO_2, 43% CO, 5% C_2H_4 and 23.1% H_2).

For the laboratory-scale and semi-industrial-scale experiments involving combustion and gasification, different biomass-based solid fuels were used. Wood chips were used in the 12-MW_{th} CFB boiler for OCAC operation, and pellets of char were used in the fluidized bed reactor. The results of the analyses of the fuels used in this thesis are displayed in Table 3. Further details regarding the fuel analysis are given in **Paper II** and **Paper III**. A reference database wood example is provided for comparison.

Table 3. Analyses of the fuels, given in [wt.%]. Ash, S, C, H and O are given on a dry basis and elemental analysis of the ash is given as g/kg dried fuel. The fuels were converted into ash at 550°C.

Sample	*Dry basis*					*Elemental composition of the ash*							
	Ash	***S***	***C***	***H***	***O***	***Fe***	***Ca***	***Mg***	***Mn***	***Al***	***K***	***P***	***Si***
Wood-Chips Sample	0.5	<0.02	49.2	6.1	42	0.66	23	3.8	1.5	0.53	12	1.3	1.7
*Wood Pellets Sample**	0.4	<0.02	50.3	6.2	43	0.89	22	3.6	2.7	1.1	9.6	1.4	4.0
Wood Pellets Char Sample	3.4	0.02	90.4	<0.5	3	3.9	21	4.8	2.9	1.5	5.8	1.3	6.6
German Wood Char	7.2	0.02	85.3	2.6	4.4	1	12	0.97	0.37	1	4.4	0.35	12
*Wood Reference***	1.4	0.03	49.7	6.0	43	0.01	24	3.6	1.5	0.02	14	2.2	0.13

**Analysis of wood pellets was not performed on the same batch of pellets as the one used to produce the wood pellets char samples but had the same provider.*
***The reference sample analysis is based on a mean calculated for 24 different stem-wood fuels in the Chemical Fractionation Fuel database of Åbo Akademi.*

The solid fuels used in the experimental campaign in **Paper IV** using the 10-kW_{th} continuous chemical looping reactor system were: Black Pellets (BP); Pine Forest Residue (PFR); and crushed straw pellets (ST). The results of the analyses of these fuels are shown in Table 4. The BP were steam-exploded pellets provided by Arbaflame AS, Norway. This was used as a reference fuel with more fixed carbon and low level of alkali. The pellets were crushed and sieved to obtain a size in the range of 0.7–2.8 mm. PFR was provided by the National Renewable Energy Centre (CENER), Spain. This fuel is more complex than BP and contains more volatiles. The PFR was crushed to obtain a size in the range of 0.7-3.0 mm. Straw pellets were provided by Stohfelder, Austria. Straw is known for having high levels of alkali, chloride and silica in the ash, which are problematic for the operation of combustion processes [22,76]. The straw pellets were crushed to obtain a size fraction in the range of 0.7–3.5 mm.

Table 4. Analysis of the fuel used in the 10-kW_{th} pilot-scale chemical-looping reactor. Values are given for the as-received fuel. LHV stands for Lower Heating Value.

Component	*Unit(s)*	*Black pellets (BP)*	*Pine forest residue (PFR)*	*Straw*
Moisture	%	5.7	9.2	8.8
Ash	%	0.3	1.8	7.9
Volatiles	%	74.2	80.0	67.5
Fixed Carbon	%	19.8	9.0	15.8
C	%	49.6	46.9	42.0
H	%	6.5	5.7	6.1
N	%	<0.1	0.35	0.7
O	%	43.6	36.0	43.0
Si	mg/kg dry fuel	<530	-	19000
Ca	mg/kg dry fuel	820	-	7700
K	mg/kg dry fuel	460	2080	11000
Na	mg/kg dry fuel	<53	27	260
LHV	MJ/kg	18.7	18.0	15.1

2.3 Experimental units

For this thesis, experiments were performed to evaluate the performance of LD slag as an oxygen carrier at different process scales. The laboratory scale batch fluidized bed reactor was the main item of equipment for these experiments. Experiments at pilot scale and semi-industrial scale were used to evaluate the specific abilities of LD slag and to assess the batch reactor results. In the following subsections, the different experimental units are presented in order of size, starting with the smallest.

2.3.1 *Horizontal tubular furnace*

For the stationary interaction experiments between oxygen carriers and ash elements, a horizontal tubular furnace system was used. A schematic overview of the system is presented in Figure 5. Here, mixtures of oxygen carriers and either of four potassium salts (K_2CO_3, KCl, K_2SO_4 and KH_2PO_4), totaling 2–5 g, were placed in an alumina crucible in the middle of a horizontal tubular furnace. The furnace was heated to 900°C to investigate the oxygen carrier-alkali interactions under reducing conditions in presence of steam. The potassium salt was crushed in a mortar and pestle before being mixed with the oxygen carrier, so that the salt would distribute evenly around the oxygen carrier particles. The amount of salt was determined so that the final mixing contained 4 wt.% potassium, which is the same amount of potassium that was observed in an ilmenite sample after 3 weeks of operation in the 12-MW_{th} CFB boiler [62]. Details regarding the execution of the experiments can be seen in **Paper VI**.

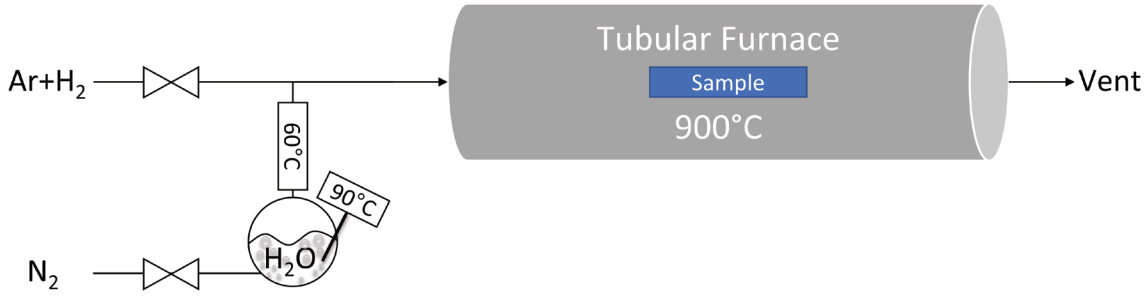

Figure 5. Schematic overview of the horizontal tub furnace setup.

The advantage of this system is that it is simple to operate and requires only small samples. It represents the worst-case scenario for the bed material and ash interactions, as since there is constant contact with the particles.

2.3.2 *Laboratory scale batch fluidized bed reactor*

The main equipment that was used to determine the reactivity of the different oxygen carriers was a small-scale batch fluidized bed reactor. The reactor in this system comprises a quartz tube with an inner diameter of 22 mm, which is equipped with a porous plate where the bed material is located (Figure 6). For the experiments presented in this thesis, samples weighing 15–40 g were used in this reactor system.

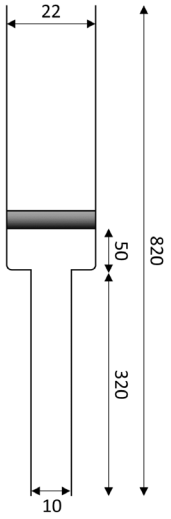

Figure 6. Design of the quartz glass reactor with a porous plate where the bed material is mounted for exposures. The flow direction for a fluidized bed is from the bottom up. Distances are given in mm.

The layout of the system where the reactor is located inside a vertical furnace is depicted in Figure 7. The system is divided into three different parts: Gas preparation, Furnace, and Flue gas analysis. In the Gas preparation section (to the left side in Figure 7), gas mixtures are prepared using different gases that contain synthetic air, CO/H_2 mixture (syngas), CO, CH_4, N_2, SO_2 in N_2 etc. All the incoming gaseous flows are measured using mass flow controllers. Liquid fuels with relatively low boiling points, such as benzene, can be introduced into the system by saturating a carrying stream of nitrogen. Details of the system can be found elsewhere [95].

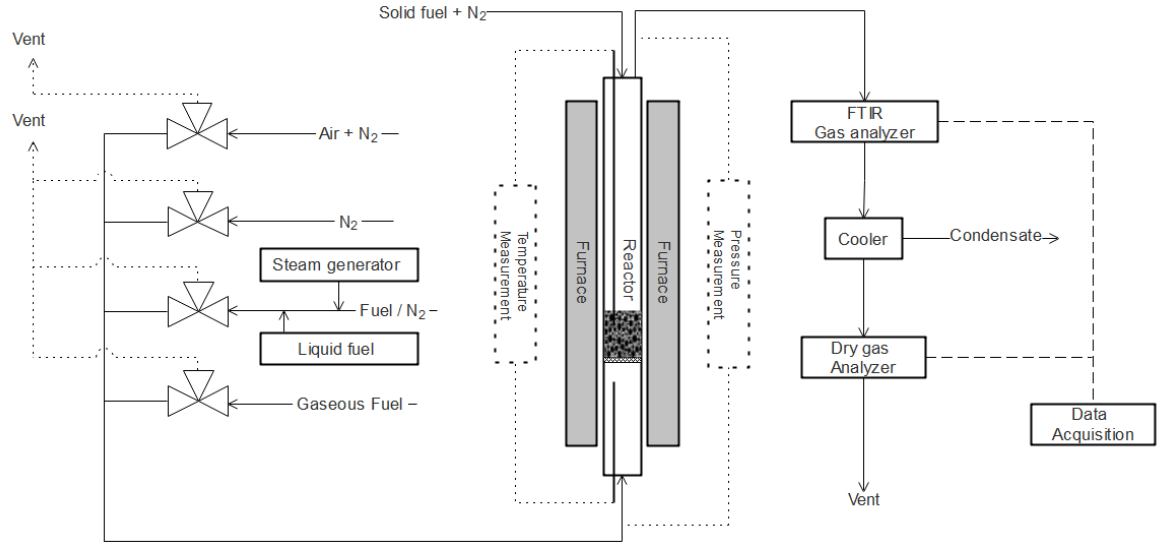

Figure 7. Schematic of the layout of the setup for the laboratory batch fluidized bed reactor.

The prepared gas mixture selected by the magnetic valves is inserted into the bottom of the quartz reactor mounted inside the furnace. This is the second part of the reactor system (middle part of Figure 7). The magnetic valves are sequenced so as to expose the bed material to the desired conditions. The quartz reactor is equipped with two K-type thermocouples protected by a quartz glass mantle.

The fluidization of the bed in the reactor is monitored using a pressure sensor that measures the pressure difference between the top and bottom of the reactor. The pressure sensor is a Honeywell pressure transducer that measures pressure at a frequency of 20 Hz.

Solid fuel can be introduced at the top of the reactor using a set of sealing valves. Solid fuel is inserted together with a span gas of N_2, to push the particles into the reactor. The size of the solid fuel is dependent upon the density but is normally larger than the denser bed material to avoid char blow-out due to reaching the terminal velocity of the solid fuel. For these experiments, 40 g of bed material were used and 0.2 g, 0.4 g or 0.6 g of solid char was added as fuel. These amounts of char correspond to theoretical bed reductions of roughly 1 wt.%, 2 wt.% and 3 wt.%, with the assumption that all the char is converted to CO_2. The bed was fluidized with a mixture of nitrogen and steam.

The third part of the reactor system is the flue gas analysis (on the right side in Figure 7). Initially, the uncondensed flue gases are assayed continuously using the Thermo-Scientific IS50 Fourier Transform Infrared (FTIR) spectrometer to measure CO, CO_2, CH_4, H_2O and C_6H_6. FTIR was mainly used for evaluation of the experiments that used benzene.

Downstream of the FTIR, the gases are condensed to remove water vapor and introduced into a dry gas analyzer. The dry gas analyzer used was a Rosemount NGA 2000 equipped with IR/UV sensors for CO, CO_2 and CH_4, as well as a thermal conductivity sensor for H_2 and a paramagnetic gas sensor for O_2. For experiments with sulfur, a different Rosemount analyzer was used in which the sensor for H_2 was exchanged for an IR/UV sensor to detect SO_2. After the analysis, the gases are vented or for shorter periods of time bagged into gas-tight Al-bags. Bagging of the flue gases was used for the sulfur analyses where H_2S and SO_2 were measured using Dräger tubes. More information about the features of this reactor system can be found elsewhere [95].

There are many different procedures that can be utilized in the laboratory fluidized bed reactor, more than are described in this thesis. For more alternative procedures, the reader is directed elsewhere [95]. In Section 2.4, the methods, calculations and assumptions related to the gaseous and solid fuels are explained further.

2.3.3 The 10-kW_{th} chemical looping reactor

Chalmers's 10-kW_{th} chemical looping unit for solid fuel was inspired by the previous successfully used reactor system for gaseous fuel. However, the fuel reactor was redesigned for solid fuels and mounted in an electrically heated furnace to maintain the operational temperature [101]. In Year 2019, the fuel reactor was redesigned to operate more effectively with biofuels that contained a large fraction of volatiles. A volatile distributor was inserted into the bed to ensure better conversion of the volatile fuel. A schematic overview of the process is shown in Figure 8, where the volatile distributor is indicated as two dashed lines in the fuel reactor. In comparison to the previous version of the reactor that lacked a volatile distributor, this unit showed a higher level of gas conversion, indicating more-effective contacts between the oxygen carriers and volatiles. A typical bed inventory of the system entails 20–30 kg of bed material [102].

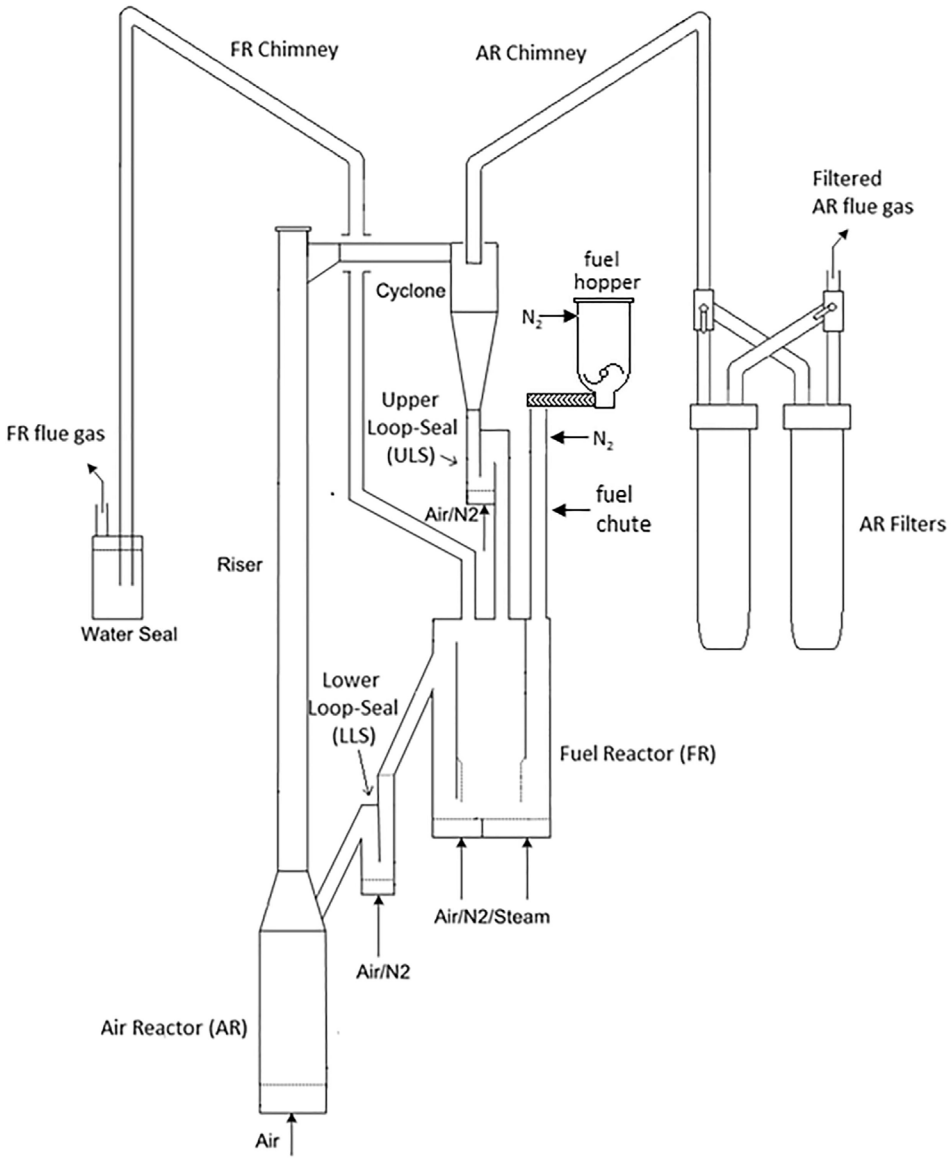

Figure 8. Schematic of the layout of the 10-kW solid fuel chemical looping reactor system equipped with a volatile distributor in the fuel reactor [102].

The focus of this thesis is related to tars generated from CLG experiments in the 10-kW unit. Besides LD slag, ilmenite and sand were used as bed materials for reference. Three different solid fuels were used, more about these fuels in Table 4 in section 2.2.

For the tar samples, flue gases were extracted from the fuel reactor chimney just above the furnace using a Venturi pump system inserted into a heated line. From this heated line, a 100-ml gas sample was extracted while passing through a hot filter to remove particles, using a pneumatic pump system. The pneumatic pump was connected to the system by a syringe through a septum. Tars from the gas sample were collected in a Solid Phase Adsorption (SPA) column. See Figure 9 for an overview of the tar sampling system. The SPA column was the Superclean^{TM} Envi-Carb^{TM}/LC-NH_2 in 3-ml tubes delivered by Supelco. The tar-measuring method using these types of SPA columns has been evaluated [103] and used in previous studies [30,96]. For every operational setting of the system, two tar samples were collected after the extraction system was pre-heated and filled with flue gas.

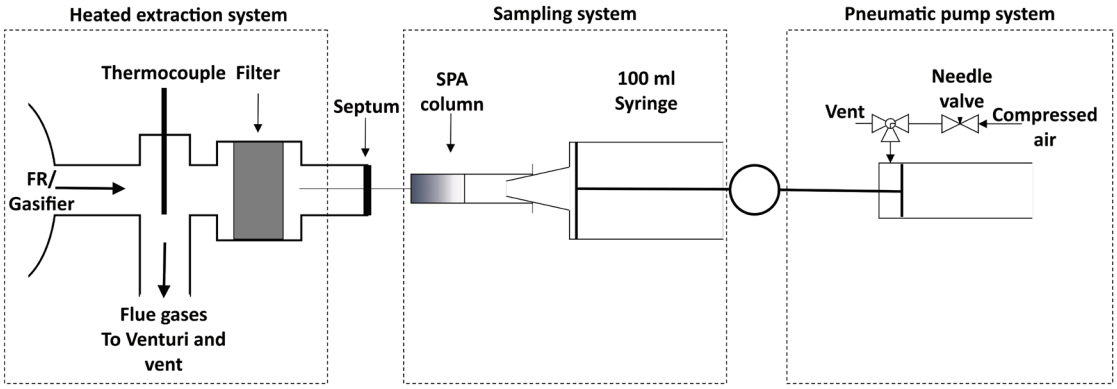

Figure 9. Illustration of the overall tar sampling system. Left panel: Heated extraction system where the flue gas is extracted from the fuel reactor (FR). Middle panel: The sampling system in which a needle pierces a septum to extract 100 ml of filtered hot flue gas and in which the tars are absorbed onto the SPA column. Right panel: The pneumatic pump system is used to control the syringe, so as to extract at the same suction rate for every sample.

The tar sample captured in the SPA column was directly cooled to prevent the evaporation of volatile tar species. At 1–2 days after the experiments, the samples were eluted using a standardized elution solution. The samples were analyzed with gas chromatography (GC) using the Bruker GC430 GC equipped with a 30-m mid-polar column and connected to an flame ionization detector (FID), using hydrogen as the carrier gas. The results of the GC analysis were then related to the dry gas composition of the fuel reactor. Further details regarding the sampling, elution, calculations and assumptions can be found in **Paper IV**.

2.3.4 Chalmers 12-MW_{th} CFB boiler

LD slag was used as the bed material in the 12-MW_{th} CFB boiler at Chalmers University of Technology [50]. For this, 28 metric tonnes of LD slag with particle size of 150–400 µm were received from SSAB Merox AB, Sweden. The boiler was originally designed to use of coal at a maximum load of 12 MW_{th}. However, with the usage of biomass, the maximum load is reduced to roughly 8 MW_{th}, although the boiler is normally operated at 5–6 MW_{th}. The boiler is used to produce hot water for district heating during the cold season.

The boiler is equipped with an integrated gasifier in the form of a secondary bubbling fluidized bed. This gasifier can be included or excluded from operation by activation or deactivation of the two fluidized loop seals. Bed materials can be extracted from several positions during operation. Bed materials were extracted from the bottom of the boiler and fly ash samples were acquired from the secondary cyclone and the textile filter (Figure 10).

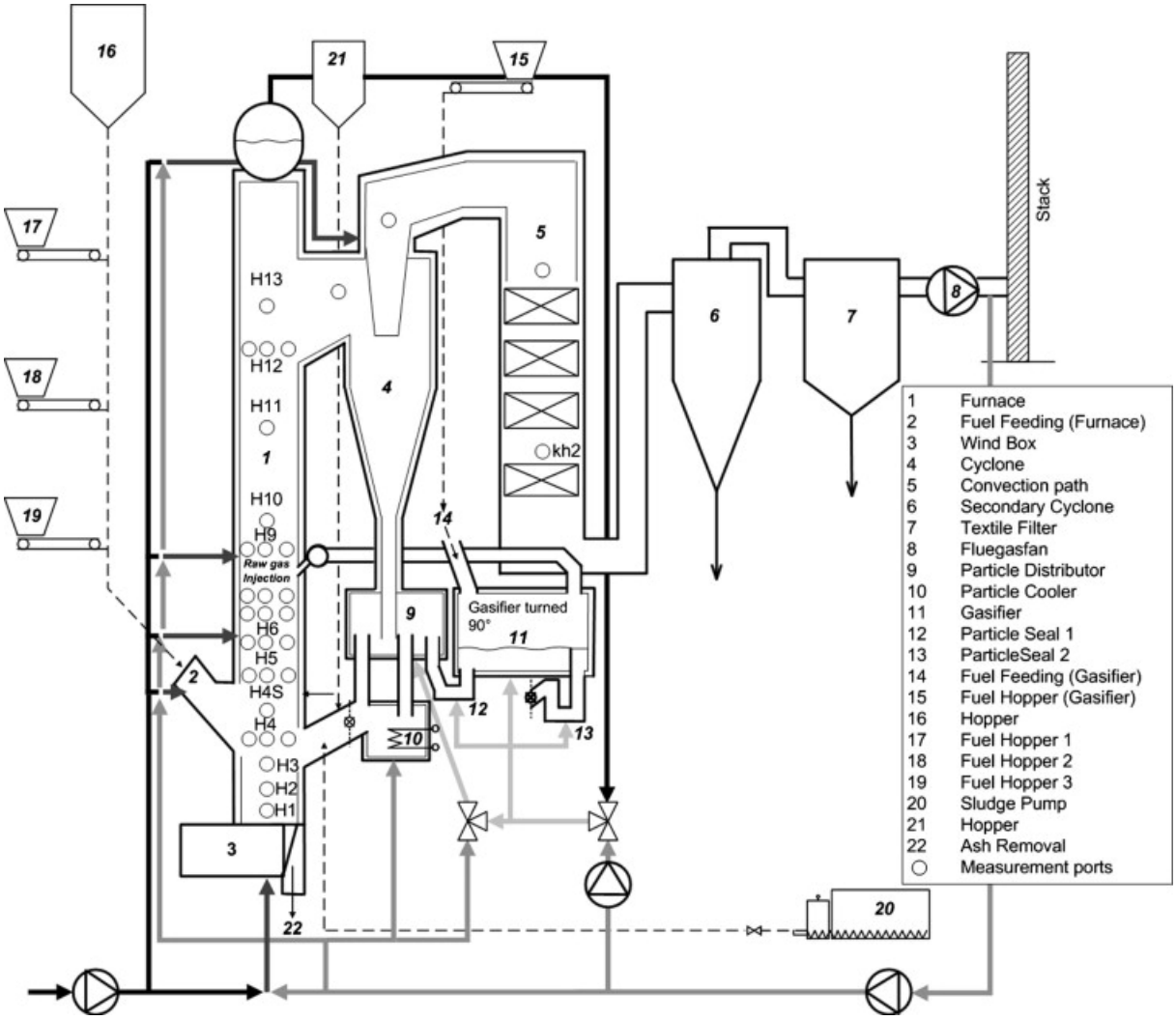

Figure 10. Schematic of the process layout of the Chalmers 12-MW_{th} CFB boiler equipped with a 2–4-MW_{th} gasifier. Bed material can be extracted from various points in the boiler. The bed material used in the experiments of this thesis were extracted from a port located between H2 and H3 [8].

During the tests with LD slag as the bed material in the boiler, the boiler was operated for 1 week under OCAC conditions without any use of the gasifier. During this week, the boiler was operated using only LD slag as bed inventory, with no regeneration of the bed and a total bed inventory of about 2,000 kg. Some additional LD slag was added during boiler operation due to a pressure loss caused by partial loss of bed material mass. The boiler was operated at around 860 °C using woodchips as fuel. Fuel feed to the boiler was 1600-1700 kg/h with a primary air flow set at 1.4-1.5 kg/s. Two samples of roughly 1 kg each of bed material were extracted twice a day.

2.4 Experimental procedures and evaluation

The main unit used for investigating the properties of LD slag was the laboratory batch fluidized bed reactor as described in section 2.3.2. In this section, the methods, assumptions and calculations are explained for the two main experiments.

2.4.1 Evaluation of gaseous fuels

Thanks to the flexibility of the laboratory batch fluidized bed reactor, many different fuel and conditions could be investigated. In the setup, samples are normally exposed to gases in a "cycle" comprised of several sequences using different gases. One such cycle involves *Inert-Reducing-Inert-Oxidation* periods, performed on initially oxidized particles. Oxidation is normally performed until consumption of oxygen is no longer observed, i.e., the outlet O_2 concentration is the same as the inlet O_2 concentration, after which the particles are considered to be "fully oxidized". For some experiments, the oxygen carrier was pre-reduced to reach a lower oxidation state before the conversion of fuel was measured. In these cases, the cycle was designated as: *Inert-"Pre-Reduction"-Inert-Reducing-Inert-Oxidation*. The gas volumetric flows, compositions and exposure times are displayed in Table 5.

Table 5. Gas mixtures introduced into the laboratory fluidized bed reactor when using gaseous fuel in the different papers.

Phase	*Gas mixture*	*Gas flow [ml_N/min]*	*Temperature [°C]*	*Time [s]*	
Oxidizing	5% O_2, 95% N_2	1000	800-950	300-1200	***All papers***
Inert	100% N_2	1000	800-950	180	
Reducing – Activation	50% CO, 50% H_2	900	850	20	
Reducing – Syngas	50% Steam, 45% 50/50 CO/H_2, 5% N_2	1000	800-950	20	***Papers I & V***
Reducing – CH_4	50% Steam, 35% CH_4, 15% N_2	1000	800-950	20	
Reducing – C_6H_6	50% Steam, 50% N_2 containing 1.4% C_6H_6, 20% N_2	1000	800-950	20-60	
Reducing – Syngas Dry	100% 50/50 CO/H_2	900	670-970	20	***Papers II & IV***
Reducing – CO Dry	50% CO, 50% N_2	900	670-970	5-20	
Reducing – SO_2	25% CO, 25% H_2, 1% SO_2, balance is N_2	1000	870	20	***Paper III***
Reducing – SO_2 and C_6H_6	50% Steam, 1.46% C_6H_6, 0.4% SO_2, N_2 balance	1000	850	60	
Oxidizing – SO_2	5% O_2, 1.5% SO_2. balance is N_2	1000	870	90 min	

Prior to all the experiments, the bed material was "activated". This was carried out by altering the oxidizing conditions (first row in Table 5) and reducing conditions (third row in Table 5) until stable conversion of the syngas was obtained. It is normal in these types of experiments that the oxygen carrier shows greater deviations in reactivity during the initial cycles, and this is a way to stabilize the behavior. Usually, 7–20 cycles were used to activate the samples.

The resulting data were logged every second, and an example of a concentration profile acquired over time can be seen in Figure 11.

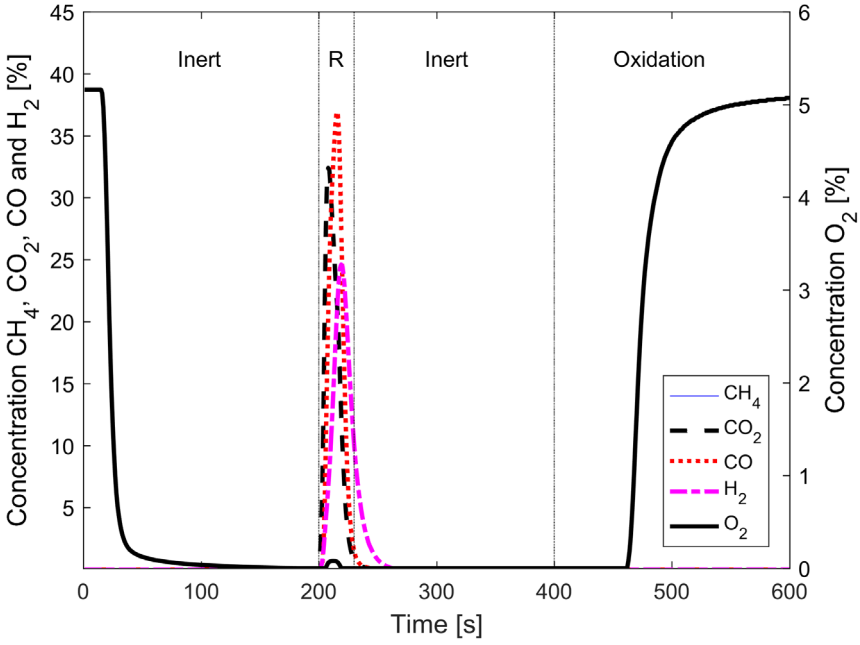

Figure 11. One entire cycle displaying the dry gas analysis for calcined LD slag exposed to syngas (50% CO in H_2). "R" stands for reduction.

The gas yield for gaseous exposures was calculated over the entire cycle for all the gas species, and the yield was calculated accordingly to Equation (E1).

$$\gamma_{Fuel} = \int_{t_{red}=0}^{t_{red}=end} \frac{x_{Fuel,in} * \dot{n}_{in} - x_{Fuel,out} * \dot{n}_{out}}{x_{Fuel,in} * \dot{n}_{in}} dt * 100\% \quad \text{(E1)}$$

Besides the total conversion over a cycle, the interim CO conversion (γ_{CO}) was calculated for gaseous exposures that did not involve steam, accordingly to Equation (E2).

$$\gamma_{CO,i} = \frac{x_{CO_2,i}}{x_{CO_2,i} + x_{CO,i}} \quad \text{(E2)}$$

There are a few different ways to calculate the degree of oxidation of the oxygen carrier. The level of transferred oxygen can be calculated from the outgoing levels of CO_2 and H_2. The degree of oxidation of the oxygen carrier (ω) can thereby be calculated from Equations (E3) and (E4) for a syngas [48]:

$$\omega = \frac{m}{m_{ox}} \quad \text{(E3)}$$

$$\omega_i = \omega_0 - \int_{t_0}^{t_i} \frac{\dot{n}_{out} M_O}{m_{ox}} (2x_{CO_2} + x_{CO} - x_{H_2}) \quad \text{(E4)}$$

Limitations associated with this approach using Equations (E3) and (E4) are that the equations cannot be used for fuel mixtures that containing a lot of oxygen or when steam is used. This is because the mass balance do not include the oxygen from the steam, which can oxidize the oxygen carrier or react directly with the gases. In addition, the steam measurement is limited by the measurement frequency of the FTIR. This instrument requires rather long measurement intervals during which stable steam production must be maintained. Since the cycles may be short in duration, it is difficult to obtain a trustworthy result from the FTIR. Therefore, other calculation techniques were utilized.

By comparing the O_2 concentrations at the outlet during the oxidation of the oxygen carrier to an inert reference material, the difference in O_2 signals can be calculated. This difference reflects the amount of oxygen absorbed by the oxygen carrier and corresponds to the amount of oxygen transferred to the fuel during the entire cycle. This amount of oxygen is referred to as ω_{uptake} and is calculated accordingly to Equation (E5):

$$\omega_{uptake} = \int_{t_{ox}=0}^{t_{ox}=end} \left(x_{O_2,ref} - x_{O_2,sample}\right) * \dot{n}_{out} \quad \text{(E5)}$$

Equation (E5) can also be used for solid fuel experiment and will, after considering the amount of oxygen required to combust the remaining char in the reactor, be equivalent to the amount of oxygen transferred from the oxygen carrier to the fuel. The limitation of this equation is that the oxygen level can only be measured and calculated at the end of the cycle and not as a function of time during the reduction sequence, as is the case for Equations (E3) and (E4).

An example of an experiment layout with pre-reduction is presented in Figure 12. Here, LD slag was evaluated when it was reduced to wüstite ($Fe_{1-x}A_xO$). These tests were performed to gauge whether LD slag could be oxidized with steam to produce H_2 via the water-splitting reaction (Reaction R8 in Section 3.1). Further details of the execution of this experiment are listed in **Paper II**. The experimental layout and raw data plot for these experiments are shown in Figure 12.

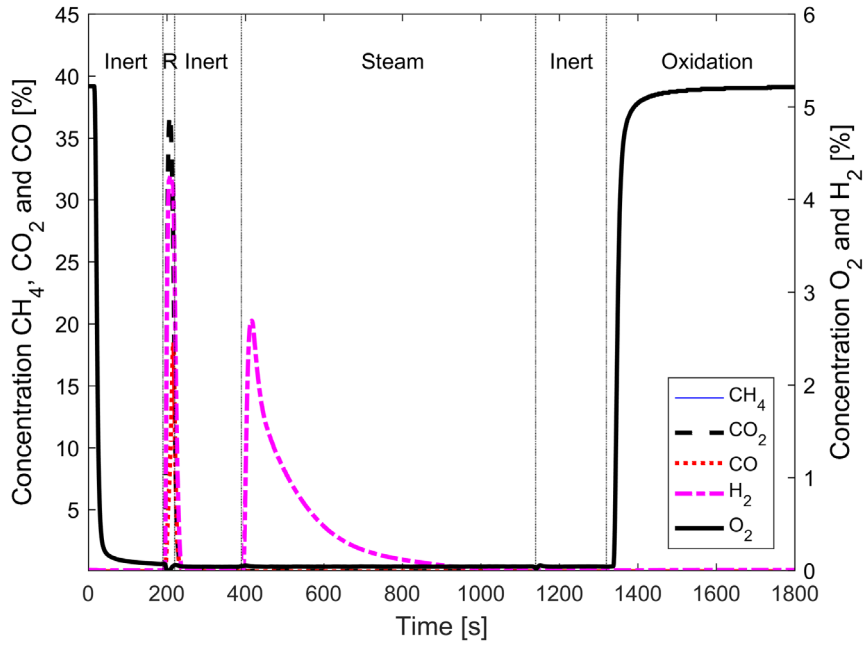

Figure 12. One cycle of a water splitting experiment using LD slag at 850°C. The formation of H_2 is clearly observed when the sample is oxidized using steam. "R" stands for reduction.

2.4.2 Evaluation of solid fuels

Solid fuel gasification experiments were performed to evaluate the effects on gasification of a fuel in presence of an oxygen carrier or additive. Here, the fuel used was devolatilized wood pellets. The production of these pellets is described in **Paper II**.

The oxidizing and inert flows were the same as for the gas experiments (see Table 5), and the same general experimental layout with oxidizing-inert-reducing-inert cycles back to oxidizing was used. Figure 13 displays a cycle of solid fuel gasification.

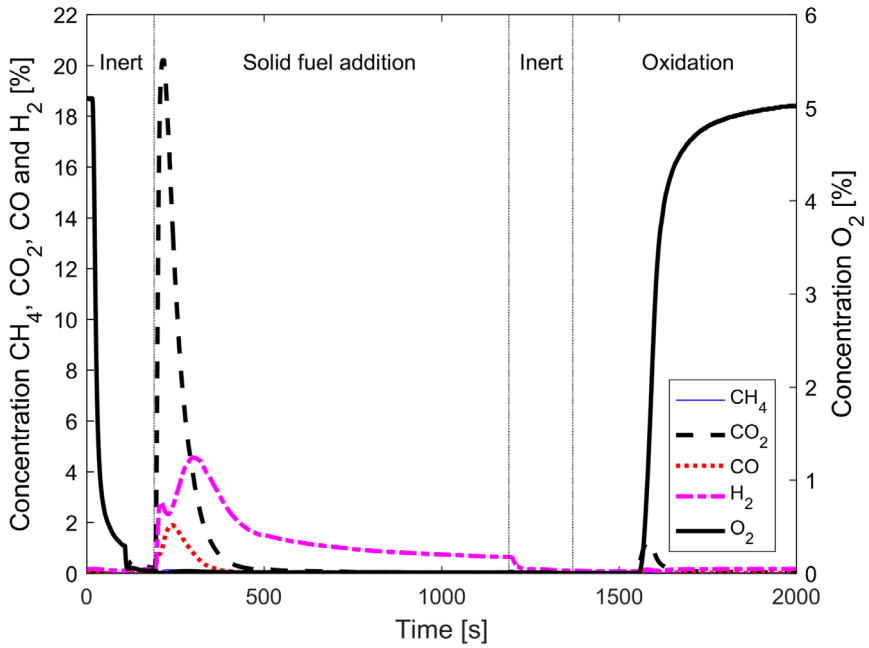

Figure 13. One cycle of char gasification at 970°C using LD slag as the bed material in the laboratory scale batch fluidized bed reactor system

The outgoing amount of gas from these experiments can be calculated according to Equation (E6).

$$n_{i,tot} = \int_{t_1}^{t_2} x_{i,out}(t) * \dot{n}_{out}(t)dt \quad \text{(E6)}$$

In Equation (E6), the total molar flow is calculated from the known volumetric flow of N_2 according to Equation (E7) [29].

$$\dot{n}_{out} = \frac{P}{RT} * \frac{\dot{V}_{N_2,in}}{1 - (x_{CO_2} + x_{CO} + x_{H_2} + x_{CH_4})} \quad \text{(E7)}$$

Char conversion was calculated as the fraction of gasified carbon, X_c. $X_c(t)$ as defined in Equation (E8) where the mass of carbon, $m_c(t)$, at time t is defined as the integral from t_{red}=0 to t_{red}=t according to Equation (E9). The total amount of carbon was calculated from t_{red}=0 to t_{red}=$t_{red,end}$.

$$X_c(t) = \frac{m_c(t)}{m_{c,tot}} \quad \text{(E8)}$$

$$m_c(t) = M_c \int_{t_1}^{t_2} \dot{n}_{out}(t) \left(x_{CO}(t) + x_{CO_2}(t) + x_{CH_4}(t) \right) dt \quad \text{(E9)}$$

The gasification rate (r_w) was defined and calculated using Equation (E10), as a time derivate of fuel conversion of char X_c. Using Equation (E11), the gasification rate was normalized to the amount of remaining carbon in the bed. Calculations of the gasification rate were performed for $0.3<X_c<0.7$. Here, the first and last 30% is not included to avoid impacts from the of remaining volatiles and the last part of gasification where the solid fuel in the bed is very small, something which was also done in earlier studies [104].

$$r_w = \frac{dX_c(t)}{dt} = \frac{\dot{m}_c(t)}{m_{c,tot}} \quad \text{(E10)}$$

$$r = \frac{r_w}{1 - X_c(t)} \quad \text{(E11)}$$

For the water-gas-shift reaction, Reaction R9 in Section 3.2, the equilibrium constant K_{eq} is defined as in Equation (E12) and the reaction quotient Q_i at time i as in Equation (E13). The temperature dependence of the equilibrium is empirically defined as Equation (E14) [105,106].

$$K_{eq} = \frac{x_{CO_2} * x_{H_2}}{x_{CO} * x_{H_2O}} \quad \text{(E12)}$$

$$Q_i = \frac{x_{CO_2,i} * x_{H_2,i}}{x_{CO,i} * x_{H_2O,i}} \quad \text{(E13)}$$

$$K_{eq} = \exp\left(-4.33 + \frac{4577.8}{T}\right) \quad \text{(E14)}$$

2.5 Material characterization

LD slag is a very complex material that contains many different elements and phases. Interactions with ash, potassium salts, sulfur and other bed materials increase the complexity further. Therefore, different measurement techniques are used, to understand both the bulk properties and the phase interactions.

2.5.1 SEM-EDS

SEM-EDS (Scanning Electron Microscopy – Energy-Dispersive x-ray Spectroscopy) was one of the main techniques used to determine the interactions between LD slag and the other investigated bed materials. SEM-EDS was performed with the FEI Quanta 200 FEG ESEM on either whole particles or cross-sections of the particles. Whole particles were mounted on carbon tape. The cross-sections of the particles were exposed by stabilizing the particles in epoxy and polishing until exposure of the cross-sectional surface. To avoid charging of the sample, the epoxy was coated with gold and conducted with copper tape to the sample holder in the SEM-EDS.

The program used for the analysis of the SEM-EDS data was the Aztec software. With this program, areas with similar elemental composition were combined into groups for further analysis. Carbon from the epoxy and oxygen was excluded from the formulation of these compositional groups. This was to simplify the analysis of the remaining components in the particles.

2.5.2 XRD

Powder X-Ray Diffraction (XRD) was used to identify the crystalline phases of the materials. It is important to note that only the crystalline phases are detected by XRD, and not the amorphous phases that are also present in LD slag. XRD was performed with the Brucker D8 ADVANCE/Brucker D8 DISCOVER equipped with a Cu Kα-radiation source. Step sizes of 0.05° for the Advance system and of 0.02° for the Discover system were used and the angle was 10°–90° for both machines.

Due to the complexity of the LD slag, the XRD diffractograms contained many interacting peaks and solid solutions in different phases, resulting in broadening of the peaks. For this reason, the phases identified in this thesis have been generalized, e.g., $Fe_{1-x}A_xO$ (wüstite) for phases that contained mainly Fe and having the same crystal structure as wüstite. This was regardless of whether "A" in the phase with best fit was, e.g., Mn or Mg with different ratios of "x" to Fe.

2.5.3 *Thermal gravimetric analysis (TGA)*

The TA Instruments thermogravimetric analyzer Q500 was used for the thermal gravimetric analysis (TGA). The analyzer was equipped with a gas mixing system similar to that used for the laboratory-scale, batch fluidized bed system, albeit without steam or liquid fuel. The properties investigated with TGA were: the carbonation/calcination temperatures at different partial pressures of CO_2; and the total amount CO_2 absorbed by carbonatization. Also investigated were the reactions related to the heating up of the outdoor-stored LD slag samples, as well as some oxygen-reduction cycles, to determine how much oxygen could be transported by the material (the so-called 'oxygen carrier potential'). However, a limitation of the TGA experiments is that the oxygen carrier potential was evaluated without steam, which limits the reduction potential of the reducing gas.

2.5.4 *Free calcium quantification*

To quantify the free calcium, i.e., CaO and $Ca(OH)_2$, in the LD slag, 1.0 g of LD slag was ground and leached in 100 ml of 10% sucrose sugar solution for 25 min under constant stirring. This time period was deemed sufficient to dissolve all the free calcium components in the water solution, so as to form $Ca(OH)_{2(aq)}$. Thereafter, the mixture was filtered and rinsed. The filtrate was titrated with 0.075 M H_2SO_4 using phenolphthalein as a pH indicator, until neutral pH was reached. The free calcium content was calculated from the acid consumption as CaO-equivalents in the sample [107].

2.5.5 *Elemental analysis*

Elemental analyses of the bed materials were performed externally by ALS using ICP-SFMS (Inductively Coupled Plasma – Sector Field Mass Spectrometry) according to ISO 17294-2:2016. The particles were melted together with $LiBO_2$ and then dissolved in HNO_3 before analysis with ICP-SFMS. The results provide the elemental compositions, which are normally given as the most thermodynamically favorable metal oxides at that temperature, i.e., at roughly 1,000°C. Loss On Ignition (LOI) was also derived as the weight loss during heating to 1,000°C in air. A high LOI value can be due to the presence of hydrates and carbonates, which are not stable at these high temperatures.

Besides ICP-SFMS, XRF (X-Ray Fluorescence) was used to analyze the elemental compositions of the bed material samples. For the samples analyzed by the provider, the sample was dissolved in $B_4Li_2O_7$ with continuous stirring and cast into a glass bead. This glass bead was analyzed by XRF to determine the elemental composition. In addition, XRF of powders has been performed using the Panalytical Axios XRF for elemental analysis. In these cases, the samples were both ground and analyzed as whole particles, to investigate the elements concentrated in the bulk, as compared to those on the surface of the particles [108].

Elemental analysis of fuels was performed using ICP-OES (Inductively Coupled Plasma – Optical Emission Spectroscopy). The standard used was ASTM D 3682 and the analysis was performed externally by RISE and Eurofins.

2.5.6 Bulk density

Bulk density was evaluated for the particles using the funnel method according to ISO 2923-1:2008. The test was repeated three times and the mean value was calculated. Oversized particles, such as rocks and char from the 12-MW_{th} boiler samples, were removed and not measured.

2.5.7 Size distribution

The size distribution of the particles was measured by sieving through 6–7 sieves spanning from 45 µm to 500 µm, which were stacked together during sieving. A sample of 20–30 g was analyzed, and an automatic vibrator was used for 20 min for the sieving process.

2.5.8 BET surface area

The specific surface area of the particles was evaluated using Brunauer-Emmett-Teller (BET) analysis. The Micromeritics TriStar 3000 surface area and porosity analyzer operated with liquid nitrogen was used for these analyses. Prior to the analysis, the samples were degassed under a flow of nitrogen, for 1 h at 90°C, followed by 4–16 h at 250°C.

2.5.9 Attrition

Mechanical strength was measured using a customized jet cup attrition rig (Figure 14). The rate of particle attrition was determined using a sample of 5 g in the size range of 125-180 µm. The cup at the bottom of the rig where the sample is placed has a conical inner diameter of 13/25 mm and a height of 39 mm. A nozzle with an inner diameter of 1.5 mm is placed from the side at the bottom of the cup. During operation, air is flushed into the nozzle, reaching a velocity of approximately 100 m/s. This creates a vortex that causes the particles to swirl upwards towards the settling chamber. In the settling chamber, the velocity is decreased to roughly 0.005 m/s, allowing the particles with higher terminal velocity to fall back into the cup. Particles that are small enough to exit the settling chamber, ideally particles <10 µm, are collected in a filter after the settling chamber. The filter is weighed every 10 min during the 1-hour test to determine the attrition rate of the particles and their overall attrition trends. Details of the analysis and regarding the determination of the attrition rate index and trends can be found elsewhere [109].

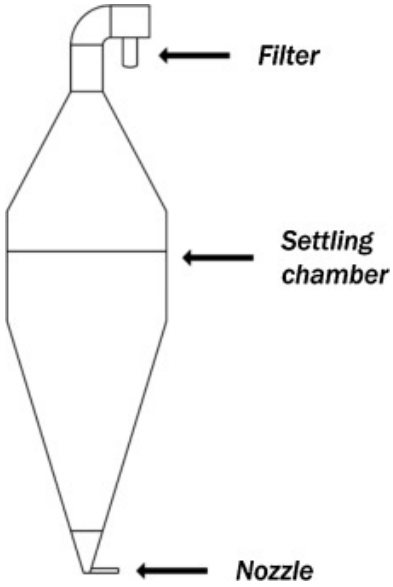

Figure 14. Schematic representation of the customized jet cup attrition rig [109].

The actual values from the jet cup attrition rig should not be regarded as an exact predictor of attrition in a large-scale unit, although Rydén et al. have shown clear correlations to the results obtained in pilot operations [109]. This is due to the accelerated attrition that is achieved using the high velocity in the jet cup, as well as to the fact that it is conducted at room temperature without any stresses to the particles as altering reducing and oxidizing conditions provides. However, the attrition rate index may indicate the attrition trend of bed material and the measured attrition rate index can be compared easily to other materials evaluated in the same rig. Another common method to estimate the attrition of an oxygen carrier is by measuring the crushing strength of single particles and calculate a mean value [24,109]. Since the number of tested particles in the attrition rig are much larger compared to crushing strength, where only a few single particles are evaluated, the attrition rig provides a more trustworthy value for the evaluation of attrition.

Chapter 3

3. Chemical properties of LD slag as an oxygen carrier

3.1 LD slag phases related to oxygen transport and activation

In **Paper I** the oxidized LD slag phases for the as-received, heat-treated and LD slag operated in the 12-MW_{th} boiler in OCAC mode were investigated, see Table 6. It was observed that the XRD diffractograms were very similar for the samples from different operational times in the boiler, and that the main difference associated with the heat treatment was the decomposition of $CaCO_3$ and $Ca(OH)_2$ when compared to the as received sample. It is noteworthy that the detection limit of XRD is a few wt.%, and the diffractograms contained a very high number of peaks, which meant that no phases containing ash could be identified with certainty.

Table 6. Identified phases using XRD and free calcium content in LD slag samples given as CaO quantified using leaching. "A" in identified phases indicates dopant metals such as Mg and Mn. "B" indicates elements such as Mg, Mn, Al and Si.

Sample	*Detected phases*	*Free CaO + $Ca(OH)_2$ [wt.%]*
LD slag as received "Fresh"	$Mg_{1-x}Fe_xO$, $Ca_2Fe_{2-x}B_xO_5$, $(CaO)_xSiO_2$, $Ca(OH)_2$, $CaCO_3$, CaO	6.2±0.3
LD slag heat treated "Ox 24 h"	$Mg_{1-x}Fe_xO$, $Ca_2Fe_{2-x}B_xO_5$, $(CaO)_xSiO_2$, CaO	4.0±0.1
LD slag used in the boiler "OCAC 65 h"	$Mg_{1-x}Fe_xO$, $Fe_{3-x}A_xO_4$, $Ca_2Fe_{2-x}B_xO_5$, $(CaO)_xSiO_2$, CaO	2.6±0.1

It should be noted in Table 6 that no magnetite phase ($Fe_{3-x}A_xO_4$) was detected in the fresh and heat-treated (Ox 24 h) LD slag sample. However, after being used in the laboratory fluidized bed reactor, the XRD diffractogram was more similar to the OCAC boiler samples in terms of having the magnetite phase. This indicates that magnetite appears as the oxidized form in LD slag after the particles have been activated by cyclic oxidation and reduction. Note here that the laboratory scale batch fluidized bed reactor tests were conducted with distinct reducing/oxidizing conditions, as in CLC, while OCAC has less distinct reducing and oxidizing areas in the boiler. Therefore, it is reasonable to assume that the LD slag will have similar oxidized/reduced phases in a chemical-looping application as in OCAC.

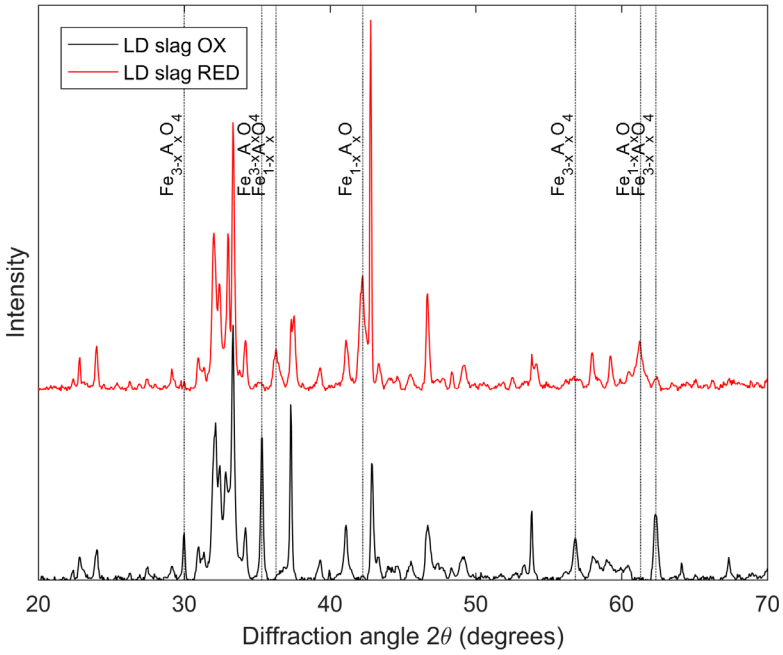

Figure 15. XRD diffractogram of oxidized LD slag and LD slag reduced using syngas and steam. The lines indicate phases that are pronounced in only one sample, but not the other. "A" in the given phases indicates dopants in the crystal structure, such as Mg and Mn.

It was found that the oxidized LD slag contained magnetite while the reduced LD slag contained a $Fe_{1-x}A_xO$ (wüstite-structure) phase, where "A" indicates dopants such as Mg. The reduced sample was reduced using a syngas and steam, according to Table 5. The results from the XRD analyses of the reduced and oxidized materials in Figure 15 clearly indicate that oxygen transport is dominated by the magnetite-wüstite phase transition, as illustrated by R7 where an oxygen atom (O*) is available for reaction with a fuel. This is likely due to a kinetic limitation associated with oxidation to hematite, as magnetite is expected to oxidize to hematite according to thermodynamic calculations made with 5% oxygen in nitrogen at temperatures relevant for CLC. This unexpected behavior could be due to the inclusion of dopants. In the laboratory batch fluidized bed reactor and in the TGA tests, it was concluded that LD slag has an oxygen-carrying capacity of 1.0–1.2 wt.% [110]. The latter corresponds to the theoretical maximum oxygen transfer through R7 for a material that contains 17% iron, which is the iron content of this sample of LD slag.

However, since iron is also present in phases such as the srebrodolskite structure ($Ca_2Fe_{2-x}B_xO_5$), which are not identified as an oxygen-carrying phase, dopants and other unidentified phase changes might contribute to the oxygen transport.

$$Fe_{3-x}A_xO_4 \underset{Ox}{\overset{Red}{\rightleftarrows}} 3Fe_{1-x}A_xO + O^* \quad \{R7\}$$

For oxygen carriers that contain iron, R7 is not the common oxygen transport reaction. Normally, it is the hematite-magnetite reaction that provides oxygen to these systems at high levels of conversion and partial pressures of oxygen [43]. Since wüstite is formed during reduction, even in the presence of steam, a water-splitting reaction can occur, according to reaction R8. Here, steam is acting as an oxidant to form magnetite. Experimental evaluation of this phenomenon was conducted in **Paper II**, both during solid fuel experiments and in sequence using gaseous fuel. The results from the gaseous fuel experiments are shown in Figure 12 in section 2.4.1. During these experiments, it was concluded that LD slag could absorb additional oxygen after being oxidized with steam, indicating that phases other than magnetite-wüstite can transport oxygen. These phases could represent either a minor formation of hematite ($Fe_{2-x}A_xO_3$) or other minor phases not oxidized with steam. This strengthens the hypothesis that the formation of hematite is kinetically hindered.

$$3Fe_{1-x}A_xO + H_2O \rightarrow Fe_{3-x}A_xO_4 + H_2 \quad \{R8\}$$

3.2 Free calcium in LD slag

A significant amount of free calcium, i.e. CaO, $Ca(OH)_2$ and $CaCO_3$, is known to be present in LD slag, normally accounting for a few percent [69,107]. For this batch of LD slag, the free calcium content was measured using leaching, and was found to be 4 wt.% for the heat-treated sample (see **Paper I**). In the boiler, the free calcium content of the LD slag was reduced to stabilize at around 2.5 wt.% after 1 day of operation with minimal regeneration.

The free calcium in the LD slag affects the chemistry of the material in several different ways. At temperatures relevant for CLC, CaO is the stable phase of free lime. The presence of a significant amount of CaO can affect the ability to use LD slag as an oxygen carrier in any technical application, e.g. CLC, CLG or OCAC. CaO has effects on the gas-phase composition in chemical-looping applications and is reactive towards elements introduced with the fuel. The major features of CaO are:

- CaO is catalytic towards the water-gas shift (WGS) reaction, R9 [111,112], as discussed in **Paper II** and in Sections 4.1 and 4.3.1.
- CaO is catalytic towards tars, as discussed in **Paper IV** and in Section 4.2.2.
- CaO is reactive, forming stable phases with ash elements such as phosphorus (see **Paper VI** and Section 3.3), as well as with other metals, such as Cu and Mn (see **Paper V** and Section 4.5). CaO can also react with sulfur that are discussed in **Paper III** and Section 3.5.
- If high partial pressure of CO_2 are obtained, $CaCO_3$ can be formed according to the equilibrium reaction, R10. When transported to the air reactor $CaCO_3$ can decompose, leading to a lower carbon capture efficiency. This is discussed further in **Paper I** and can be dismissed as a phenomenon in CLC and CLG applications.
- CaO reacts at ambient temperatures with water to form $Ca(OH)_2$ according to R11. $Ca(OH)_2$ is leachable, which affects the storage of the material. This is discussed further in **Paper VII** and Section 5.2.

$$CO + H_2O \leftrightarrow CO_2 + H_2 \quad \{R9\}$$

$$CaO + CO_2 \leftrightarrow CaCO_3 \quad \{R10\}$$

$$CaO + H_2O \rightarrow Ca(OH)_2 \quad \{R11\}$$

The effects of the CaO present in LD slag are indeed many and are mediated in many different ways. CaO can react under different conditions and is catalytic towards the WGS reaction and tars. In the beginning of these studies, there was a concern that carbon could be transported from the fuel reactor to the air reactor through the formation of $CaCO_3$ in the fuel reactor, which would decompose to CaO and CO_2 in the air reactor. This carbonation reaction, described by R10, is an equilibrium reaction that is affected both by CO_2 partial pressure and temperature [113]. However, since the temperature in both CLC and CLG is most likely >800°C, the CO_2 concentration needs to be in the range of 50%-80% for the sample to remain as a carbonate. This could be the case with CLC if coal (containing almost entirely carbon) is used as fuel and fluidized with CO_2. However, since the temperature in CLC is estimated to be >900°C [59], especially in the case of CLC with

coal which can operate at higher temperature, carbonate formation is unlikely to take place under normal operating conditions. Still, it is clear that the mechanism is possible with this material, and this may be of interest for processes for which a high H_2/CO ratio is desired, as the carbonation could promote the WGS reaction, R9.

Besides its chemistry at higher temperatures, CaO will also at ambient temperature absorb humidity and water to form $Ca(OH)_2$, according to R11. $Ca(OH)_2$ was also found in the as-received samples (Table 6). When inserting this material into a combustion process, the material will heat up. At higher temperatures, $Ca(OH)_2$ will decompose into CaO and steam, and the steam will leave the combustion zone, resulting in decreased bed mass. The amount of steam produced from $Ca(OH)_2$ corresponds to a maximum of 13 kg/t of fresh material, according to the free calcium content in the heat-treated sample. $CaCO_3$ present in the material will also calcine, contributing to the decreased bed mass upon insertion into a boiler.

3.3 Interactions with potassium and synthetic ash

The inorganic compounds in a fuel are the ash-forming matter remaining after thermal conversion of the fuel. The amount and chemical composition of the ash are very different for different fuels [22]. For biofuels, the ash depends both on the species and specific growth conditions at the location of the fuel. In a combustion process using biofuels, there are some common operational issues that originate from the ashes of the fuel, such as deposit formation, corrosion of superheaters, and bed agglomeration in fluidized bed boilers. Both corrosion and agglomeration have been associated with fuels that contain high levels of alkali. Alkali together with chloride has been identified as the most aggressive combination in terms of causing corrosion [22]. Furthermore, alkali and silica sand have been identified as forming potassium silicates with low melting temperatures, resulting in agglomeration of the fluidized bed [22,76].

To investigate how alkali species present in the biomass ash affect LD slag in large-scale boiler operations, synthetic ash components have been used. The alkali components used in this work that have been used also in previous studies [81,110,114,115] are: K_2CO_3, KCl, K_2SO_4 and KH_2PO_4. Störner and coworkers [110] have investigated how LD slag interacts with these ash species in a fixed bed, while Mattisson and colleagues [116] have studied how LD slag particles doped with K_2CO_3 interact when used in a batch fluidized bed reactor. Here, it was observed that only a minor amount of the alkali was bound into the LD slag, same observation as with the ash interactions in the 12-MW_{th} boiler presented in **Paper I**. This indicates that most of the potassium forms phases that evaporate in the humid atmosphere. The Ca from LD slag reacted with KH_2PO_4, preventing the formation of gas-impermeable KPO_3 observed in similar experiments with ilmenite [110,114]. Furthermore, it was observed that K_2CO_3 deactivated the LD slag.

Based on the different ash interaction mechanisms observed with both LD slag and ilmenite, a blend of the two materials could be used, as suggested in **Paper VI**. Here, it was concluded that alkali binds to the ilmenite rather than the LD slag in a mixture of the two materials. It was also observed that the Ca from LD slag moderated the agglomeration of ilmenite and KH_2PO_4, when present. In the present study, the effects of blending silica sand with either LD slag or ilmenite together with the ash components were also investigated. Experiments were performed in a horizontal tubular furnace at 850°C in a reducing atmosphere that contained steam; further information about the experimental setup is available in **Paper VI**.

It was observed that alkali preferentially bound into the structure of the silica sand rather than the ilmenite and into the structure of the ilmenite rather than the LD slag. This resulted in all the experiments that used sand showing agglomeration due to the melting of the formed potassium silicates (see Figure 16 for LD slag together with silica sand and K_2CO_3). From this observation, three aspects must be considered in future studies: i) if high levels of silica and potassium are present in the fuel, it may not matter if one has ilmenite to remove alkali, as the potassium could bind to the silica sand rather than to the ilmenite; ii) dilution of the oxygen carrier with silica sand in a full-scale fluidized bed may not be the best way to improve the resistance of the bed to alkali; and iii) experiments conducted in quartz tube reactors with alkali and any of the tested oxygen carriers may show that most of the alkali is interacting with the tube rather than with the oxygen carrier.

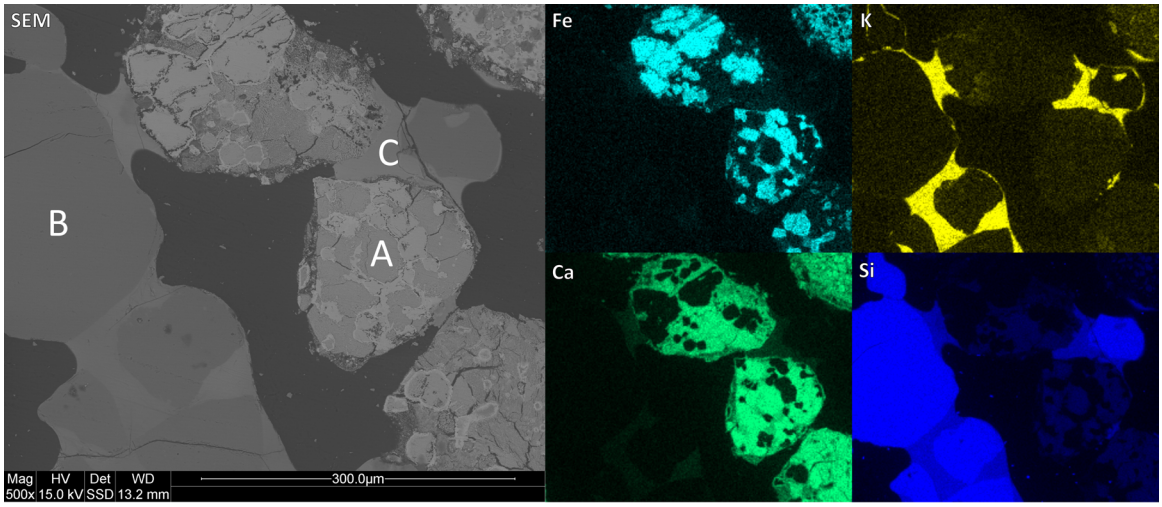

Figure 16. LD slag and silica sand exposed to 4wt.% K in the form of K_2CO_3. The experiments were performed in a horizontal tubular furnace under reducing conditions with H_2 and steam at 850°C for 3 hours. A: LD slag particle; B: Sand particle; C: Melt of potassium silicate.

That potassium exhibits only weak interactions with LD slag compared to silica sand was also observed in the experiments of **Paper I**. Here, samples of LD slag that were employed for only a few hours under OCAC conditions in the 12-MW_{th} Chalmers boiler were used in the laboratory-scale, batch fluidized reactor for conversion experiments. The samples were diluted with sand to allow a better comparison of the gas conversion between the samples. Once the blend of particles was heated to around 840°C, it defluidized due to the formation of potassium silicates (Figure 18). This outcome was the same as that observed in the horizontal fixed bed experiments with synthetic ash in **Paper VI**.

Combustion of fuels with high levels of phosphorus is known to experience issues with agglomeration [76,117]. It is known that Ca has positive effects in terms of reducing agglomeration for these types of fuels [22,117]. Ca available in the LD slag has an important effect on the K-P-Ca system as observed by Störner *et al.* decreasing the agglomeration severity and prevents deactivation [110]. Similar effects was also observed when LD slag was blended with other bed materials, such as with ilmenite as shown in Figure 17. This suggest that LD slag could be a suitable bed material for either OCAC or CLC for fuels with high levels of phosphorus.

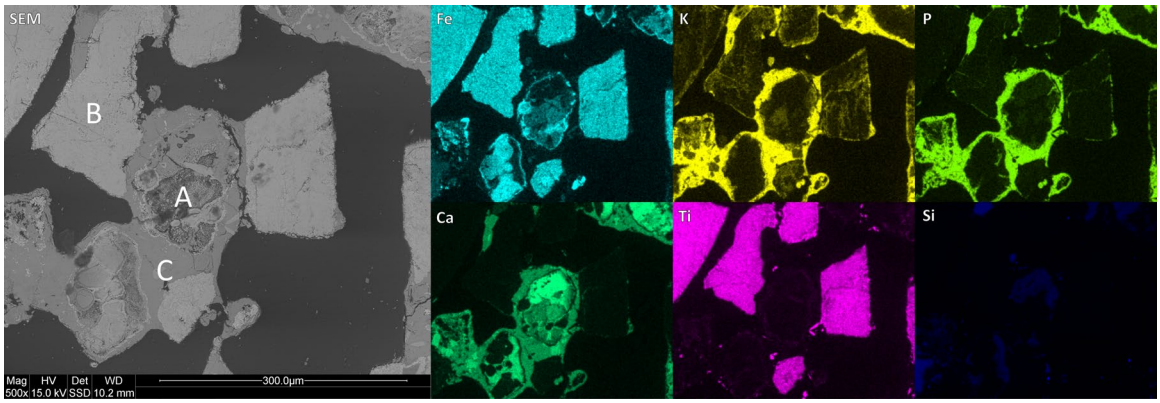

Figure 17. LD slag and ilmenite exposed to 4wt.% K in the form of KH_2PO_4. The experiments were performed in a horizontal tubular furnace under reducing conditions with H_2 and steam at 850°C for 3 hours. A: LD slag particle; B: Sand particle; C: Melt of Ca-K-P phase.

3.4 Interactions with ash in the Chalmers 12-MW_{th} CFB boiler

When LD slag was first investigated as an oxygen carrier for solid fuel conversion technologies, only small-scale reactor experiments were performed. Due to a combination of promising initial results, high availability, and low cost, it was decided to use LD slag as the bed material in the Chalmers 12-MW_{th} CFB boiler operated under OCAC conditions [50]. Bed samples were extracted during operation, and the elemental compositions of these samples were analyzed, with the results reported in **Paper I**.

The trends show that elements that are commonly found in wood ash, i.e., K, P and S, accumulate in the bed during operation. Elements that are commonly found in LD slag, i.e., Ca, Fe, Mg, Mn and V, were diluted with these ash elements. It was observed that the potassium content of the bed was only 1.6 wt.% after roughly 68 h of operation. This can be compared to a potassium content of closer to 4 wt.% in ilmenite bed samples after 72 h of operation, with similar fuels and also partial bed regeneration using ilmenite and sand [62]. Fly ash, especially the textile filter ash, contains a very high concentration of alkali. This indicates that the absorption of potassium by the LD slag is limited. Instead, alkali appears to a greater extent in the gas phase during boiler operation, and accumulates in the cooler downstream areas. The same observation was made for LD slag used in a 10-kW chemical-looping reactor operated under CLG conditions [118]. XRD analyses indicate that some of the alkali can react with the LD slag to form $KAlSiO_4$ [116]. Furthermore, in **Paper I**, areas that contained K, Si and Al were identified using SEM-EDS in the cross-sections of LD slag particles that underwent operation in the 12-MW_{th} CFB boiler.

The fact that LD slag does not have the same tendency to bind alkali as, for example, sand and ilmenite, implies different effects in different applications. For OCAC applications, a high vapor pressure of alkali will increase the CO emissions, as observed in the 12-MW CFB boiler experiments [50]. In chemical-looping applications such as CLC and CLG, this limited reaction between LD slag and alkali will result in most of the alkali being emitted from the fuel reactor. This has positive effects on both the char gasification rate and tar cracking, as observed in **Paper IV**.

A negative consequence of LD slag not binding to alkali is that it can react with, for example, sand that originates from the fuel or as dilution of the bed and create melts. As was the case with potassium salt, discussed in **Paper VI** and Section 3.3, when samples collected from the 12-MW CFB boiler were diluted with sand agglomeration occurred. This happened as soon as the temperature reached 840°C and for all the samples, even for the first sample that was collected after only 17 h of operation. In Figure 18, the interactions between sand particles and LD slag particles are clear, resulting in the formation of a melt between particles that contains K and Si, identified as potassium silicate, which has a low melting temperature [76]. Similarly, in the agglomeration tests performed externally, LD slag samples without sand did not agglomerate, while LD slag samples that contained 30% silica sand agglomerated [50].

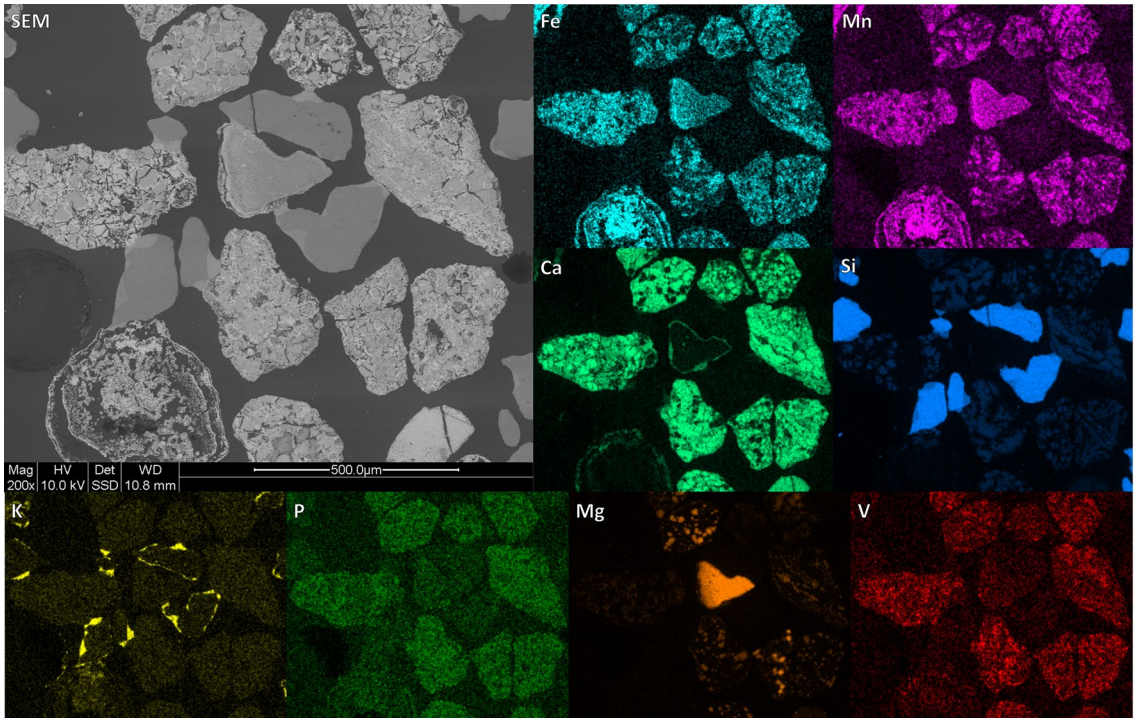

Figure 18. LD slag particles operated for 17 h under OCAC conditions in the 12-MW_{th} CFB boiler mixed with sand, showing agglomeration in the fluidized bed reactor after reaching ≈840°C. The "bridges" between the silica and LD slag particles contain mainly Si and K, in addition to O.

3.4.1 Ash layer formation

To understand in a quantitative way the difference between the ash layer and the bulk of the particles, XRF analysis was performed on whole particles compared to ground particles. This method was also used in another study of ilmenite particles [108]. XRF analysis was performed on OCAC samples collected after 65 h of operation in the 12-MW_{th} CFB boiler (see XRF results in Table 7). Comparing the elements associated with the surface and with the bulk, higher concentrations of S, K and P were detected on the surface. Lower concentrations of Si, Fe, Al and Ca were also observed on the surface, as compared to the bulk. From Figure 19, it could be expected that the difference between the surface and bulk for the concentration of V would be higher than that shown in Table 7. This discrepancy could be due to the fact that the surface layer is still very thin compared to the sampling depth of XRF.

Table 7. Comparison of the XRF results for whole particles (surface analysis) and ground particles (bulk analysis) that were operated under OCAC conditions in the 12-MW CFB boiler for 65 h. A heat-treated sample is presented as a reference for comparison.

Sample	Fe	Ca	Mg	Mn	Al	V	K	P	Si	S	Ti
LD slag heat treated	14.7	29.3	1.9	2.2	0.6	1.8	0.0	0.2	4.6	0.1	0.6
OCAC 65 h bulk	14.5	26.0	2.7	2.3	0.7	1.5	1.7	0.4	4.3	0.5	0.7
OCAC 65 h surface	12.0	23.0	2.7	2.2	0.3	1.6	2.0	0.7	1.8	1.1	0.4

To elucidate the surfaces of the LD slag particles in more detail, compositional phase analysis was performed on the cross-sections of bed particles following operation for 65 h in the 12-MW CFB boiler (Figure 19). On the surfaces of the particles, elements such as K, S and P were present, as was V. Since there are only very low amounts of vanadium in the fuel, this element must have migrated towards the surface from the slag. In the surface layer, there was also a relatively high level of Ca. The total amounts of K and S increased towards the outer surface. The molar ratio of K to S was roughly 2:1, suggesting the presence of K_2SO_4. Similar analysis of the same material after operation in the laboratory batch fluidized bed reactor did not show the same K:S ratio in an outer shell. Neither in the samples mixed with sand for syngas/benzene exposures nor in the samples without sand that have been exposed with methane. This suggests that sulfur has been re-emitted, most likely already during activation, where CO can react with sulfates and produce SO_2 [120].

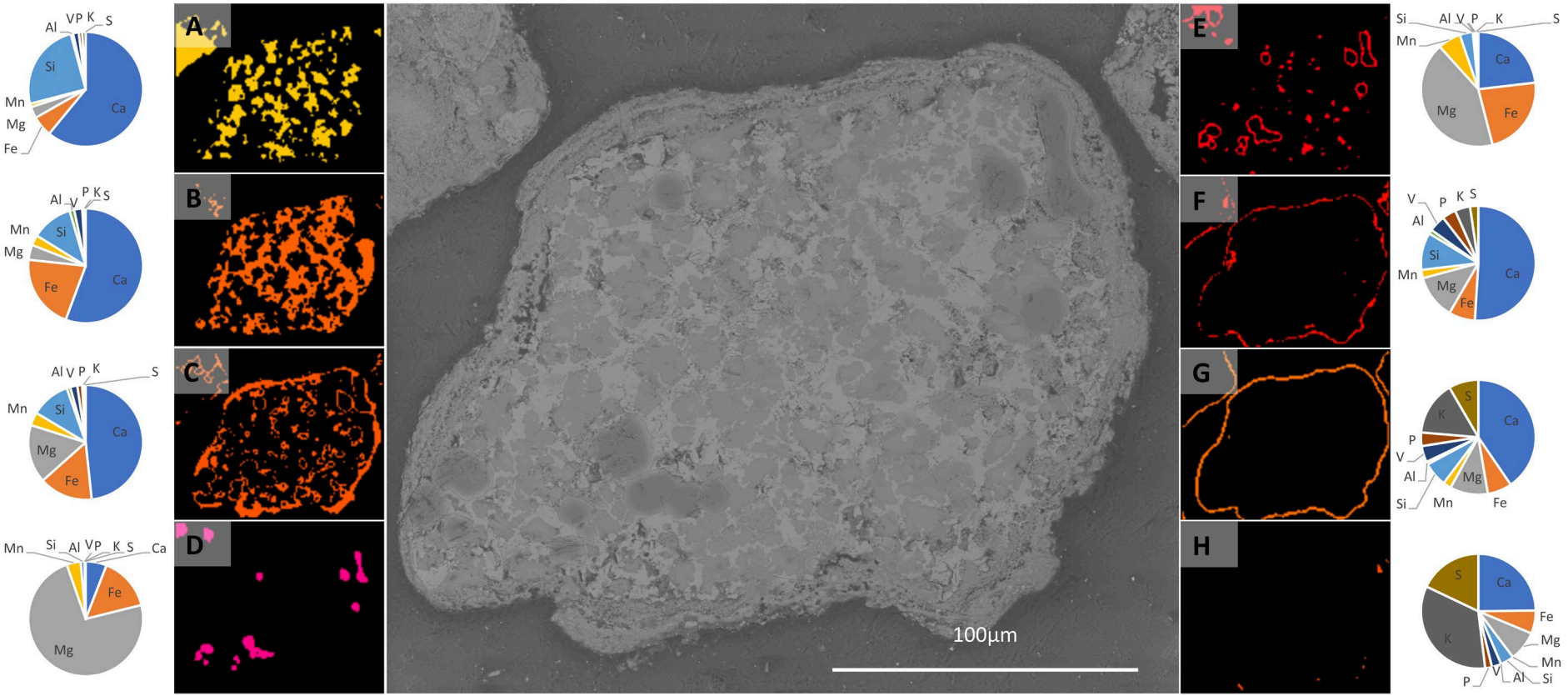

Figure 19. Compositional mapping using SEM-EDS data for a cross-section of an LD slag particle extracted from the 12-MW_{th} CFB boiler after 65 h of OCAC operation with wood chips. The detected groups are correlated to phases detected using XRD. The shares in the pie diagrams are based on mol%.

A) The group likely dominated by $(CaO)_xSiO_2$.

B) The group most likely dominated by $Ca_2Fe_{2-x}B_xO_5$. This latter group has been indicated to be the continuous phase with dispersed groups of "A" and "D".

C) The group similar to that in B but with more magnesium, maybe containing the $Fe_{3-x}A_xO_4$ phases that are associated with oxygen transport.

D) The group dominated by $Mg_{1-x}Fe_xO$.

E) Transition group between D and C, indicating concentration gradients in the material.

F–H) Groups present in the outer crust that contain elements related to ash, such as P, K and S, as well as migrated V.

F is the innermost group, followed by G and H, which contain more ash elements. It should be noted that the atomic ratio of K to S is 2:1, as in K_2SO_4.

3.5 Interaction with sulfur

LD slag has two abilities that are highly relevant for the sulfur chemistry in both OCAC and chemical-looping applications: i) LD slag contains high concentrations of calcium, which can form $CaSO_4$ in the presence of sulfur; and ii) there is no stable phase with alkali in LD slag, resulting in a high vapor pressure of K in the boiler, which in turn suggests an increased need for excess sulfur to prevent corrosion of the superheaters. Both of these aspects were observed for LD slag operation in the 12-MW boiler during OCAC operation. Elementary sulfur was added as a way to reduce the high emissions of CO that were believed to be associated with a high vapor pressure for the alkali. The addition of sulfur had some impact, although the effect was not long-lasting, suggesting that the sulfur was bound into the calcium structure of the LD slag [50]. When the bed material from **Paper I** was investigated it could be concluded that sulfur was bound into the structure of the particle. As shown in Figure 19, the sulfur was mostly associated with calcium and potassium on the surfaces of the particles.

To investigate further the sulfur interactions, batch experiments with both solid and gaseous fuels were carried out, the results of which are given in **Paper III**. Here, it was observed that high levels of sulfur could indeed be integrated into the structure of the LD slag, forming $CaSO_4$. Under reducing conditions, it will form both $CaSO_4$ and CaS. These can react and form SO_2 under inert conditions, eventually being released in the loop seals and in the air reactor. Even small amounts of sulfur affected the reactivity towards both CO and char. In **Paper III**, the effect of sulfur was observed to increase the overall reactivities of both LD slag and ilmenite, and also shown was how sulfur is affecting the oxygen carriers in different ways. Sulfur has been previously observed to increase the gasification rate of char due to improved oxygen transport to the char particle [20]. A summary of the interactions of LD slag, sulfur and solid char particles of fuel is provided in Figure 17.

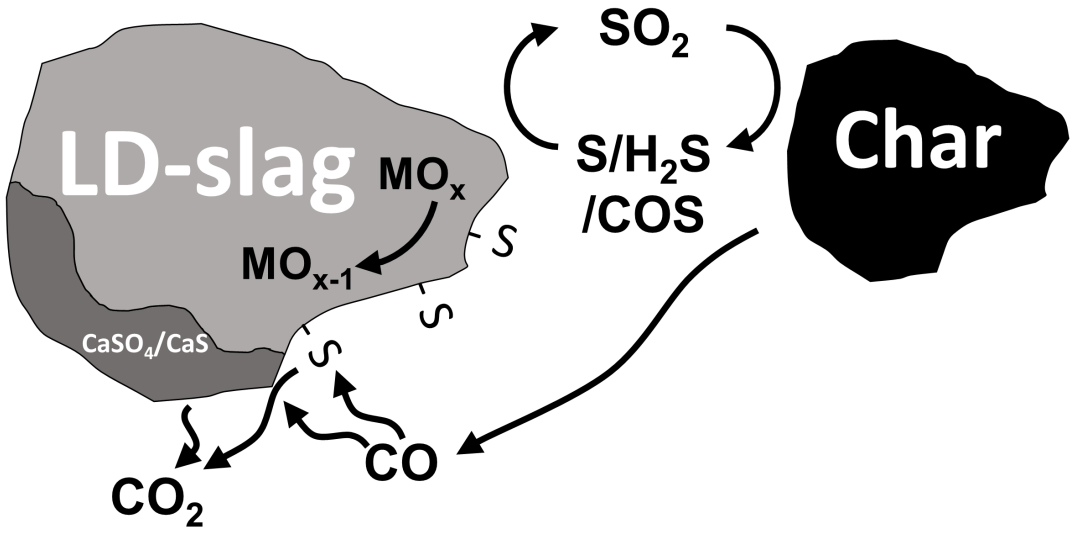

Figure 20. Graphical description of how sulfur interacts with LD slag. Three main reactions are described: i) the formation of $CaSO_4$ with oxygen-carrying potential; ii) surface-active sulfur increasing the reaction rate; and iii) gaseous sulfur acting as an intermediate increasing oxygen transport rate to char from the oxygen carrier.

It was also clear that sulfur bound into the LD slag particles had a lasting effect on the reactivity. In subsequent experiments without gaseous sulfur addition, it became clear that sulfur was both released in the gas phase and increased the reactivities towards both solid and gaseous fuels. The increased reactivity towards gaseous fuels was partly associated with $CaSO_4$/CaS, although it might also be attributable to surface-active sulfur on the particle.

The $CaSO_4$/CaS that formed in the LD slag in the presence of sulfur in the ingoing gas might exert effects in chemical-looping applications. These phases can contribute oxygen-carrying ability but the will also react to form SO_2 under inert conditions. As mentioned above, this suggests that SO_2 could be released in the loop seals and also partly in the air reactor. This is not a favorable event since this requires further flue gas treatment of the gases out from the air reactor. If significant formation of $CaSO_4$/CaS are formed in LD slag also in the presence of ashes needs to be investigated further. In OCAC, with ongoing oxidizing conditions, the formation of $CaSO_4$/CaS should only mean that co-combustion or the addition of sulfur in the bed is less-efficient than is the case with other oxygen carriers, as indicated by the experiments conducted in the 12-MW CFB boiler [50].

Chapter 4

4. Reactivity of LD towards fuels

In the previous chapter, it was discussed how LD slag transport of oxygen and its other material characteristics might affect the usability and reactivity of the material in an applied process. In this chapter, the effects of utilizing LD slag as an oxygen carrier are studied with respect to fuel conversion at different scales, using different fuels and setups.

4.1 Reactivity toward gaseous fuels

The reaction kinetics of a chemical looping process are dependent upon several factors. The choice of metal in the oxygen carrier is one parameter that needs to be considered carefully. Ni and Cu are known to have high reaction rates compared to Mn, while Mn in turn has a higher reaction rate than Fe [17]. Even though the metal itself may be identical in two different materials, the overall reactivity of the material may not be the same due to the accompanying elements. This becomes obvious when comparing different ores and waste products for oxygen carrier applications [56,121]. The conversion of CO as a function of the oxidation level of the oxygen carrier can be a useful tool to describe the kinetics of a reaction.

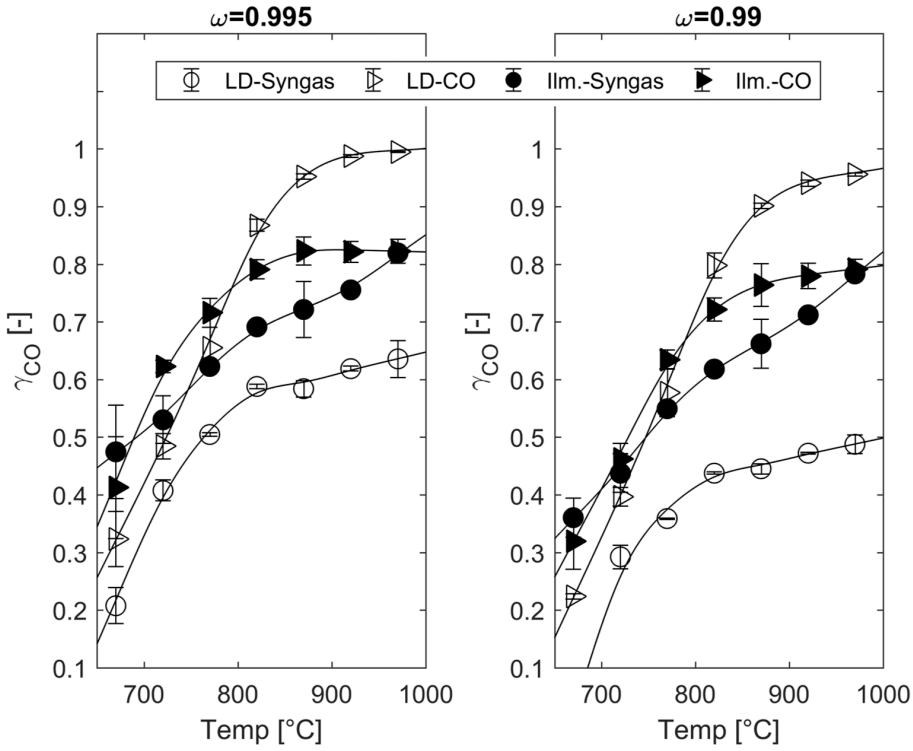

Figure 21. The conversion of CO (γ_{CO}) for LD slag and ilmenite at two different reduction levels (ω values) using 50% CO in N_2 and 50% CO in H_2 (syngas).

In Figure 21, the conversion rates of CO (γ_{CO}) are displayed at two different oxidation levels (ω-values), using LD slag and ilmenite. Here, it is apparent that the conversion of CO using LD slag is highly dependent upon the presence of H_2. This study was conducted for CLG, as described further in **Paper II**. Two different fuels were used, either 50% CO in N_2 or 50% CO in H_2. Here, it is evident that the level of CO conversion is high for LD slag when no H_2 is present. However, in the presence of H_2, the level of CO conversion is lower. In contrast to ilmenite, where the CO conversion decreased by only about 10% in the presence of H_2, the decrease in CO conversion for LD slag was 40%–50%. At the highest temperature used in these experiments, 970 °C, the equilibrium constant, K_{eq}, for the WGS reaction was 0.65 [105]. This means that the reaction is shifted more towards CO at higher temperatures than at lower temperatures, see Equations (E12) and (E14). If the reaction is shifted towards CO, the CO conversion (γ_{CO}) will be lower. It has been shown in earlier studies that CaO in the presence of the oxygen carrier ilmenite catalyzes the WGS reaction [122]. Therefore, it has been suggested that the decreased CO conversion seen in this work is related to the presence of free calcium in the LD slag. Free calcium in the form of CaO catalyzes the WGS reaction, shifting the reaction more towards CO when H_2 is present, as compared to when only CO is converted to CO_2 and the WGS reaction is not possible. Since CO_2 and H_2O are the main components in the flue gas from the fuel reactor in a CLC unit and LD slag contains CaO, LD slag may affect the outgoing gas composition due to the WGS reaction.

Methane is a common gaseous fuel, and it has been observed previously that iron-based oxygen carriers have low reactivities towards methane [12,49]. The same has been observed with LD slag and ilmenite, as shown in Figure 29 in Section 4.4. In **Paper V**, experiments were conducted to evaluate whether additions of reactive elements would increase the rate of methane conversion. It was concluded that addition of the reactive element Ni, Cu, Mn or Ce could indeed increase the level of reactivity towards methane, see Figure 31 in Section 4.5.

4.2 Reactivity toward tars

Tars are condensable hydrocarbons that may be formed during the conversion of fuels. Issues related to tars are mainly relevant to gasification processes where there is an under-stoichiometric oxygen supply, which results in incomplete combustion and a reducing atmosphere. Condensing tar is an issue owing to the need for increased maintenance in downstream processes. Tar may also contain a significant amount of the fuel energy, leading to decreased efficiency of the overall process if the tar is not utilized. Using oxygen carriers is one way to decrease the tar yield in a gasification process [30,123]. In CLG, where oxygen carriers are used for oxygen transport to the gasifier, the conditions in the gasifier are reducing and only a part of the fuel is combusted [27]. Thus, tar is able to form due to the incomplete combustion [124].

4.2.1 Benzene as tar surrogate

In the laboratory batch fluidized bed experiments, C_6H_6 was used as a surrogate tar to simulate tar conversion with oxygen carrier particles. Benzene is relatively easy to measure and feed into the laboratory batch fluidized bed system, and it has been used in earlier studies with similar scopes [125]. Benzene is also a common component of tar and it has been found to contribute to a significant amount of the tars produced in gasification systems [103,124]. It has also been observed that if the amounts of other condensable tars decrease, so does the level of benzene [126]. Thus, benzene is a very useful indicator molecule for general tar conversion, and it is probably the most stable and difficult-to-convert hydrocarbon species.

The rates of conversion of benzene for both heat-treated LD slag and ilmenite were similar, and relatively high compared to what has been seen in other studies [125]. When ash was present with the LD slag particles, the conversion of benzene tended to decrease the longer the particles had been used in the 12-MW_{th} boiler (see Figure 29 from **Paper I**). Therefore, it can be expected that tar removal over time will decrease for LD slag that ages inside a boiler. Sulfur was added at the end of the experimental campaign and bed samples were extracted as described in **Paper I**. For the bed samples to which sulfur had been added, increased conversion of the surrogate tar (benzene) was observed, indicating a decrease in the impact of LD slag aging. Regeneration of the bed with fresh material might increase the rate of tar removal. Unfortunately, there is high variability in the measurements regarding C_6H_6 conversion shown in Figure 29. As a consequence, only general trends can be discussed. In subsequent experiments with benzene, the variability was improved by changing the duration of reduction in the cycles. With the improved stability of benzene conversion, it could be concluded that sulfur dioxide addition did not alter the conversion of benzene, as mentioned in **Paper III** when no ashes were present.

It is noteworthy that tar conversion is catalyzed by alkali [35]. This limits the usability of the laboratory fluidized batch bed reactor since this is made of quartz. This means that alkali species from the fuel or ash, which should be available for catalytic tar cracking, can react with the quartz reactor walls rather than acting as catalysts.

4.2.2 Catalytic properties towards tar in the 10-kW chemical looping unit

LD slag contains high levels of calcium, which are known to affect tar cracking [127,128]. Alkali metals are also known to be catalytic towards tar [35]. LD slag contains phases with weak capabilities to form stable phases that contain alkali metals such as K, as discussed in Section 3.3. This results in a high vapor pressure of K in the fuel reactor, which is available for catalytic cracking of tars [118,127,128]. Both of these properties suggest that LD slag is a good oxygen carrier for CLG applications with possibilities of low levels of tars.

To investigate the potential catalytic properties of LD slag, a pilot-scale study was conducted in a 10-kW chemical-looping unit. Here, different operational parameters and three different fuels were investigated with respect to tar yield, comparing LD slag to both ilmenite and sand. **Paper IV** describes in detail the findings from this study.

It was found that LD slag indeed generated lower total amounts of tars compared to both sand but also ilmenite. More importantly for LD slag was that the tar composition had a lower ratio of heavy 3-ring to 4-ring tar components. This is the opposite to ilmenite, which in **Paper IV** and in previous studies [30] has been shown to generate relatively high levels of 4-ring tar components. In Figure 22, the tar yields for sand, ilmenite and LD slag are compared at two different temperatures, with the same load and fuel for all the points.

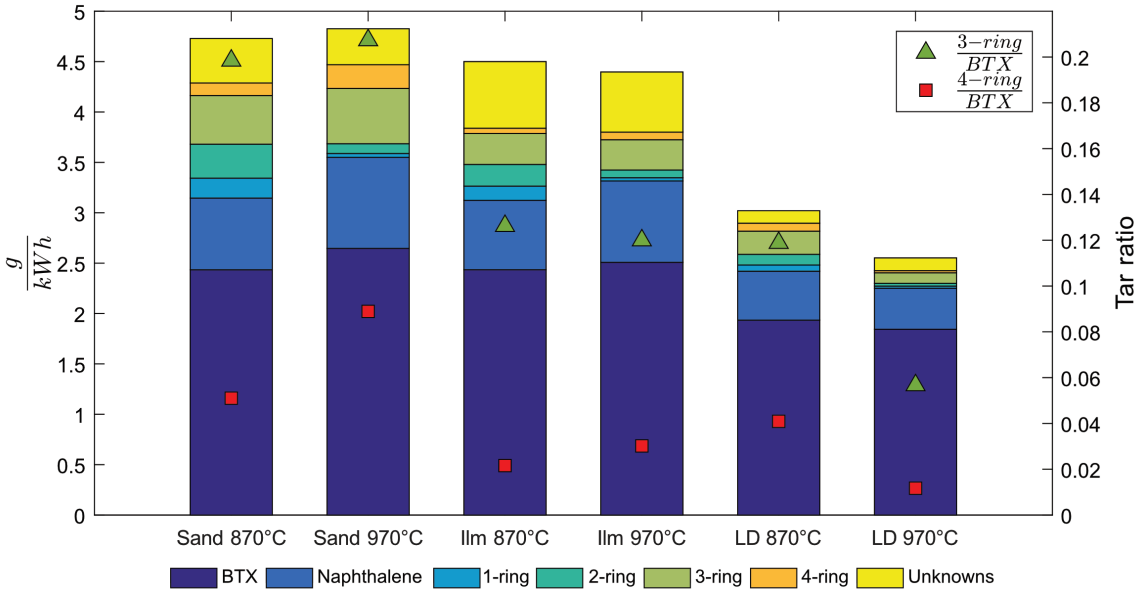

Figure 22. Measured and identified tar levels for Sand, LD slag and Ilmenite used as bed materials for CLG operation in the 10-kW chemical-looping reactor operated with PFR fuel with a load of 8 kW and at different temperatures. The ratios of identified 3-ring and 4-ring tar components in relation to BTX are indicated in the figure.

It was noted that the fuel load had a minimal effect on the obtained tar ratio. When using a fuel that contained a high level of alkali, in this case straw, the generated tar amount was lower and was even less affected by the fuel load. The most significant finding was that a higher temperature generated lower levels of heavy tar components when using LD slag, as shown in Figure 22. This contrasts with what has generally been observed for tar cracking, where higher temperatures favor the polymerization reaction that forms the heavier tars [124]. This increased formation of heavy tars was also observed during the operation of the 10-kW chemical-looping reactor with sand. However, when operated with LD slag, both the total amount of tar and the heavy tar ratio decreased when the temperature was increased.

To control the oxygen flow from the air reactor to the fuel reactor, the circulation of the oxygen carrier needs to be controlled. In the studies described in **Paper IV**, it was found that oxygen carrier circulation had limited effects on the tar yield and heavy tar ratio; even though the oxygen transport was observed to increase three-fold, the tar yield remained more or less the same.

Ageing of the LD slag bed material was also observed to have an effect on the tar yield. The same bed material was used for several days in a row, with only minimal addition of fresh material to compensate for losses of elutriated material. When repeating the same experiments with 2 operational days in between, it was observed that the total amount of tars and the ratio of heavy tars were higher for the aged sample. This was the case even if the same experimental conditions, same fuel, and similar cold gas efficiency of the outgoing gas were applied. However, the tar yield was still lower than those obtained for ilmenite and sand as the bed materials.

Comparing these results to previous results obtained in the 2–4-MW_{th} semi-industrial-scale gasifier operated with wood pellets, it was found that LD slag decreased the levels of formed tars [129]. Decreased tar formation for gasification at the semi-industrial scale was also noted in previous experiments using other oxygen carriers, such as ilmenite [30]. When the LD slag was reduced further, by using a lower circulation rate and increased fuel flow, the conversion rate of tar increased [129]. The same difference in tar yield was not detected when ilmenite was reduced further in a similar manner.

4.3 Reactivity towards solid fuels

When a solid fuel is converted in a combustion process the fuel undergoes three stages: drying, pyrolysis and gasification. First, the fuel is dried and water is evaporated. Second, the fuel is pyrolyzed, which converts the fuel to combustible volatiles and solid char composed mainly of carbon. Finally, char is converted via gasification to CO_2 and the combustible gases CO and H_2. The gasification step is normally the slowest, and is therefore the rate-determining step [130] when designing a reaction vessel for the fuel reactor. For systems with two interconnected fluidized beds, such as CLC and CLG, CO_2 and H_2O are suggested gasification agents. If the oxygen carrier has CLOU properties, O_2 is also released and it can convert the solid char [17].

LD slag was compared with ilmenite, sand and olivine. Olivine is a commonly available material that has been used in gasification systems with fluidized beds due to its tar cracking properties and ability to avoid agglomeration [131]. In these experiments, it was observed that both oxygen carriers had significantly higher reaction rates at high temperatures compared to the materials that had no oxygen-carrying capacities (Figure 23).

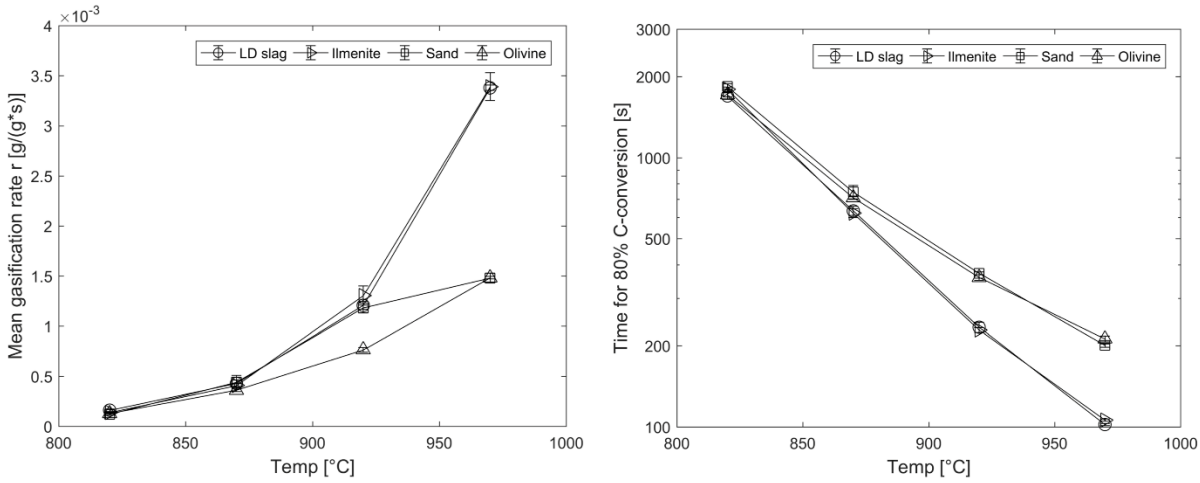

Figure 23. Left panel: Average gasification rates (r) of char in the interval of $0.3<X_c<0.7$ for the investigated bed materials. Right panel: Time required to convert 80% of the carbon in the biochar to CO, CO_2 and CH_4. Here, the two oxygen carriers show a clear difference to the sand and olivine.

It is important to note that in Figure 23 the bed materials are only heat-treated and activated through several redox cycles prior to use. The materials are not affected by either alkali or ash products to any great extent; only very small amounts of ash are included with the fuel during the experiments. In particular, potassium has been observed to both catalyze the char conversion and affect the properties of different bed materials and oxygen carriers [18,96,132,133].

In Figure 24, the gasification rate and flue gas concentrations are plotted against the char conversion degree (X_c) for one representative cycle at 870°C using 0.2 g char as fuel. The most-significant difference between the LD slag and the other evaluated bed materials is that the gasification rate of LD slag decreases around a conversion degree of X_c=0.5 compared to the other particles, which show increases in the gasification rate as the value of X_c increases. This is most likely coupled to the hydrogen generation with LD slag that occurs due to the formation of a wüstite structure, which leads to water-splitting

(Reaction R8). However, the H_2 generated from the gasification reacts at a lower rate at lower degrees of oxidation. The increased hydrogen generation results in hydrogen inhibition of the carbon [134,135]. However, the decreased gasification rate is still within the same range as the rates for the other evaluated bed materials.

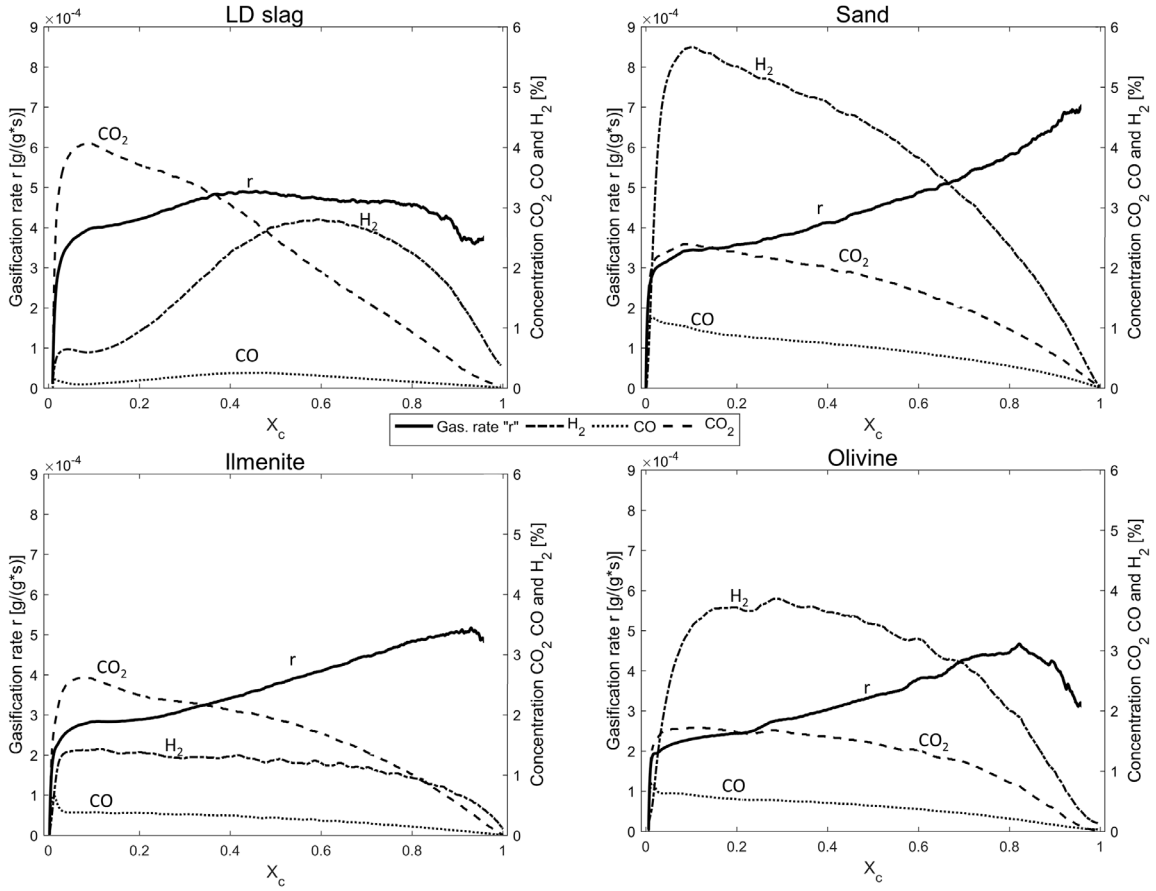

Figure 24. Gasification rates (r) and the concentrations of outgoing H_2, CO and CO_2 as a function of the char conversion degree (X_c) for the four different investigated bed materials at 870°C. Devolatilized pellets of char (0.2 g) were used for the bed of 40 g, corresponding to a theoretical bed weight reduction of approximately 1 wt.%.

In addition to the H_2 generation for LD slag, the CO curve proportionally follows the H_2 curve. This may be a result of the WGS reaction, which shifts the carbon towards CO with increased H_2 and high CO_2 contents in the gas, as indicated also in Figure 21 and Figure 26.

Another clear difference between the oxygen carriers compared to sand and olivine is the increased generation of CO_2. Partial combustion of the gasification products is one of the reasons for the increased CO_2 generation, which is especially pronounced during the initial mixing of char and oxygen carrier (see the initial period in the curve for LD slag and ilmenite in Figure 24). Although this is a well-known phenomenon, it indicates that there could be optimization issues with respect to limiting oxidation in the fuel reactor in a real CLG system.

4.3.1 *Effects on raw gas composition using LD slag*

In a system such as the laboratory batch fluidized bed reactor, it is not surprising to find that the levels of CO and H_2 generation for both LD slag and ilmenite are lower than those for quartz sand and olivine. This is due to the available oxygen in the oxygen carriers, resulting in partial combustion of the gasified fuel. In a continuous system, both the heat balance and mass balance need to be adjusted so as to be autothermal. Since this partial oxidation is necessary for CLG to solve the energy balance for an autothermal process [27], it is instead the H_2/CO ratio that is of interest for these experiments. It should be noted that sand and olivine, which are used for indirect gasification in a conventional DFB gasifier, are not supposed to transport oxygen to achieve an autothermal process. Here, partial combustion of the char in the combustor is necessary to achieve an autothermal process, and this results in a diluted CO_2 stream exiting the combustor.

The H_2/CO ratio obtained for LD slag was significantly higher at low temperatures, making it more relevant for CLG, as compared to the other tested materials (Figure 25). It was found that the water-splitting reaction (R8) contributes significantly to this effect, as described in **Paper II**. The effect of hydrogen generation through water-splitting can also be observed in Figure 24.

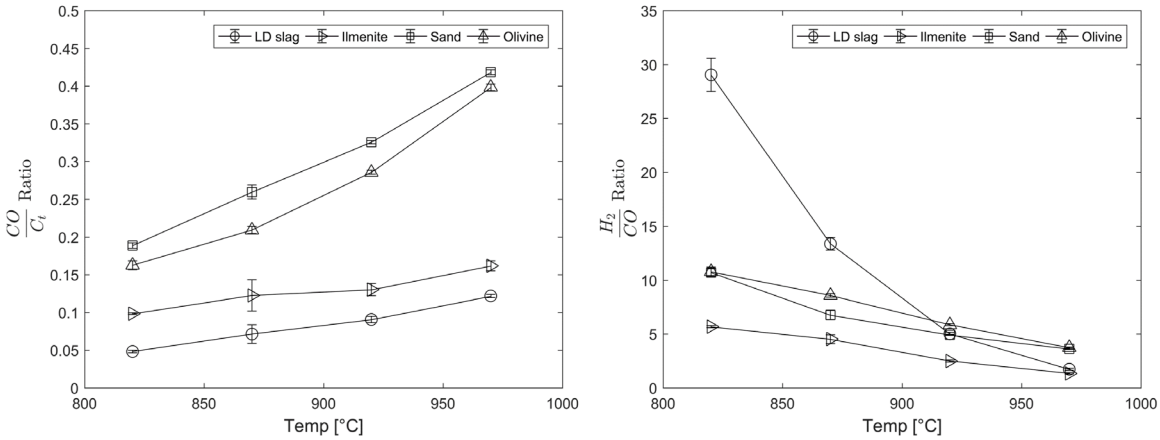

Figure 25. CO/C_t ratios (left panel) and H_2/CO ratios (right panel) for the outlet gases when gasifying char from wood pellets in the laboratory-scale, fluidized bed reactor at different temperatures. C_t is the total amount of carbon emitted from the reactor in the forms of CO, CO_2 and CH_4. The calculations are performed for char conversion degree in the interval of $0.3<X_c<0.7$.

The relative CO generation in comparison to the total carbon emissions is higher at higher temperatures for all the bed materials, as shown in Figure 25. LD slag and ilmenite have lower CO to total carbon (CO/C_t) ratios compared to olivine and sand. This is a result of the partial combustion of the gasification gases. At higher temperatures, more CO is converted to CO_2 and, therefore, the difference between the oxygen carriers and the "inert" bed materials is larger at 970°C than it is at 820°C.

From the gasification experiments, it is clear that LD slag is active towards the WGS reaction. LD slag, the Q_i value (the ratio of the gases related to the WGS reaction), as defined in Equation (E13), is much closer to the WGS equilibrium K_{eq} compared to the other tested bed materials [105,106], as shown in Figure 26. This is most likely related to the CaO content of the material, as discussed in Sections 3.2 and 4.1.

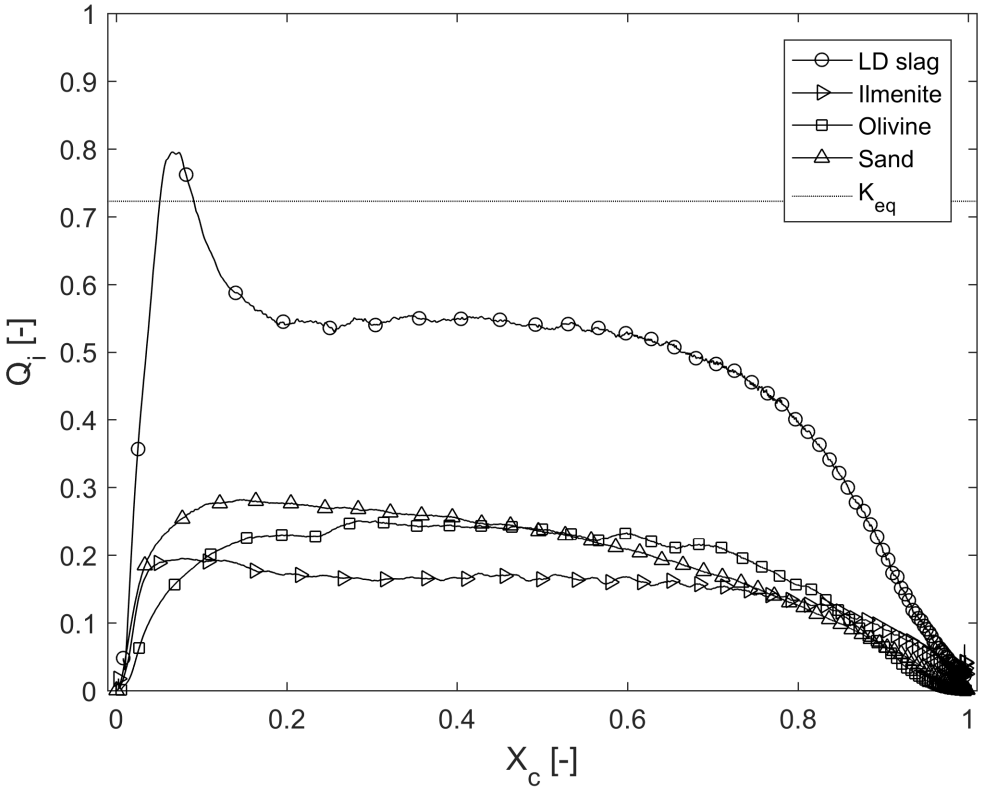

Figure 26. The reaction quotient Q_i for LD slag plotted against the char conversion degree (X_c) compared to other bed materials and the equilibrium constant K_{eq} for the same cycles at 870°C as in Figure 24. Since the steam concentrations in the outgoing gases were not measured, it was assumed that the outgoing concentration was roughly the same as the ingoing concentration, e.g., 50%.

4.3.2 *Effects of an increased fuel-to-bed ratio*

In a continuously operated CLC or CLG plant, oxygen transport to the fuel is regulated by the circulation rate, dilution of the oxygen carrier or by controlling the oxidation degree of the oxygen carrier in the air reactor. In CLG, the oxygen transport is very important for achieving an autothermal and efficient gasification process [27,32,33]. In a batch fluidized bed, the oxygen transport from the oxygen carrier can be adjusted by changing the fuel-to-bed ratio. Increasing the amount of fuel to achieve a higher fuel-to-bed ratio results in an increased degree of reduction. The average values for these cycles and the reduction rate at the end of the cycle are listed in Figure 27. Here, a clear difference between the LD slag and ilmenite is evident. By increasing the amount of fuel, the levels of H_2 and CO generation are increased while the level of oxygen transport remains more or less the same for LD slag. This is not the case for ilmenite, whereby the levels of H_2 and CO generation remain roughly the same as the oxygen transport increases. This indicates that ilmenite requires a higher fuel-to-bed ratio for the gasification processes with regulated oxygen transport, as compared to LD slag. Indications that hydrogen generation is increased by increases in the fuel-to-bed ratio were also observed at the semi-industrial scale in the 2-4-MW_{th} gasifier [129].

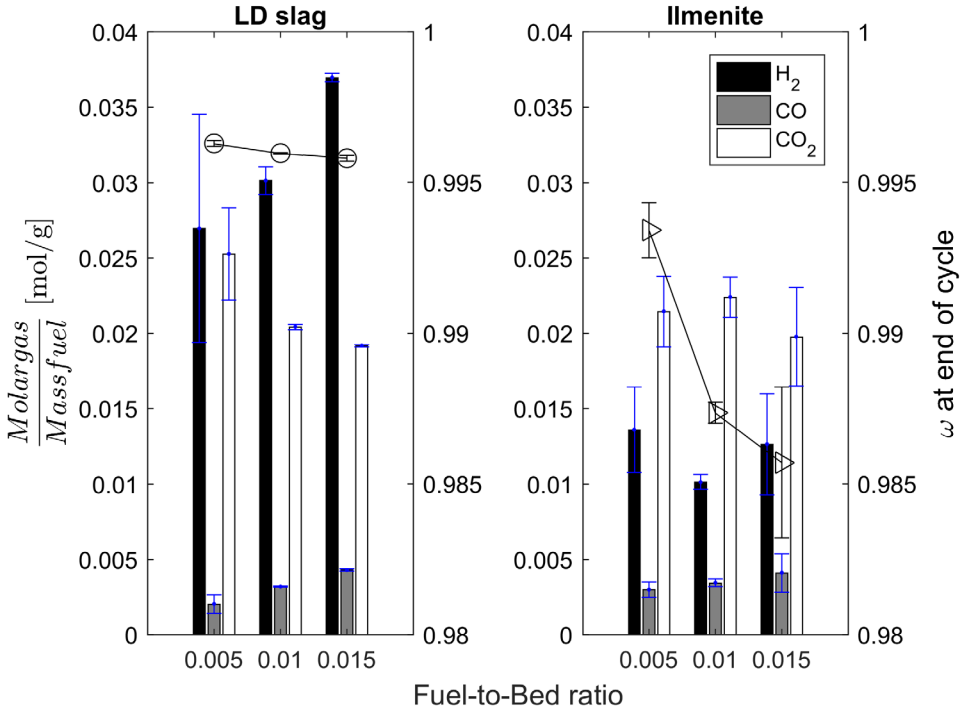

Figure 27. Molar gas production per gram of fuel with LD slag and ilmenite as bed materials at 870°C and using three different fuel-to-bed ratios. These ratios correspond to fuel additions of 0.2, 0.4 and 0.6 g to a bed that contains 40 g of oxygen carrier. Calculations of the gases are made for average at the char conversion degree in the interval of 0.3<X_c<0.7, to avoid the effects of volatiles. On the right axis is the ω-value at the end of the cycle, calculated from the amount of oxygen absorbed during oxidation.

It is important to note that the ω-value is calculated at the end of the cycle. LD slag is, therefore, affected to some extent by the water-splitting reaction, where the material is oxidized with steam. Nevertheless, the trend of increased levels of desired gasification products and decreased CO_2 concentrations is an important observation even at these fuel-to-bed ratios. However, higher concentrations of H_2 also affect the gasification rate through H_2-inhibition. Thus, an increased H_2 concentration results in a decreased relative gasification rate, as shown in Figure 28. Here, it can be seen that the gasification rate for LD slag is lower than that for ilmenite at higher fuel-to-bed ratios.

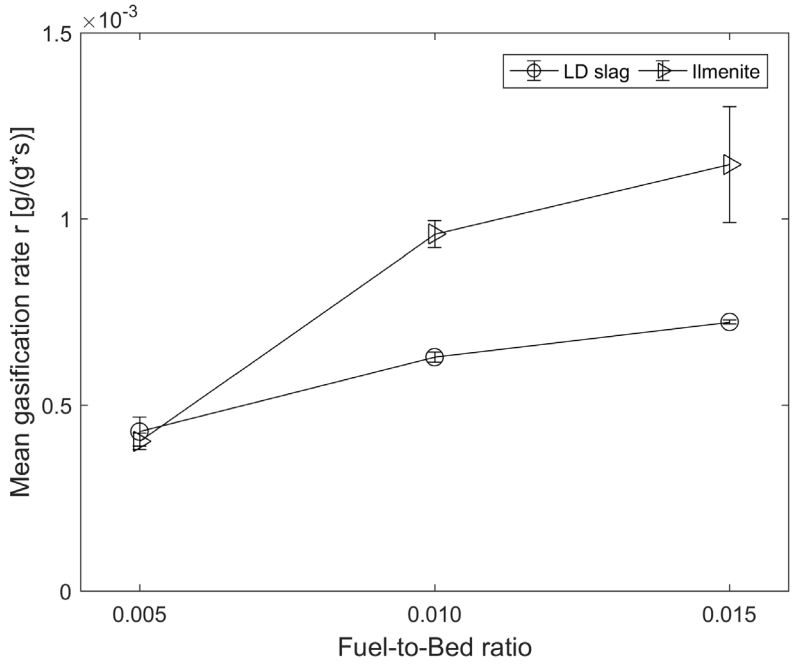

Figure 28. The mean gasification rates for LD slag and ilmenite with different fuel-to-bed ratios. These ratios correspond to the addition of 0.2, 0.4 and 0.6 g of char to a bed that contains 40 g of oxygen carrier.

Since the gasification rate is affected by the fuel-to-bed ratio, which in turn affects the syngas composition, it seems likely that a balance between these parameters will be struck in an industrial process. This will then affect the general design of the process equipment.

4.4 Effects of ash and non-carbon species from the fuel on the reactivity of LD slag

Elements such as potassium are known to increase the levels of reactivity of active bed materials such as olivine [126,136] and ilmenite [80,137,138]. In this section, the results for interactions between the LD slag and non-carbon species are used to define the expected reaction properties of LD slag towards fuels.

The ways in which the conversion rates of gases are affected by the presence of ash were evaluated in a laboratory batch fluidized bed reactor that was operated with LD slag samples extracted from the 12-MW_{th} boiler, and exposed to different gases. The tested gases, CO/H_2, CH_4 and C_6H_6, were introduced into the laboratory scale batch fluidized bed reactor, with or without steam. Fuel mixtures were used according to Table 5. LD slag and ilmenite that were only heat-treated were compared to the LD slag extracted from the 12-MW_{th} boiler. The results of these exposures are shown in Figure 29. All the samples were activated through oxidizing-reducing cycles until a stable conversion rate for CO was attained [139].

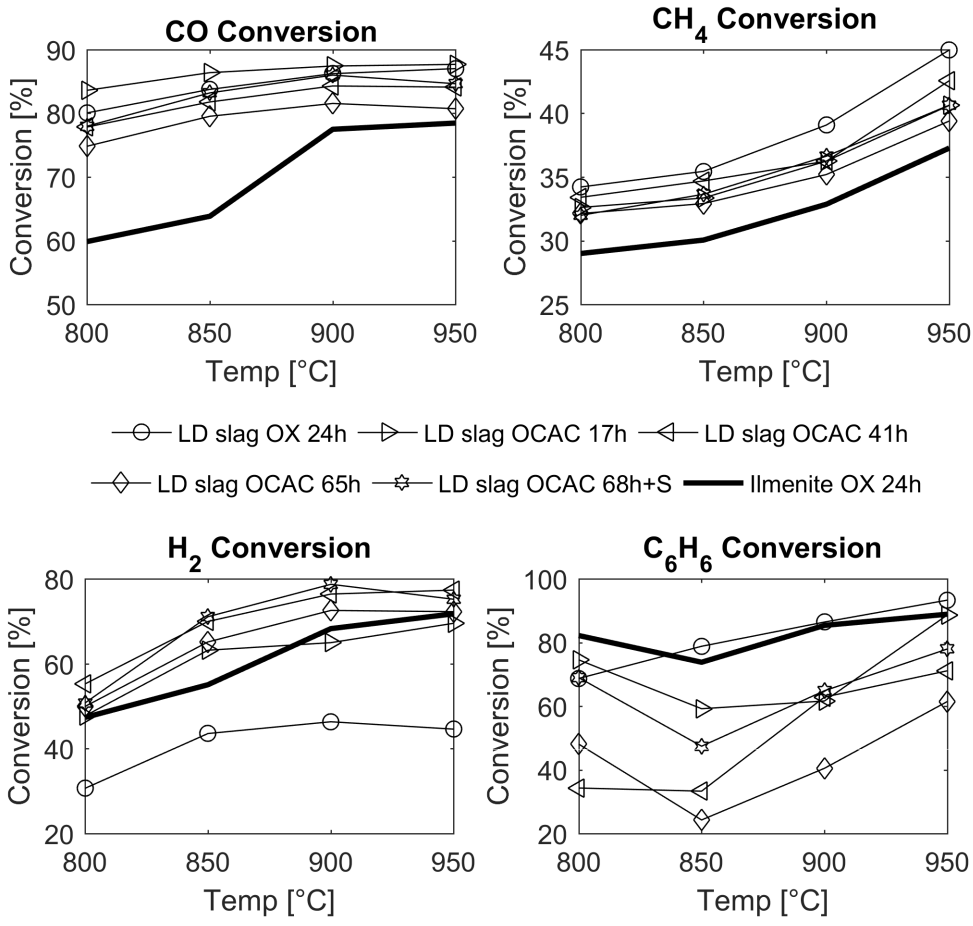

Figure 29. Average conversion of four different common fuel gases mixed with steam using LD slag operated for different numbers of hours in the 12-MW_{th} OCAC CFB boiler, as compared with a heat-treated ilmenite sample. It is well-known that ilmenite increases in reactivity in the presence of alkali and ash components.

Compared to ilmenite, LD slag performed similarly or slightly better for the conversion of H_2 and CO, as well as for the conversion of CH_4. The sample of LD slag that had not been used in the boiler showed a significantly lower H_2 conversion rate. This might be due to the high content of CaO in this sample, which would catalyze the WGS reaction.

The ageing effect on the samples in respect to operational over time in the boiler could be observed to decrease the reactivity of LD slag slightly towards CO, CH_4 and C_6H_6. The addition of elemental sulfur (the sample noted "LD slag OCAC 68 h+S" in Figure 29), suggests that the aging of LD slag could to some level restore some of its reactivity. It was only towards H_2 that the conversion rate increased over time. However, the overall conversion of especially H_2 is dependent upon three parallel reactions: i) the WGS reaction; ii) the water-splitting reaction; and iii) the oxidation of CO and H_2. These reactions are present simultaneously in system. Of these reactions, both water-splitting and the oxidation of CO and H_2 correlate with the oxidation level of the oxygen carrier.

Ash has a significant effect on the gasification rate of a solid fuel. Figure 30 shows a comparison of the gasification rates seen in the laboratory batch fluidized bed reactor between heat-treated slag and activated LD slag (as a reference) with bed samples extracted from the 12-MW_{th} boiler after 65 h of operation in OCAC mode. It is clear that the gasification rate for the OCAC slag sample is several times higher than that for the reference LD slag. Similar experiments have been conducted with heat-treated olivine compared to samples extracted from the 12-MW_{th} [140]. In those cases, it was observed that the gasification was initially higher, but after a few cycles was similar to that of the reference. However, the difference was not as significant as when the LD slag was used. Furthermore, for LD slag, the gasification rate started to decline after four cycles, albeit slowly. This indicates that the oxygen transfer to the solid fuel is strongly affected by potassium and sulfur present in the ash with the aged samples from the boiler.

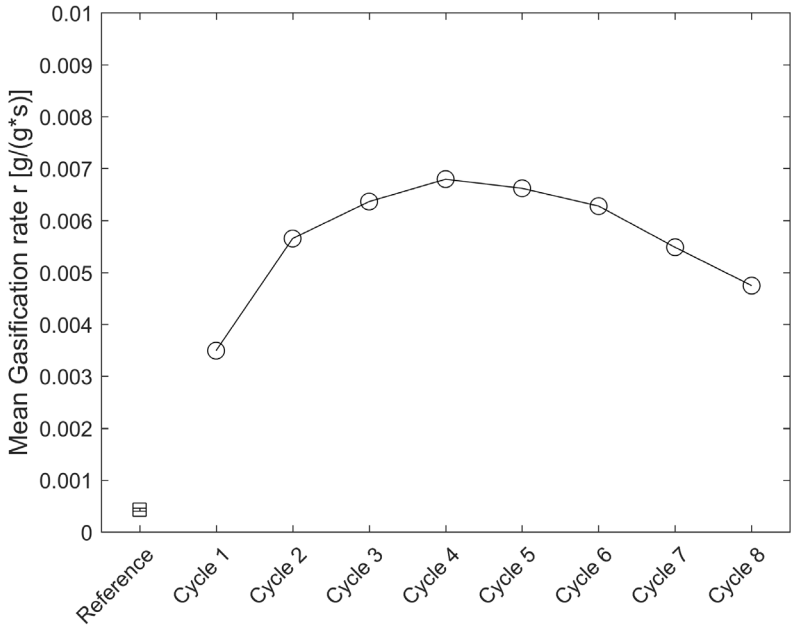

Figure 30. Mean gasification rates calculated for char conversion degrees in the interval of 0.3<Xc<0.7 for heat-treated LD slag (reference) and the first eight cycles using LD slag samples collected from the 12-MW CFB boiler operated under OCAC conditions for 65 h.

Alkali metals are known to have catalytic properties for char conversion [18] and have been observed to increase significantly the gasification rate, also with other oxygen carriers [141]. However, a previous study conducted with LD slag at Åbo akademi in Finland indicated that an anion with a potassium ion had a significant effect on the reactivity of LD slag. Thus, is was found the K_2SO_4 increased the reactivity of LD slag towards CO in the presence of steam, whereas K_2CO_3 decreased this reactivity [110].

In experiments carried out with sulfur and solid fuels (see **Paper III**), it was observed that sulfur exerted a positive effect on the gasification rate when used together with LD slag. Without sulfur, the reaction rates for LD slag and ilmenite are more or less the same. When sulfur is added, the intermediate transport of oxygen from the oxygen carrier to the char particle via SO_2-H_2S/S/COS can occur, as illustrated in Figure 20. This contributes to increasing the reaction rate for both LD slag and ilmenite, but not for sand, which has no oxygen to transport. An indication of an increased gasification rate in the presence of sulfur has also been seen in previous studies [20]. This may indicate that sulfur recirculation in both CLC and CLG is highly favorable for increasing the rate of char gasification.

From the studies performed with sulfur in **Paper III**, it is apparent that the reduced phase of LD slag also has an important effect on the sulfur. Reduced LD slag forms H_2 due to water-splitting in the presence of steam (further discussed in Section 4.3.1). H_2 reduces SO_2 to form H_2S, which is the reason why the SO_2 level drops when LD slag is reduced further in the gasification experiments with LD slag and SO_2. This might influence different technical applications. In CLG, it is already estimated that H_2S is the dominating sulfur-containing gas species, while in CLC, with over-stoichiometric oxygen, SO_2 is dominating [89–93]. When there is close-to-stoichiometric conversion in CLC, more H_2 might be present, resulting in H_2S becoming the dominant sulfur-containing gas species when using LD slag. However, since heat transport rather than oxygen transport is estimated to be limiting in CLC [57], the conditions should always be over-stoichiometric and SO_2 should be the dominant sulfur-containing gas species.

In summary, LD slag experiences increases reactivity towards both gaseous and solid fuels when ashes and sulfur are present. This could be related to the increased oxygen transfer seen with sulfur and the catalytic properties of alkali, both of which properties are favorable for CLC and CLG. This means that LD slag allows both sulfur and alkali to be available in the gas phase to interact with the fuel. However, the reactivities of LD slag towards gaseous fuels, such as methane, are low.

4.5 Increasing reactivity by impregnation

A general issue associated with iron based-oxygen carriers is that they have lower reactivity towards hydrocarbons than other well studied transition metals such as Ni, Cu, Co and Mn [142]. It is however known that the reactivity of oxygen carriers can be improved by cyclic reduction and oxidation (activation) [121,139] or by the addition of alkali metals to improve the reactivity, at least in the case of ilmenite [80,138]. Activation of LD slag can be achieved with both multiple redox cycles and ash (see the experiments related to **Paper I**, as shown in Figure 29). This activation was observed as increased reactivity for the LD slag that was initially utilized at the semi-industrial scale, as compared to the reference sample that was only heat-treated and activated through several redox cycles. This activation by the ash may not be associated specifically with potassium, as has been observed for ilmenite with K_2CO_3 [137]. K_2CO_3 has been shown to instead deactivate LD slag, removing the possibility for it to be reduced by CO [110].

To achieve increased reactivity, doping of an inexpensive oxygen carrier has been tested in different studies. Examples of doped materials are Cu doped onto iron ore [97] and red mud [143], and Ce doped onto iron particles [144], all of which exhibited increased reactivity. In **Paper V**, LD slag was doped with small amounts of four different elements (Ni, Cu, Mn and Ce) that are known to have high reactivities towards gaseous fuels. Increased reactivities were observed for all these dopants, even with the addition of only 2% dopant. Figure 31 displays the degrees of conversion for methane for the reference sample and for the samples that were doped with the different elements.

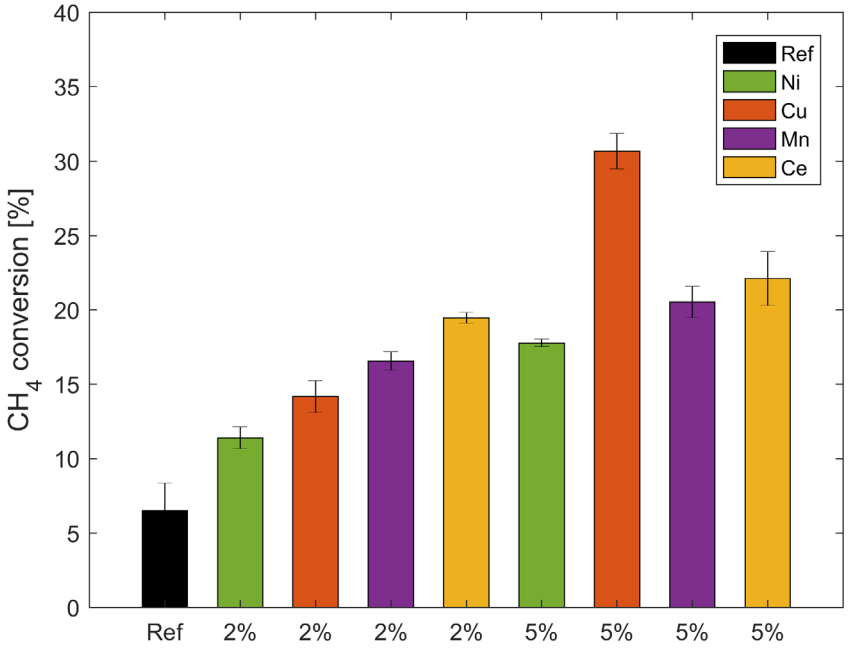

Figure 31. Conversion of methane for LD slag reference compared with LD slag doped with 2% or 5% of either Ni, Cu, Mn or Ce.

In this study, it was observed that Mn and Cu both formed phases in the LD slag together with either Ca or Fe, resulting in CLOU properties. While both Ni and Ce showed increased reactivity, they did not interact to the same extents with the slag itself. This suggests also how these elements might interact if present in the fuel ash.

Chapter 5

5. Physical properties identified for LD slag used as an oxygen carrier

The oxygen carrier needs to have sufficient mechanical strength to allow it to be fluidized in thermal conversion applications. The particles need to retain their fluidization properties over many cycles with acceptable levels of attrition and must also be able to undergo storage without changing their properties. In this section, some of these properties are discussed for LD slag.

5.1 Bulk density, attrition and the effect of fines

During operation of the 12-MW_{th} CFB boiler with LD slag under OCAC conditions, the development of the physical appearance of the material could be observed. A summary of the physical data related to bulk density, BET surface area and attrition is presented in Table 8. During heat treatment of the material, it was observed that the bulk density of the LD slag decreased. This was mainly due to the decomposition of $Ca(OH)_2$ and carbonates. At the same time, the BET surface area decreased, most likely due to sintering of the pores. The attrition rate was not affected by the heat treatment.

Table 8. Basic properties of the as-received, heat-treated (HT) LD slag operated in the 12-MW_{th} CFB boiler under OCAC conditions for 65 h, as compared with the benchmark material ilmenite.

Sample	*Bulk density [kg/m^3]*	*BET surface area [m^2/g]*	*Attrition [wt.%/h]*
LD slag as-received	1560	4.4	2.2
LD slag HT oxidized for 24 h	1410	1.0	2.2
LD slag Used OCAC 65 h	1640	0.41	0.43
Ilmenite HT oxidized 24 h	1831	0.21	0.53

For the slag samples that were used in the CFB boiler under OCAC conditions, the bulk density was higher and the surface area and attrition rate were lower compared to the heat-treated samples. This combination indicates that loose fines adherent to the particles are easily removed by attrition. In the SEM investigations of fresh and heat-treated samples (Figure 32), slag particles that had agglomerated fines or were composed of agglomerated fines were detected. These types of particles could not be found in the LD slag samples taken from the boiler, the OCAC samples. Furthermore, during the operation of the boiler with LD slag, there was a high level of consumption of the bed material, together with high levels of generation of fines in the secondary cyclone and textile filter. Compared to operation with sand, the level of fines generated during a comparative 24-h period with LD slag was 3-fold higher [50]. The material from the secondary cyclone and textile filter had an elemental composition similar to that of the original material, as shown in **Paper 1**. When operated under CLG conditions in the 10-kW unit, the lifetimes of the oxygen carriers were estimated from the fines obtained in the air reactor filter and fuel reactor chimney. Here, the lifetime of the LD slag was estimated to be 800 h, which was very similar to the 850 h lifetime of ilmenite [145].

Fines contribute to a large surface area in relation to weight, which is why the surface area decreased when the fines were eroded and elutriated in the boiler. This was also clear from the high attrition rate, which was attributed to the fact that the agglomerated fines were removed early in the test, resulting in a logarithmic decay in the attrition profile. The OCAC samples showed a more linear attrition pattern with a relatively low attrition rate, comparable to those of ilmenite [109] and manganese ores [48]. This suggests that while LD slag has sufficient strength, longer exposures in the boiler are needed to be able to define the lifetime of the particles. However, the production of the material needs to be monitored to avoid fines that will contribute to increased fly ash generation. This is because fly ash, depending on the fuel source, is expensive to dispose of in an environmentally safe way [146].

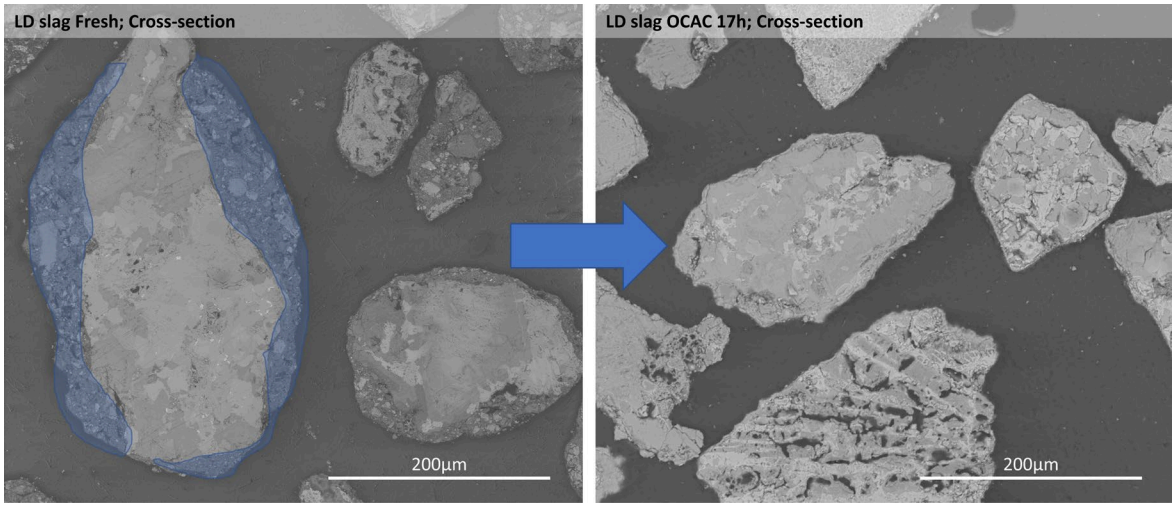

Figure 32. SEM images of cross-sections of the as-received fresh LD slag (left) and a sample of LD slag that had been operated in the boiler under OCAC conditions for approximately 17 h (right). The blue area on one of the fresh LD slag particles indicates an area of fines that is associated with the surfaces of the fresh LD slag particles. These fines are not seen in any of the LD slag samples extracted from the boiler.

The remaining fines in the material or the formation of these agglomerates of fines on the particles could result from insufficient sieving and drying of the particles. To investigate the optimal production of the particles within a desired size range, further studies using different pre-treatment techniques, such as crushing, sieving and drying, are needed. In addition, the aspect of weathering is interesting from the perspective of the fines generated. The yield of the material produced in the desired size range for this work was 20%-25% [50]. This can be compared to the yield of roughly 50% obtained for the generation of other crushed oxygen carrier material in a previous study [75], suggesting that there is room for improvements.

5.2 Storage and weathering of LD slag

LD slag has been considered for use as a construction material in both the cement industry and in road construction; however, there are issues related to this. For example, in Korea, the use of LD slag aggregates in common cement has been prohibited, due to the danger that expansion of unaged material would weaken the cured cement [147]. The expansion of LD slag aggregates is related to the presence of free lime in the structure. The free lime reacts with water to form $Ca(OH)_2$, which if in contact with air will over time form $CaCO_3$. A feature that has been suggested to be accounted for to decrease, at least on paper, the CO_2 emissions from steel manufacturing since the present CaO removes CO_2 from the atmosphere [148]. CaO is also leachable from the structure and will be released from the slag over time if exposed to water. The use of LD slag in road construction in Germany has shown that up to 7% and 4% free lime content can be integrated into unbound representative asphaltic layers without any serious issues. However, in these studies, the MgO concentration was also low [69].

To increase the stability of LD slag, it can be weathered, i.e., exposed to water over time. This requires that the slag yards are expanded and that the material is spread so that rain can leach and stabilize the material over time. The weathering can be enhanced by the addition of water, which decreases the duration of weathering [69]. If collected in an appropriate way, the leached liquid can be used to manufacture lime [149], which can be reused in the steel manufacturing process.

In **Paper VII**, a sample of heat-treated and sieved LD slag particles was exposed outdoors to weathering for about 1.5 years. The material was exposed to rain and weather in a drainage container in which some of the leached fluids could be collected. It was clear that the material had leached CaO, forming a white powder at the bottom of the leach collector. The bulk of the material was still in powder form, while the upper part of the material had agglomerated to form a thick crust (Figure 33). This agglomerate was bound together by reacted CaO forming $CaCO_3$.

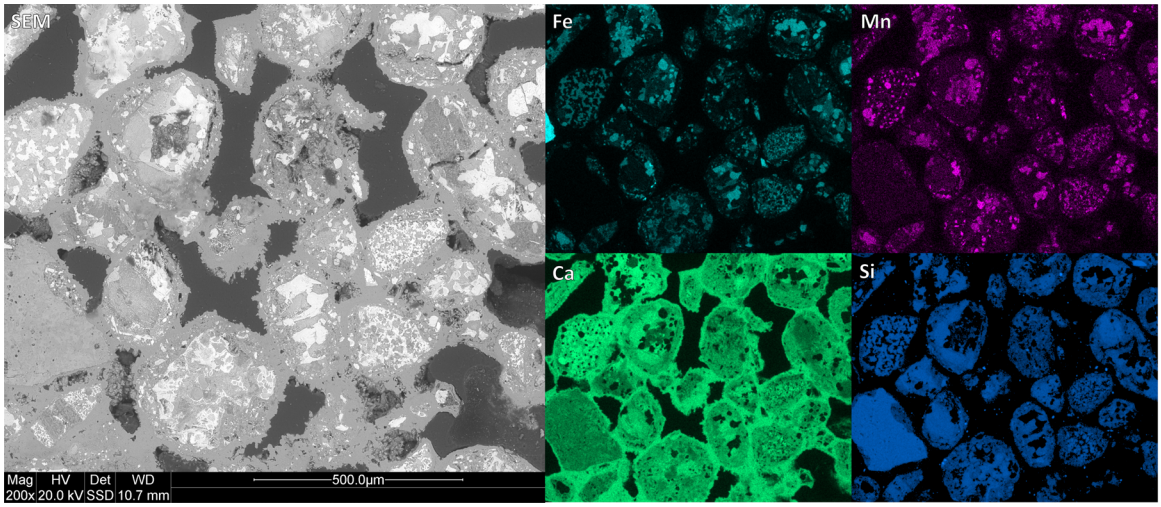

Figure 33. SEM-EDS analysis of the particles in the upper part of the weathered LD slag particles, the "crust", which had undergone agglomeration as a result of the formation of $CaCO_3$ from the leached CaO.

When comparing the particles' physical properties, there was significant degradation of these properties after weathering. The bulk density of the particles had decreased due to the leaching. Furthermore, the attrition rate had increased. The attrition of LD slag was already determined to be very high for fresh particles, as evidenced by the large amounts of fines emitted from the cyclone when it was used in the 12-MW_{th} boiler [50].

The difference in reactivity between the weathered and fresh LD slag was minimal when tested in the laboratory batch fluidized bed reactor. The CaO content of the material was almost unchanged after weathering and it was still active towards, for example, the WGS reaction. Similar reaction conversion rates for both solid fuel and gaseous CO were observed for the weathered and fresh materials.

Overall, it can be concluded that weathering should be avoided when LD slag particles of the desired size have been achieved and heat-treated. This is not because of changes in the reactivity of the material but is instead attributed to the degraded physical integrity of the LD slag particles, resulting in higher levels of attrition and agglomeration due to the formation of $CaCO_3$. Therefore, it is recommended that LD slag particles be stored in a dry silo and not outdoors.

Chapter 6

6. Discussion

In the previous chapters, different aspects of LD slag have been discussed separately and in detail. In this chapter the usability and needed studies of LD slag as an oxygen carrier for chemical looping applications will be discussed.

6.1 Understanding LD slag

When this work was initiated only a limited number of small-scale studies had been conducted on LD slag in the application of bed material for thermal conversion of fuels. In 2004, the first reports of LD slag as a bed material for OCAC were published [74]. Subsequently, LD slag was investigated in 2014 and 2017 as a bed material at Chalmers [56,73]. The first report [74] described the issues with the catalytic properties, increasing the formation of NOx. Nonetheless, with the new approach of adding ammonium sulfate to reduce NOx formation [150], NOx emissions can now be handled more easily in conventional combustion processes and OCAC. The later publications indicated the possibilities of LD-slag in the forms of good reactivity and low cost.

LD slag was utilized as a bed material during the winter season of 2017–2018 in the Chalmers 12-MW_{th} boiler. This initiated the work of this thesis and provided the material for **Paper I**. The boiler operation confirmed that NOx formation increased compared to silica sand [50] and showed that LD slag generates a significant level of fines. These investigations also provided understanding on ash interaction, specifically regarding how LD slag interacts with alkali, and the resulting high levels of CO emissions. Alkali interactions were then investigated in greater depth in **Paper VI** using synthetic ash, to examine the issues related to mixing sand with LD slag in presence of alkali. Elemental

sulfur and ammonium sulfate were tested in the boiler experiments for their abilities to handle CO emissions. [50]. The interaction of sulfur with LD slag was further investigated in **Paper III** with the results suggesting that some sulfur can be bound into the structure of LD slag. In the same study it was identified how sulfur can act as an intermediate transporter of oxygen from an oxygen carrier to a solid fuel. A very interesting and important aspect of sulfur since it increases the gasification rate. This finding suggests that sulfur recirculation and fuel with high sulfur content could be favorable for chemical looping applications while using LD slag.

The reactivity of LD slag with fuel is, of course, of great importance. The main equipment used in this work has been the laboratory batch fluidized bed reactor. This reactor is highly suitable for gaseous fuel experiments and for comparative experiments involving gasification. In the same reactor, the catalytic effects on the WGS reaction were investigated, as well as how the gasification rate of the fuel can be affected by, for example, the oxidation state of the oxygen carrier and hydrogen inhibition (**Paper II**). Moreover, the addition of reactive elements to increase the rate of gas conversion could easily be evaluated in this setup (**Paper V**).

Some of the limits of the small quartz reactor, such as low reactivity with volatiles and the alkali-quartz reactor interaction, can be avoided when advancing to the pilot scale reactor made of steel. In the larger scale, the alkali interaction with quartz is avoided and continuous circulation between the two reactors can be achieved. This enables one to study the effects of alkali and the catalytic properties of LD slag during continuous gasification and combustion under chemical-looping conditions. Alkali emissions [118] and operational performance [145] besides the tar yield (**Paper IV**) could be investigated for LD slag and compared with other oxygen carriers using different fuels. From this, it is evident that LD slag are a suitable oxygen carrier for CLG.

It is apparent that LD slag is affected by alkali and other ash components. This was clear when the LD slag used in the 12-MW_{th} boiler was evaluated in the gasification experiments (Figure 30). Here, the gasification rate was an order of magnitude greater for the used particles from the boiler than for the particles that have only been heat-treated and activated through several redox cycles without ash-containing fuel. This suggests that alkali and other elements on the surfaces of the particles originating from the ash are very important for fuel gasification in the presence of LD slag. This aspect of how used materials that have interacted with ash deviates in reactivity towards gasification from fresh material needs to be considered in future studies.

The physical properties of LD slag represent perhaps the most pressing issue of LD slag implementation as an oxygen carrier, regardless of the intended application. The production of the LD slag particles gave a low yield and despite heat treatment, the LD-slag particles had a relatively low mechanical strength. This results in the generation of a lot of waste material, both at the production site and when it is used in a boiler. The rate of recovery during particle production was only 20%–25% of particles with the desired size, and a large amount of fly ash was observed due to the remaining fines generated during operation in the 12-MW_{th} boiler. Also, it was the physical properties that hindered the use of LD slag in

the Sävenäs HP2 95-MW_{th} BFB boiler; here, issues with the pneumatic transport limited the addition to roughly 7% of the slag in the bed before the operation had to be shut down [13]. However, in the much-smaller 10-kW unit, the lifetime was estimated to be 800 h, similar to that of ilmenite [145]. Taking this to consideration, if LD slag can be crushed and treated in such a way that a high percentage of the right-size fraction is recovered without attached fines, then LD slag might become favorable. Also, as investigated in **Paper VII**, it is important to store the particles in an appropriate manner to maintain the integrity of the particles.

One of the characteristic properties of LD slag is its interaction with alkali metals. LD slag and alkali do not form products with low melting points, as happens with silica sand and alkali. Neither does LD slag absorb the alkali to form high-melting-point structures to the same degree as ilmenite. Instead, more of the alkali will be in the gas phase and available for reactions. This is favorable for both CLC and CLG, in which a high level of gas-phase alkali contributes to increasing the gasification rate of char and cracking of tars as investigated and reported in **Paper IV**. A higher level of alkali is, however, not favorable for OCAC, since this results in higher emissions of CO, which need to be handled with the addition of, for example, ammonium sulfate. Ammonium sulfate is also required to manage the higher levels of NOx emissions linked to the use of LD slag in OCAC [50,150].

CLG is an application for which LD slag could be an attractive choice for CO and H_2 production. In addition to the higher concentrations of alkali, which have positive effects on the char conversion and tar cracking, CaO catalyzes the tar cracking, as shown in **Paper VI**, which is advantageous for downstream processes. Another effect of the high calcium content of the slag is that CaO is catalytic for the WGS reaction, as shown in **Paper II**. This, together with the possibility for water-splitting of the reduced oxygen carrier, as observed in **Paper II**, can be used to adjust the H_2/CO ratio to more H_2 and less CO which is advantageous for Fischer-Tropsch synthesis. This could reduce the demand and energy-consuming downstream processes that would otherwise be needed for adjusting the H_2/CO ratio. A techno-economic study carried out on the subject of LD slag as an oxygen carrier for CLG has concluded that, for example, the catalysis of the WGS reaction has positive effects [151].

Another application in which the water-splitting ability of LD slag can potentially be exploited is Chemical Looping with Water Splitting (CLWS). Here, the reduced oxygen carrier from the fuel reactor is exposed to steam, to produce hydrogen before the oxygen carrier is circulated to the air reactor [152]. Producing hydrogen through CLWS could be an efficient method to extract more than heat and power from a CLC process. Given the active phases of LD slag and the evident hydrogen produced when reduced LD slag was exposed to steam, as shown in Figure 12, LD slag could be suitable for CLWS. Also, as high-level reduction of oxygen carriers is utilized in CLWS [153], LD slag has a weaker tendency to agglomerate compared with other iron-based oxygen carriers when highly reduced [154]. This means that LD slag can be less problematic than other iron-based oxygen carriers at high-level reduction.

Furthermore, due to its high content of calcium, LD slag could be used in favorable thermal processes with fuels that contain high levels of phosphorus, such as agriculture residues or waste; this is valid for all technical applications, such as OCAC, CLC and CLG. Given the higher levels of phosphorus in such fuels, the agglomeration occurs through the second mechanism, as described in Section □. Higher levels of calcium are favorable because they induce higher melting temperatures in the Ca-P-K system [155] and the Ca-Si-K system [76]. This suggests that LD slag could be used as an additive in a conventional fluidized bed boiler, based on both its OCAC properties and interactions with the ash. However, since the phosphorus system is very complex and LD slag itself contains phosphorus, the interactions with phosphorus-containing ash need to be further investigated, and compared with the results obtained with synthetic ashes in **Paper VI** and in the paper of Störner et al. [156]. All in all, the chemistry of LD slag is very complex and can influence the performance differently both in respect to fuel and application. Further, the composition of LD slag differs depending on the origin and may vary in e.g. iron, calcium, magnesium and vanadium content.

6.2 Future access of and demand for LD slag as an oxygen carrier

The future availability of LD slag is dependent upon the dominant process for steelmaking. The steel industry is currently facing one of the greatest transitions since the start of the industrial revolution: producing steel using hydrogen instead of coal. Producing steel with hydrogen does not entail producing a better product, and it is neither safer nor easier than using conventional methods. The transition is related to the goals of rendering the steel industry in Europe carbon-neutral and producing steel from renewable energy sources [157]. Thus, using hydrogen is the most convenient and efficient method to use renewable energy sources and to minimize carbon emissions from the industry. However, the production of carbon-neutral hydrogen is associated with high demands for renewable and low-cost electricity [158].

This transition will affect the usability of LD slag as an oxygen carrier in two major ways. First, in a steel manufacturing process that uses hydrogen, no LD slag is formed. The reason for this is that the sponge iron formed in the hydrogen-based ironmaking process is converted to steel in an electric arc furnace rather than in an LD converter [157]. This suggests that the amount of LD slag produced during steelmaking would decline in the future and will only be produced by the older coal-based plants. Second, the hydrogen produced on a large scale for these processes will probably come from electrolysis using renewable energy. The production of large amounts of hydrogen by electrolysis will generate pure oxygen as a byproduct. Given the large amounts of hydrogen needed in steel manufacturing, oxygen may become a bulk product in the future that is locally available at a comparatively low price. Low-price, high-purity oxygen would dramatically reduce the cost of oxyfuel combustion, since one of the most expensive components of the process (the air separation unit) would be unnecessary [159]. Retrofitting a conventional boiler to an oxyfuel boiler is also possible and is not too difficult [5], which is an advantage of the oxyfuel technology compared to, for example, CLC. Suggestions have been made regarding the retrofitting of a conventional fluidized bed boiler with a fuel reactor to form

a CLC plant [10]. However, potential issues with heat transport and ensuring sufficient circulation suggest that larger units should be designed for CLC from the beginning. Examples of full-scale designs also emphasize the need for designed units to achieve sufficient circulation [57].

Access to LD slag is dependent upon technological developments and energy costs, as is the demand for LD slag. The shortest path to implementation of an oxygen carrier at conventional scale is OCAC. It is, however, debatable whether LD slag is favorable for OCAC applications, as discussed in Section 6.1. Today, the commercialization of chemical looping, either CLC or CLG, on an industrial scale in which large amounts of LD slag would be consumed, is not imminent. Should LD slag become the preferred oxygen carrier for, e.g., CLG, it would most likely be because it offers a combination of benefits regarding decreased levels of tars and effects on the raw gas composition. These benefits would need to be balanced against the cost of handling the waste streams containing the additional dust in the fly ash from LD slag. As such, a comprehensive economic study of concerning this is required.

Chapter 7

7. Conclusion

In this thesis, LD slag, which is a byproduct of steelmaking, was investigated for usage as bed material in thermal conversion processes based on fluidized beds. More specifically, the main objective of the evaluation of LD slag was to understand whether LD slag is a suitable oxygen carrier for OCAC, CLC and/or CLG. Reactors ranging in size from laboratory scale to semi-industrial scale and several characterization methods were used to acquire a better understanding of the chemical and physical properties of the LD slag. For comparison, a range of other well-known materials was also investigated.

From these studies it can be concluded that LD slag has several beneficial properties for usage in a thermal conversion process of solid fuels. To summarize, LD slag possesses the following properties:

- Sufficient oxygen carrying capacity.
- The oxygen carrying phases is mainly magnetite-wüstite, thereby enables hydrogen formation of steam via the water splitting reaction.
- Reactivities towards gaseous and solid fuels that are similar to those of the benchmark, iron-based oxygen carrier ilmenite.
- Initially high amounts of fines, however, gradually decreased attrition to acceptable levels.
- A lower tendency to agglomerate compared to sand in the presence of alkali.
- A lack of ability to bind alkali in a stable phase, resulting in higher amounts of alkali in the gas phase being available for other reactions. This results in:
    - Potentially increased CO emissions during OCAC operation;
    - Higher level of tar conversion;
    - Increased gasification rate;

    - When alkali is available or LD slag that contains ash is mixed with silica, the silica can react with the available alkali rather than the LD slag, thereby generating potassium silicate with a low melting point, leading to agglomeration.
- Contains free calcium oxide, resulting in:
    - Catalytic properties towards the WGS reaction;
    - Catalytic towards conversion of tars;
    - Can react with sulfur forming $CaSO_4$ and CaS;
    - Can interact with phosphorus containing ash resulting in a higher melting temperature, decreasing the risk of agglomeration;
    - Affects the storage properties of LD slag since it can react with humidity.

Given these properties, it can be concluded that LD slag could be a suitable oxygen carrier for both chemical looping applications as well as OCAC. In particular, it may be applicable for processes that should avoid the use of a virgin bed material, such as waste combustion. For any application purposes, it needs to be considered that the high amounts of alkali will be present in the gas phase where the fuel is added. This suggests that LD slag is most suitable for CLG, where alkali is available for the gasification and tar cracking and the material is at the same time catalytic towards the WGS reaction. LD slag also has a low oxygen-carrying potential, which makes it suitable for a process like CLG that encounters problems associated with a strong relationship between oxygen transfer and heat transfer.

Should LD slag be considered as an oxygen carrier in a full-scale process, the entire supply chain needs to be considered, from the future availability of the slag and the process of extracting the appropriate size fraction to recycling and waste management. Given the transition currently occurring in the steel manufacturing industry, the supply of LD slag may dwindle. Nevertheless, LD slag will continue to be produced for the upcoming years and are already stored for extensive use.

Abbreviations and Nomenclature

BECCS	Bio-Energy with Carbon Capture and Storage
CLC	Chemical Looping Combustion
CLG	Chemical Looping Gasification
CLOU	Chemical Looping with Oxygen Uncoupling
CLWS	Chemical Looping with Water Splitting
DFB	Dual Fluidized Bed
OCAC	Oxygen Carrier Aided Combustion
WGS	Water-Gas-Shift
SEM-EDS	Scanning Electron Microscopy – Energy Dispersive X-ray Spectroscopy
XRD	X-Ray Diffraction
CO/C_t	Ratio of carbon monoxide to total carbon (CO, CO_2, CH_4)
H_2/CO	Ratio of hydrogen to carbon monoxide
n_i	Amount of substance *i* [mol]
m_i	Mass of substance *i* [g]
x_i	Fraction of substance *i* in gas [mol/m^3]
K_{eq}	Equilibrium constant for the WGS reaction
Q_i	The reaction quotient at the time *i*
P	Pressure [Pa]
V	Volume [m^3]
R	Gas constant in Ideal Gas Law
T	Temperature [K]
t	Time [s]
r	Char conversion rate as a function of time [(g/s)/g]
γ_{CO}	CO_2 yield from the conversion of CO
ω	Mass conversion on oxygen carrier, with a valued between 0 and 1
X_c	Conversion degree of char, with a value between 0 and 1
$\dot{}$	Indicates a flow

References

1. United Nations *Convention on Climate Change: Climate Agreement of Paris.*; 2015;
2. Conference of the Parties *Decision-/CP.26 Glasgow Climate Pact*; 2021;
3. IPCC; Masson-Delmotte, V.; Zhai, P.; Pirani, A.; Connors, S.L.; Péan, C.; Berger, S.; Caud, N.; Chen, Y.; Goldfarb, L.; et al. *Climate Change 2021: The Physical Science Basis. Contribution of Working Group I to the Sixth Assessment Report of the Intergovernmental Panel on Climate Change*; Cambridge University Press, 2021;
4. Masson-Delmotte, V.; Zhai, P.; Pörtner, H.O.; Roberts, D.; Skea, J.; Shukla, P.R.; Pirani, A.; Moufouma-Okia, W.; Péan, C.; Pidcock, R.; et al. *IPCC, 2018: Global Warming of 1.5°C. An IPCC Special Report on the Impacts of Global Warming of 1.5°C above Pre-Industrial Levels and Related Global Greenhouse Gas Emission Pathways, in the Context of Strengthening the Global Response to the Threat of Cli*; 2018;
5. IPCC; Metz, B.; Davidson, O.; de Coninck, H.C.; Loos, M.; Meyer, L.A. *IPCC Special Report on Carbon Dioxide Capture and Storage.*; 2005; Vol. 33;.
6. Azar, C.; Lindgren, K.; Obersteiner, M.; Riahi, K.; Detlef, ·; Van Vuuren, P.; Michel, · K; Den Elzen, G.J.; Möllersten, K.; Larson, E.D.; et al. The Feasibility of Low CO 2 Concentration Targets and the Role of Bio-Energy with Carbon Capture and Storage (BECCS). *Climatic Change* **2010**, *100*, 195–202, doi:10.1007/s10584-010-9832-7.
7. IPCC *Climate Change 2014: Mitigation of Climate Change. Summary for Policymakers and Technical Summary*; 2014; ISBN 9781107415416.
8. Thunman, H.; Lind, F.; Breitholtz, C.; Berguerand, N.; Seemann, M. Using an Oxygen-Carrier as Bed Material for Combustion of Biomass in a 12-MWth Circulating Fluidized-Bed Boiler. *Fuel* **2013**, *113*, 300–309, doi:10.1016/j.fuel.2013.05.073.
9. Berdugo Vilches, T.; Lind, F.; Rydén, M.; Thunman, H. Experience of More than 1000 h of Operation with Oxygen Carriers and Solid Biomass at Large Scale. *Applied Energy* **2017**, *190*, 1174–1183, doi:10.1016/j.apenergy.2017.01.032.
10. Lyngfelt, A. Chemical Looping Combustion: Status and Development Challenges. *Energy and Fuels* **2020**, *34*, 9077–9093, doi:10.1021/acs.energyfuels.0c01454.
11. Zhao, X.; Zhou, H.; Sikarwar, V.S.; Zhao, M.; Park, A.H.A.; Fennell, P.S.; Shen, L.; Fan, L.S. Biomass-Based Chemical Looping Technologies: The Good, the Bad and the Future. *Energy and Environmental Science* **2017**, *10*, 1885–1910, doi:10.1039/c6ee03718f.
12. Adánez, J.; De Diego, L.F.; García-Labiano, F.; Gayán, P.; Abad, A.; Palacios, J.M. Selection of Oxygen Carriers for Chemical-Looping Combustion. *Energy and Fuels* **2004**, *18*, 371–377, doi:10.1021/ef0301452.
13. Störner, F.; Lind, F.; Rydén, M. Oxygen Carrier Aided Combustion in Fluidized Bed Boilers in Sweden—Review and Future Outlook with Respect to Affordable Bed Materials. *Applied Sciences (Switzerland)* **2021**, *11*, 7935, doi:10.3390/app11177935.

14. Mantripragada, H.C.; Zhai, H.; Rubin, E.S. Boundary Dam or Petra Nova – Which Is a Better Model for CCS Energy Supply? *International Journal of Greenhouse Gas Control* **2019**, *82*, 59–68, doi:10.1016/j.ijggc.2019.01.004.

15. Strömberg, L.; Lindgren, G.; Jacoby, J.; Giering, R.; Anheden, M.; Burchhardt, U.; Altmann, H.; Kluger, F.; Stamatelopoulos, G.N. Update on Vattenfall's 30 MWth Oxyfuel Pilot Plant in Schwarze Pumpe. *Energy Procedia* **2009**, *1*, 581–589, doi:10.1016/j.egypro.2009.01.077.

16. Boot-Handford, M.E.; Abanades, J.C.; Anthony, E.J.; Blunt, M.J.; Brandani, S.; Mac Dowell, N.; Fernández, J.R.; Ferrari, M.C.; Gross, R.; Hallett, J.P.; et al. Carbon Capture and Storage Update. *Energy and Environmental Science* **2014**, *7*, 130–189, doi:10.1039/c3ee42350f.

17. Adánez, J.; Abad, A.; Mendiara, T.; Gayán, P.; de Diego, L.F.; García-Labiano, F. Chemical Looping Combustion of Solid Fuels. *Progress in Energy and Combustion Science* **2018**, doi:10.1016/j.pecs.2017.07.005.

18. Sutton, D.; Kelleher, B.; Ross, J.R.H. Review of Literature on Catalysts for Biomass Gasification. *Fuel Processing Technology* **2001**, *73*, 155–173, doi:10.1016/S0378-3820(01)00208-9.

19. Lyngfelt, A.; Linderholm, C. Chemical-Looping Combustion of Solid Fuels - Technology Overview and Recent Operational Results in 100 KW Unit. *Energy Procedia* **2014**, *63*, 98–112, doi:10.1016/j.egypro.2014.11.011.

20. Leion, H.; Mattisson, T.; Lyngfelt, A. The Use of Petroleum Coke as Fuel in Chemical-Looping Combustion. *Fuel* **2007**, *86*, 1947–1958, doi:10.1016/j.fuel.2006.11.037.

21. Mattisson, T.; Lyngfelt, A.; Leion, H. Chemical-Looping with Oxygen Uncoupling for Combustion of Solid Fuels. *International Journal of Greenhouse Gas Control* **2009**, *3*, 11–19, doi:10.1016/j.ijggc.2008.06.002.

22. Zevenhoven, M.; Yrjas, P.; Hupa, M. 14 Ash-Forming Matter and Ash-Related Problems. In *Handbook of Combustion Vol.4: Solid Fuels*; Lackner, M., Winter, F., Agarwal, A.K., Eds.; WILEY-VCH Verlag GmbH & Co. KGaA, 2010; pp. 493–531 ISBN 978-3-527-32449-1.

23. Zevenhoven, M.; Yrjas, P.; Skrifvars, B.J.; Hupa, M. Characterization of Ash-Forming Matter in Various Solid Fuels by Selective Leaching and Its Implications for Fluidized-Bed Combustion. *Energy and Fuels* **2012**, *26*, 6366–6386, doi:10.1021/ef300621j.

24. Adánez, J.; De Diego, L.F.; García-Labiano, F.; Gayán, P.; Abad, A.; Palacios, J.M. Selection of Oxygen Carriers for Chemical-Looping Combustion. *Energy and Fuels* **2004**, *18*, 371–377, doi:10.1021/ef0301452.

25. Bhavsar, S.; Najera, M.; Solunke, R.; Veser, G. Chemical Looping: To Combustion and Beyond. *Catalysis Today* **2014**, *228*, 96–105, doi:10.1016/j.cattod.2013.12.025.

26. Knutsson, P.; Linderholm, C. Characterization of Ilmenite Used as Oxygen Carrier in a 100 KW Chemical-Looping Combustor for Solid Fuels. *Applied Energy* **2015**, *157*, 368–373, doi:10.1016/j.apenergy.2015.05.122.

27. Mattisson, T.; Keller, M.; Linderholm, C.; Moldenhauer, P.; Rydén, M.; Leion, H.; Lyngfelt, A. Chemical-Looping Technologies Using Circulating Fluidized Bed Systems: Status of Development. *Fuel Processing Technology* **2018**, *172*, 1–12, doi:10.1016/j.fuproc.2017.11.016.

28. Ge, H.; Guo, W.; Shen, L.; Song, T.; Xiao, J. Experimental Investigation on Biomass Gasification Using Chemical Looping in a Batch Reactor and a Continuous Dual Reactor. *Chemical Engineering Journal* **2016**, *286*, 689–700, doi:10.1016/j.cej.2015.11.008.

29. Ge, H.; Guo, W.; Shen, L.; Song, T.; Xiao, J. Biomass Gasification Using Chemical Looping in a 25 KW Th Reactor with Natural Hematite as Oxygen Carrier. *Chemical Engineering Journal* **2016**, *286*, 174–183, doi:10.1016/j.cej.2015.10.092.

30. Larsson, A.; Israelsson, M.; Lind, F.; Seemann, M.; Thunman, H. Using Ilmenite to Reduce the Tar Yield in a Dual Fluidized Bed Gasification System. *Energy and Fuels* **2014**, *28*, 2632–2644, doi:10.1021/ef500132p.

31. Pissot, S.; Berdugo Vilches, T.; Maric, J.; Cañete Vela, I.; Thunman, H.; Seemann, M. Thermochemical Recycling of Automotive Shredder Residue by Chemical-Looping Gasification Using the Generated Ash as Oxygen Carrier. *Energy and Fuels* **2019**, *33*, 11552–11566, doi:10.1021/acs.energyfuels.9b02607.

32. Dieringer, P.; Marx, F.; Alobaid, F.; Ströhle, J.; Epple, B. Process Control Strategies in Chemical Looping Gasification-A Novel Process for the Production of Biofuels Allowing for Net Negative CO2 Emissions. *Applied Sciences (Switzerland)* **2020**, *10*, 4271, doi:10.3390/app10124271.

33. Pissot, S.; Berdugo Vilches, T.; Thunman, H.; Seemann, M. Effect of Ash Circulation on the Performance of a Dual Fluidized Bed Gasification System. *Biomass and Bioenergy* **2018**, *115*, 45–55, doi:10.1016/j.biombioe.2018.04.010.

34. Larsson, A.; Gunnarsson, I.; Tengberg, F. *The GoBiGas Project - Demonstration of the Production of Biomethane from Biomass via Gasification*; 2018;

35. Thunman, H.; Seemann, M.; Berdugo Vilches, T.; Maric, J.; Pallares, D.; Ström, H.; Berndes, G.; Knutsson, P.; Larsson, A.; Breitholtz, C.; et al. Advanced Biofuel Production via Gasification – Lessons Learned from 200 Man-Years of Research Activity with Chalmers' Research Gasifier and the GoBiGas Demonstration Plant. *Energy Science and Engineering* **2018**, *6*, 6–34, doi:10.1002/ese3.188.

36. Dara, S.; Khan, I.; Al Jenaibi, E.; Dhebar, S.; Srivastava, G.; Shehata, M. Techno-Economic Assessment of Blue Hydrogen Technologies.; OnePetro, October 31 2022.

37. Moldenhauer, P.; Corcoran, A.; Thunman, H.; Lind, F. A Scale-Up Project for Operating a 115 MWth Biomass-Fired CFB Boiler with Oxygen Carriers as Bed Material.; Proceedings of the 5th International Conference on Chemical Looping, 2018; pp. 24–27.

38. Lind Fredrik et al. 12,000 Hours of Operation with Oxygen-Carriers in Industrially Relevant Scale. *VGB PowerTech* **2017**, *7*.

39. Caram, H.S.; Gupta, R.; Thomann, H.; Ni, F.; Weston, S.C.; Afeworki, M. A Simple Thermodynamic Tool for Assessing Energy Requirements for Carbon Capture Using Solid or Liquid Sorbents. *International Journal of Greenhouse Gas Control* **2020**, *97*, doi:10.1016/j.ijggc.2020.102986.

40. Mathekga, H.I.; Oboirien, B.O.; North, B.C. A Review of Oxy-Fuel Combustion in Fluidized Bed Reactors. *International Journal of Energy Research* **2016**, *40*, 878–902, doi:10.1002/er.3486.

41. Koornneef, J.; Junginger, M.; Faaij, A. Development of Fluidized Bed Combustion-An Overview of Trends, Performance and Cost. *Progress in Energy and Combustion Science* **2007**, *33*, 19–55, doi:10.1016/j.pecs.2006.07.001.

42. Adanez, J.; Abad, A.; Garcia-Labiano, F.; Gayan, P.; De Diego, L.F. Progress in Chemical-Looping Combustion and Reforming Technologies. *Progress in Energy and Combustion Science* **2012**, *38*, 215–282, doi:10.1016/j.pecs.2011.09.001.

43. Jerndal, E.; Mattisson, T.; Lyngfelt, A. Thermal Analysis of Chemical-Looping Combustion. *Chemical Engineering Research and Design* **2006**, *84*, 795–806, doi:10.1205/cherd05020.

44. Abad, A.; Adánez-Rubio, I.; Gayán, P.; García-Labiano, F.; de Diego, L.F.; Adánez, J. Demonstration of Chemical-Looping with Oxygen Uncoupling (CLOU) Process in a 1.5kWth Continuously Operating Unit Using a Cu-Based Oxygen-Carrier. *International Journal of Greenhouse Gas Control* **2012**, *6*, 189–200, doi:10.1016/j.ijggc.2011.10.016.

45. Penthor, S.; Zerobin, F.; Mayer, K.; Pröll, T.; Hofbauer, H. Investigation of the Performance of a Copper Based Oxygen Carrier for Chemical Looping Combustion in a 120 KW Pilot Plant for Gaseous Fuels. *Applied Energy* **2015**, *145*, 52–59, doi:10.1016/j.apenergy.2015.01.079.

46. Cho, P.; Mattisson, T.; Lyngfelt, A. Comparison of Iron-, Nickel-, Copper- and Manganese-Based Oxygen Carriers for Chemical-Looping Combustion. *Fuel* **2004**, *83*, 1215–1225, doi:10.1016/j.fuel.2003.11.013.

47. Rydén, M.; Leion, H.; Mattisson, T.; Lyngfelt, A. Combined Oxides as Oxygen-Carrier Material for Chemical-Looping with Oxygen Uncoupling. *Applied Energy* **2014**, *113*, 1924–1932, doi:10.1016/J.APENERGY.2013.06.016.

48. Sundqvist, S.; Arjmand, M.; Mattisson, T.; Rydén, M.; Lyngfelt, A. Screening of Different Manganese Ores for Chemical-Looping Combustion (CLC) and Chemical-Looping with Oxygen Uncoupling (CLOU). *International Journal of Greenhouse Gas Control* **2015**, *43*, 179–188, doi:10.1016/j.ijggc.2015.10.027.

49. Johansson, M. Screening of Oxygen-Carrier Particles Based on Iron-, Manganese-, Copper-and Nickel Oxides for Use in Chemical-Looping Technologies, Chalmers University of Technology, 2007.

50. Rydén, M.; Hanning, M.; Lind, F. Oxygen Carrier Aided Combustion (OCAC) of Wood Chips in a 12 MWth Circulating Fluidized Bed Boiler Using Steel Converter Slag as Bed Material. *Applied Sciences* **2018**, *8*, 2657, doi:10.3390/app8122657.

51. Mattisson, T.; Lyngfelt, A.; Cho, P. The Use of Iron Oxide as an Oxygen Carrier in Chemical-Looping Combustion of Methane with Inherent Separation of CO2. *Fuel* **2001**, *80*, 1953–1962, doi:10.1016/S0016-2361(01)00051-5.

52. Xiao, R.; Song, Q.; Zhang, S.; Zheng, W.; Yang, Y. Pressurized Chemical-Looping Combustion of Chinese Bituminous Coal: Cyclic Performance and Characterization of Iron Ore-Based Oxygen Carrier. *Energy Fuels* **2010**, *24*, 1449–1463, doi:10.1021/ef901070c.

53. Shen, L.; Wu, J.; Xiao, J.; Song, Q.; Xiao, R. Chemical-Looping Combustion of Biomass in a 10 KWth Reactor with Iron Oxide as an Oxygen Carrier. *Energy and Fuels* **2009**, *23*, 2498–2505, doi:10.1021/ef900033n.

54. Jerndal, E.; Leion, H.; Axelsson, L.; Ekvall, T.; Hedberg, M.; Johansson, K.; Källén, M.; Svensson, R.; Mattisson, T.; Lyngfelt, A. Using Low-Cost Iron-Based Materials as Oxygen Carriers for Chemical Looping Combustion Chemical Looping -An Alternative Concept for Efficient and Clean Use of Fossil Resources La Boucle Chimique -Un Concept Alternatif Pour Un Usage Propre et Efficace Des . *Oil & Gas Science and Technology – Rev. IFP Energies nouvelles* **2011**, *66*, 235–248, doi:10.2516/ogst/2010030.

55. Ksepko, E. Sewage Sludge Ash as an Alternative Low-Cost Oxygen Carrier for Chemical Looping Combustion. In Proceedings of the Journal of Thermal Analysis and Calorimetry; Springer Netherlands, June 11 2014; Vol. 116, pp. 1395–1407.

56. Xu, L.; Schwebel, G.L.; Knutsson, P.; Leion, H.; Li, Z.; Cai, N. Performance of Industrial Residues as Low Cost Oxygen Carriers. *Energy Procedia* **2017**, *114*, 361–370, doi:10.1016/j.egypro.2017.03.1178.

57. Lyngfelt, A.; Pallarès, D.; Linderholm, C.; Lind, F.; Thunman, H.; Leckner, B. Achieving Adequate Circulation in Chemical Looping Combustion─Design Proposal for a 200 MWth Chemical Looping Combustion Circulating Fluidized Bed Boiler. *Energy and Fuels* **2021**, doi:10.1021/acs.energyfuels.1c03615.

58. Pröll, T.; Mayer, K.; Bolhàr-Nordenkampf, J.; Kolbitsch, P.; Mattisson, T.; Lyngfelt, A.; Hofbauer, H. Natural Minerals as Oxygen Carriers for Chemical Looping Combustion in a Dual Circulating Fluidized Bed System. *Energy Procedia* **2009**, *1*, 27–34, doi:10.1016/j.egypro.2009.01.006.

59. Lyngfelt, A.; Leckner, B. A 1000 MWth Boiler for Chemical-Looping Combustion of Solid Fuels – Discussion of Design and Costs. *Applied Energy* **2015**, *157*, 475–487, doi:10.1016/j.apenergy.2015.04.057.

60. Zhang, W.; Zhu, Z.; Cheng, C.Y. A Literature Review of Titanium Metallurgical Processes. *Hydrometallurgy* **2011**, *108*, 177–188, doi:10.1016/J.HYDROMET.2011.04.005.

61. Leion, H.; Lyngfelt, A.; Johansson, M.; Jerndal, E.; Mattisson, T. The Use of Ilmenite as an Oxygen Carrier in Chemical-Looping Combustion. *Chemical Engineering Research and Design* **2008**, *86*, 1017–1026, doi:10.1016/j.cherd.2008.03.019.

62. Corcoran, A.; Marinkovic, J.; Lind, F.; Thunman, H.; Knutsson, P.; Seemann, M. Ash Properties of Ilmenite Used as Bed Material for Combustion of Biomass in a Circulating Fluidized Bed Boiler. *Energy and Fuels* **2014**, *28*, 7672–7679, doi:10.1021/ef501810u.

63. Corcoran, A.; Knutsson, P.; Lind, F.; Thunman, H. Comparing the Structural Development of Sand and Rock Ilmenite during Long-Term Exposure in a Biomass Fired 12 MWth CFB-Boiler. *Fuel Processing Technology* **2018**, *171*, 39–44, doi:10.1016/j.fuproc.2017.11.004.

64. World Crude Steel Production - Summary Available online: https://www.worldsteel.org/en/dam/jcr:dcd93336-2756-486e-aa7f-64f6be8e6b1e/2018%2520global%2520crude%2520steel%2520production.pdf (accessed on 2 September 2019).

65. Chand, S.; Paul, B.; Kumar, M. Sustainable Approaches for LD Slag Waste Management in Steel Industries: A Review. *Metallurgist* **2016**, *60*, 116–128, doi:10.1007/s11015-016-0261-3.

66. Roudier, S.; Sancho, L.D.; Remus, R.; Aguado-Monsonet, M. *Best Available Techniques (BAT) Reference Document for Iron and Steel Production*; 2013;

67. Yildirim, I.Z.; Prezzi, M. Chemical, Mineralogical, and Morphological Properties of Steel Slag. *Advances in Civil Engineering* **2011**, *2011*, 1–13, doi:10.1155/2011/463638.

68. Tossavainen, M.; Engstrom, F.; Yang, Q.; Menad, N.; Lidstrom Larsson, M.; Bjorkman, B. Characteristics of Steel Slag under Different Cooling Conditions. *Waste Management* **2007**, *27*, 1335–1344, doi:10.1016/j.wasman.2006.08.002.

69. Motz, H.; Geiseler, J. Products of Steel Slags an Opportunity to Save Natural Resources. *Waste Management* **2001**, *21*, 285–293, doi:10.1016/S0956-053X(00)00102-1.

70. Vachirapatama, N.; Jirakiattikul, Y.; Dicinoski, G.; Townsend, A.T.; Haddad, P.R. Effect of Vanadium on Plant Growth and Its Accumulation in Plant Tissues. *Songklanakarin Journal of Science and Technology* **2011**, *33*, 255–261.

71. Lundkvist, K.; Brämming, M.; Larsson, M.; Samuelsson, C. System Analysis of Slag Utilisation from Vanadium Recovery in an Integrated Steel Plant. *Journal of Cleaner Production* **2013**, *47*, 43–51, doi:10.1016/J.JCLEPRO.2012.09.002.

72. Attah, M.; Hildor, F.; Yilmaz, D.; Leion, H. Vanadium Recovery from Steel Converter Slag Utilised as an Oxygen Carrier in Oxygen Carrier Aided Combustion (OCAC). *Journal of Cleaner Production* **2021**, 126159, doi:10.1016/j.jclepro.2021.126159.

73. Keller, M.; Leion, H.; Mattisson, T.; Thunman, H. Investigation of Natural and Synthetic Bed Materials for Their Utilization in Chemical Looping Reforming for Tar Elimination in Biomass-Derived Gasification Gas. *Energy and Fuels* **2014**, *28*, 3833–3840, doi:10.1021/ef500369c.

74. Zinlt, F.; Ljungdahl, B. *Alternativa Bäddmaterial i Fb/Cfb-Pannor - Svensk Fjärrvärme*; 2004;

75. Rydén, M.; Hanning, M.; Corcoran, A.; Lind, F. Oxygen Carrier Aided Combustion (OCAC) of Wood Chips in a Semi-Commercial Circulating Fluidized Bed Boiler Using Manganese Ore as Bed Material. *Applied Sciences (Switzerland)* **2016**, *6*, 1–19, doi:10.3390/app6110347.

76. Elled, A.L.; Åmand, L.E.; Steenari, B.M. Composition of Agglomerates in Fluidized Bed Reactors for Thermochemical Conversion of Biomass and Waste Fuels: Experimental Data in Comparison with Predictions by a Thermodynamic Equilibrium Model. *Fuel* **2013**, *111*, 696–708, doi:10.1016/j.fuel.2013.03.018.

77. Gu, H.; Shen, L.; Xiao, J.; Zhang, S.; Song, T. Chemical Looping Combustion of Biomass/Coal with Natural Iron Ore as Oxygen Carrier in a Continuous Reactor. *Energy & Fuels* **2011**, *25*, 446–455, doi:10.1021/ef101318b.

78. Bao, J.; Li, Z.; Cai, N. Promoting the Reduction Reactivity of Ilmenite by Introducing Foreign Ions in Chemical Looping Combustion. *Industrial & Engineering Chemistry Research* **2013**, *52*, 6119–6128, doi:10.1021/ie400237p.

79. Arjmand, M.; Leion, H.; Mattisson, T.; Lyngfelt, A. Investigation of Different Manganese Ores as Oxygen Carriers in Chemical-Looping Combustion (CLC) for Solid Fuels. *Applied Energy* **2014**, *113*, 1883–1894, doi:10.1016/j.apenergy.2013.06.015.

80. El-Tawil, S.Z.; Morsi, I.M.; Yehia, A.; Francis, A.A. Alkali Reductive Roasting of Ilmenite Ore. *Canadian Metallurgical Quarterly* **1996**, *35*, 31–37, doi:10.1016/0008-4433(95)00039-9.

81. Zevenhoven, M.; Sevonius, C.; Salminen, P.; Lindberg, D.; Brink, A.; Yrjas, P.; Hupa, L. Defluidization of the Oxygen Carrier Ilmenite – Laboratory Experiments with Potassium Salts. *Energy* **2018**, *148*, 930–940, doi:10.1016/j.energy.2018.01.184.

82. Corcoran, A.; Knutsson, P.; Lind, F.; Thunman, H. Mechanism for Migration and Layer Growth of Biomass Ash on Ilmenite Used for Oxygen Carrier Aided Combustion. *Energy and Fuels* **2018**, *32*, 8845–8856, doi:10.1021/acs.energyfuels.8b01888.

83. Kuba, M.; He, H.; Kirnbauer, F.; Skoglund, N.; Boström, D.; Öhman, M.; Hofbauer, H. Mechanism of Layer Formation on Olivine Bed Particles in Industrial-Scale Dual Fluid Bed Gasification of Wood. *Energy and Fuels* **2016**, *30*, 7410–7418, doi:10.1021/acs.energyfuels.6b01522.

84. Hannl, T.K.; Faust, R.; Kuba, M.; Knutsson, P.; Berdugo Vilches, T.; Seemann, M.; Öhman, M. Layer Formation on Feldspar Bed Particles during Indirect Gasification of Wood. 2. Na-Feldspar. *Energy & Fuels* **2019**, *33*, 7333–7346, doi:10.1021/acs.energyfuels.9b01292.

85. Jamil, R.; Ming, L.; Jamil, I.; and Rizwan Jamil Application and Development Trend of Flue Gas Desulfurization (FGD) Process: A Review. *International Journal of Innovation and Applied Studies* **2013**, *4*, 286–297.

86. A History of Flue Gas Desulfurization Systems since 1850: Research, Development and Demonstration. *Journal of the Air Pollution Control Association* **1977**, *27*, 948–961, doi:10.1080/00022470.1977.10470518.

87. Montagna, J.C.; Lenc, J.F.; Vogel, G.J.; Jonke, A.A. Regeneration of Sulfated Dolomite from a Coal-Fired FBC Process by Reductive Decomposition of Calcium Sulfate in a Fluidized Bed. *Ind. Eng. Chem., Process Des. Dev* **1977**, *16*, 230–236.

88. Andersson, S.; Blomqvist, E.W.; Bäfver, L.; Jones, F.; Davidsson, K.; Froitzheim, J.; Karlsson, M.; Larsson, E.; Liske, J. Sulfur Recirculation for Increased Electricity Production in Waste-to-Energy Plants. *Waste Management* **2014**, *34*, 67–78, doi:10.1016/j.wasman.2013.09.002.

89. Wang, B.; Yan, R.; Lee, D.H.; Liang, D.T.; Zheng, Y.; Zhao, H.; Zheng, C. Thermodynamic Investigation of Carbon Deposition and Sulfur Evolution in Chemical Looping Combustion with Syngas. *Energy and Fuels* **2008**, *22*, 1012–1020, doi:10.1021/ef7005673.

90. Moldenhauer, P.; Rydén, M.; Mattisson, T.; Younes, M.; Lyngfelt, A. The Use of Ilmenite as Oxygen Carrier with Kerosene in a 300W CLC Laboratory Reactor with Continuous Circulation. *Applied Energy* **2013**, *113*, 1846–1854, doi:10.1016/j.apenergy.2013.06.009.

91. Forero, C.R.; Gayán, P.; García-Labiano, F.; de Diego, L.F.; Abad, A.; Adánez, J. Effect of Gas Composition in Chemical-Looping Combustion with Copper-Based Oxygen Carriers: Fate of Sulphur. *International Journal of Greenhouse Gas Control* **2010**, *4*, 762–770, doi:10.1016/j.ijggc.2010.04.002.

92. Adánez-Rubio, I.; Abad, A.; Gayán, P.; García-Labiano, F.; De Diego, L.F.; Adánez, J. The Fate of Sulphur in the Cu-Based Chemical Looping with Oxygen Uncoupling (CLOU) Process. *Applied Energy* **2013**, *113*, 1855–1862, doi:10.1016/j.apenergy.2013.06.022.

93. Ma, J.; Mei, D.; Wang, C.; Tian, X.; Liu, Z.; Zhao, H. Sulfur Fate during In-Situ Gasification Chemical Looping Combustion (IG-CLC) of Coal. *Chemical Engineering Journal* **2021**, *406*, 126773, doi:10.1016/j.cej.2020.126773.

94. Vigoureux, M.; Knutsson, P.; Lind, F. Sulfur Uptake during Oxygen-Carrier-Aided Combustion with Ilmenite. *Energy and Fuels* **2020**, *34*, 7735–7742, doi:10.1021/acs.energyfuels.0c00420.

95. Leion, H.; Frick, V.; Hildor, F. Experimental Method and Setup for Laboratory Fluidized Bed Reactor Testing. *Energies* **2018**, *11*, 2505, doi:10.3390/en11102505.

96. Berdugo Vilches, T.; Marinkovic, J.; Seemann, M.; Thunman, H. Comparing Active Bed Materials in a Dual Fluidized Bed Biomass Gasifier: Olivine, Bauxite, Quartz-Sand, and Ilmenite. *Energy and Fuels* **2016**, *30*, 4848–4857, doi:10.1021/acs.energyfuels.6b00327.

97. Yang, W.; Zhao, H.; Wang, K.; Zheng, C. Synergistic Effects of Mixtures of Iron Ores and Copper Ores as Oxygen Carriers in Chemical-Looping Combustion. *Proceedings of the Combustion Institute* **2015**, *35*, 2811–2818, doi:10.1016/j.proci.2014.07.010.

98. Dueso, C.; Abad, A.; García-Labiano, F.; De Diego, L.F.; Gayán, P.; Adánez, J.; Lyngfelt, A. Reactivity of a NiO/Al2O3 Oxygen Carrier Prepared by Impregnation for Chemical-Looping Combustion. *Fuel* **2010**, *89*, 3399–3409, doi:10.1016/j.fuel.2010.03.043.

99. Mattisson, T.; Järdnäs, A.; Lyngfelt, A. Reactivity of Some Metal Oxides Supported on Alumina with Alternating Methane and Oxygen - Application for Chemical-Looping Combustion. *Energy and Fuels* **2003**, *17*, 643–651, doi:10.1021/ef020151i.

100. Otsuka, K.; Wang, Y.; Sunada, E.; Yamanaka, I. Direct Partial Oxidation of Methane to Synthesis Gas by Cerium Oxide. *Journal of Catalysis* **1998**, *175*, 152–160, doi:10.1006/jcat.1998.1985.

101. Berguerand, N.; Lyngfelt, A. Design and Operation of a 10 KWth Chemical-Looping Combustor for Solid Fuels - Testing with South African Coal. *Fuel* **2008**, *87*, 2713–2726, doi:10.1016/j.fuel.2008.03.008.

102. Gogolev, I.; Soleimanisalim, A.H.; Linderholm, C.; Lyngfelt, A. Commissioning, Performance Benchmarking, and Investigation of Alkali Emissions in a 10 KWth Solid Fuel Chemical Looping Combustion Pilot. *Fuel* **2020**, 119530, doi:10.1016/j.fuel.2020.119530.

103. Israelsson, M.; Seemann, M.; Thunman, H. Assessment of the Solid-Phase Adsorption Method for Sampling Biomass-Derived Tar in Industrial Environments. *Energy and Fuels* **2013**, *27*, 7569–7578, doi:10.1021/ef401893j.

104. Azimi, G.; Keller, M.; Mehdipoor, A.; Leion, H. Experimental Evaluation and Modeling of Steam Gasification and Hydrogen Inhibition in Chemical-Looping Combustion with Solid Fuel. *International Journal of Greenhouse Gas Control* **2012**, *11*, 1–10, doi:10.1016/j.ijggc.2012.07.018.

105. Moe, J.M. Design of Water-Gas Shift Reactors. *Chem. Eng. Prog.* **1962**, *58*, 33–36.

106. Bustamante, F.; Enick, R.M.; Cugini, A. V.; Killmeyer, R.P.; Howard, B.H.; Rothenberger, K.S.; Ciocco, M. V.; Morreale, B.D.; Chattopadhyay, S.; Shi, S. High-Temperature Kinetics of the Homogeneous Reverse Water-Gas Shift Reaction. *AIChE Journal* **2004**, *50*, 1028–1041, doi:10.1002/aic.10099.

107. Waligora, J.; Bulteel, D.; Degrugilliers, P.; Damidot, D.; Potdevin, J.L.; Measson, M. Chemical and Mineralogical Characterizations of LD Converter Steel Slags: A Multi-Analytical Techniques Approach. *Materials Characterization* **2010**, *61*, 39–48, doi:10.1016/J.MATCHAR.2009.10.004.

108. Faust, R.; Lamarca, I.; Schaefer, A.; Lind, F. Magnetic Properties of Ilmenite Used for Oxygen Carrier Aided Combustion.; Fluidized Bed Conversion Conference 2022, 2022.

109. Rydén, M.; Moldenhauer, P.; Lindqvist, S.; Mattisson, T.; Lyngfelt, A. Measuring Attrition Resistance of Oxygen Carrier Particles for Chemical Looping Combustion with a Customized Jet Cup. *Powder Technology* **2014**, *256*, 75–86, doi:10.1016/j.powtec.2014.01.085.

110. Störner, F.; Hildor, F.; Leion, H.; Zevenhoven, M.; Hupa, L.; Rydén, M.; Eliasson Störner, F.; Hildor, F.; Leion, H.; Zevenhoven, M.; et al. Potassium Ash Interactions with Oxygen Carriers Steel Converter Slag and Iron Mill Scale in Chemical-Looping Combustion of Biomass – Experimental Evaluation Using Model Compounds. *Energy & Fuels* **2020**, *34*, 2304–2314, doi:10.1021/acs.energyfuels.9b03616.

111. Schwebel, G.L.; Leion, H.; Krumm, W. Comparison of Natural Ilmenites as Oxygen Carriers in Chemical-Looping Combustion and Influence of Water Gas Shift Reaction on Gas Composition. *Chemical Engineering Research and Design* **2012**, *90*, 1351–1360, doi:10.1016/j.cherd.2011.11.017.

112. Li, B.; Wei, L.; Yang, H.; Wang, X.; Chen, H. The Enhancing Mechanism of Calcium Oxide on Water Gas Shift Reaction for Hydrogen Production. *Energy* **2014**, *68*, 248–254, doi:10.1016/j.energy.2014.02.088.

113. Valverde, J.M.; Sanchez-Jimenez, P.E.; Perez-Maqueda, L.A. Limestone Calcination Nearby Equilibrium: Kinetics, CaO Crystal Structure, Sintering and Reactivity. *Journal of Physical Chemistry C* **2015**, *119*, 1623–1641, doi:10.1021/jp508745u.

114. Hildor, F.; Zevenhoven, M.; Brink, A.; Hupa, L.; Leion, H. Understanding the Interaction of Potassium Salts with an Ilmenite Oxygen Carrier under Dry and Wet Conditions. *ACS Omega* 2020, *5*, 22966–22977.

115. Sevonius, C.; Yrjas, P.; Hupa, M. Defluidization of a Quartz Bed - Laboratory Experiments with Potassium Salts. *Fuel* **2014**, *127*, 161–168, doi:10.1016/j.fuel.2013.10.047.

116. Mattison, T.; Hildor, F.; Li, Y.; Linderholm, C. Negative Emissions of Carbon Dioxide through Chemical-Looping Combustion (CLC) and Gasification (CLG) Using Oxygen Carriers Based on Manganese and Iron. *Mitigation and Adaptation Strategies for Global Change* **2019**, doi:10.1007/s11027-019-09860-x.

117. Grimm, A.; Skoglund, N.; Boström, D.; Öhman, M. Bed Agglomeration Characteristics in Fluidized Quartz Bed Combustion of Phosphorus-Rich Biomass Fuels. *Energy and Fuels* **2011**, *25*, 937–947, doi:10.1021/ef101451e.

118. Gogolev, I.; Soleimanisalim, A.H.; Mei, D.; Lyngfelt, A. Effects of Temperature, Operation Mode, and Steam Concentration on Alkali Release in Chemical Looping Conversion of Biomass-Experimental Investigation in a 10 KWthPilot. *Energy and Fuels* **2022**, *36*, 9551–9570, doi:10.1021/acs.energyfuels.1c04353.

119. Ma, T.; Fan, C.; Hao, L.; Li, S.; Jensen, P.A.; Song, W.; Lin, W.; Dam-Johansen, K. Biomass Ash Induced Agglomeration in Fluidized Bed. Part 2: Effect of Potassium Salts in Different Gas Composition. *Fuel Processing Technology* **2018**, *180*, 130–139, doi:10.1016/j.fuproc.2018.08.004.

120. Lyngfelt, A.; Leckner, B. SO2 Capture Fluidised-Bed Boilers: Re-Emission of SO2 Due to Reduction of CaSO4. *Chemical Engineering Science* **1988**, *44*, 207–213, doi:10.1016/0009-2509(89)85058-4.

121. Leion, H.; Mattisson, T.; Lyngfelt, A. Use of Ores and Industrial Products as Oxygen Carriers in Chemical-Looping Combustion. *Energy and Fuels* **2009**, *23*, 2307–2315, doi:10.1021/ef8008629.

122. Teyssié, G.; Leion, H.; Schwebel, G.L.; Lyngfelt, A.; Mattisson, T. Influence of Lime Addition to Ilmenite in Chemical-Looping Combustion (CLC) with Solid Fuels. *Energy and Fuels* **2011**, *25*, 3843–3853, doi:10.1021/ef200623h.

123. Corella, J.; Aznar, M.P.; Delgado, J.; Martinez, M.P.; Aragües, J.L. The Deactivation of Tar Cracking Stones (Dolomites, Calcites, Magnesites) and of Commercial Methane Steam Reforming Catalysts in the Upgrading of the Exit Gas from Steam Fluidized Bed Gasifiers of Biomass and Organic Wastes. *Studies in Surface Science and Catalysis* **1991**, *68*, 249–252, doi:10.1016/S0167-2991(08)62640-3.

124. Milne, T.A.; Evans, R.J. *Biomass Gasifier " Tars ": Their Nature , Formation , and Conversion*; 1998;

125. Keller, M.; Leion, H.; Mattisson, T. Use of CuO/MgAl2O4 and La0.8Sr0.2FeO3/γ-Al2O3 in Chemical Looping Reforming System for Tar Removal from Gasification Gas. *AIChE Journal* **2016**, *62*, 38–45, doi:10.1002/aic.15034.

126. Berdugo Vilches, T.; Seemann, M.; Thunman, H. Influence of In-Bed Catalysis by Ash-Coated Olivine on Tar Formation in Steam Gasification of Biomass. *Energy and Fuels* **2018**, *32*, 9592–9604, doi:10.1021/acs.energyfuels.8b02153.

127. Larsson, A.; Kuba, M.; Berdugo Vilches, T.; Seemann, M.; Hofbauer, H.; Thunman, H. Steam Gasification of Biomass – Typical Gas Quality and Operational Strategies Derived from Industrial-Scale Plants. *Fuel Processing Technology* **2021**, *212*, doi:10.1016/j.fuproc.2020.106609.

128. Arnold, R.A.; Hill, J.M. Catalysts for Gasification: A Review. *Sustainable Energy and Fuels* 2019, *3*, 656–672.

129. Pissot, S.; Berdugo Vilches, T.; Maric, J.; Seemann, M. Chemical Looping Gasification in a 2-4 MWth Dual Fluidized Bed Gasifier. In Proceedings of the 23rd International Conference on Fluidized Bed Conversion; Seoul, Korea, 2018.

130. Oka, S. *Fluidized Bed Combustion*; Marcel Decker Inc., 2004; ISBN 0-8247-4699-6.

131. Kuba, M.; Skoglund, N.; Öhman, M.; Hofbauer, H. A Review on Bed Material Particle Layer Formation and Its Positive Influence on the Performance of Thermo-Chemical Biomass Conversion in Fluidized Beds. *Fuel* **2021**, *291*, 120214, doi:10.1016/J.FUEL.2021.120214.

132. Knutsson, P.; Cantatore, V.; Seemann, M.; Tam, P.L.; Panas, I. Role of Potassium in the Enhancement of the Catalytic Activity of Calcium Oxide towards Tar Reduction. *Applied Catalysis B: Environmental* **2018**, *229*, 88–95, doi:10.1016/j.apcatb.2018.02.002.

133. Sikarwar, V.S.; Zhao, M.; Clough, P.; Yao, J.; Zhong, X.; Memon, M.Z.; Shah, N.; Anthony, E.J.; Fennell, P.S. An Overview of Advances in Biomass Gasification. *Energy and Environmental Science* **2016**, *9*, 2939–2977, doi:10.1039/c6ee00935b.

134. Hüttinger, K.J.; Merdes, W.F. The Carbon-Steam Reaction at Elevated Pressure: Formations of Product Gases and Hydrogen Inhibitions. *Carbon* **1992**, *30*, 883–894, doi:10.1016/0008-6223(92)90011-K.

135. Keller, M.; Leion, H.; Mattisson, T.; Lyngfelt, A. Gasification Inhibition in Chemical-Looping Combustion with Solid Fuels. *Combustion and Flame* **2011**, *158*, 393–400, doi:10.1016/j.combustflame.2010.09.009.

136. Marinkovic, J.; Thunman, H.; Knutsson, P.; Seemann, M. Characteristics of Olivine as a Bed Material in an Indirect Biomass Gasifier. *Chemical Engineering Journal* **2015**, *279*, 555–566, doi:10.1016/j.cej.2015.05.061.

137. Hildor, F.; Zevenhoven, M.; Brink, A.; Hupa, L.; Leion, H. Understanding the Interaction of Potassium Salts with an Ilmenite Oxygen Carrier under Dry and Wet Conditions. *ACS Omega* **2020**, doi:10.1021/acsomega.0c02538.

138. Chen, L.; Bao, J.; Kong, L.; Combs, M.; Nikolic, H.S.; Fan, Z.; Liu, K. Activation of Ilmenite as an Oxygen Carrier for Solid-Fueled Chemical Looping Combustion. *Applied Energy* **2017**, *197*, 40–51, doi:10.1016/j.apenergy.2017.03.127.

139. Adánez, J.; Cuadrat, A.; Abad, A.; Gayán, P.; Diego, L.F.D.; García-Labiano, F. Ilmenite Activation during Consecutive Redox Cycles in Chemical-Looping Combustion. *Energy and Fuels* **2010**, *24*, 1402–1413, doi:10.1021/ef900856d.

140. Berdugo Vilches, T.; Maric, J.; Knutsson, P.; Rosenfeld, D.C.; Thunman, H.; Seemann, M. Bed Material as a Catalyst for Char Gasification: The Case of Ash-Coated Olivine Activated by K and S Addition. *Fuel* **2018**, *224*, 85–93, doi:10.1016/j.fuel.2018.03.079.

141. Mei, D.; Lyngfelt, A.; Leion, H.; Linderholm, C.; Mattisson, T. Oxygen Carrier and Alkali Interaction in Chemical Looping Combustion: Case Study Using a Braunite Mn Ore and Charcoal Impregnated with K2CO3or Na2CO3. *Energy and Fuels* **2022**, doi:10.1021/ACS.ENERGYFUELS.2C00553/ASSET/IMAGES/LARGE/EF2C00553_0015.JPEG.

142. Yu, Z.; Yang, Y.; Yang, S.; Zhang, Q.; Zhao, J.; Fang, Y.; Hao, X.; Guan, G. Iron-Based Oxygen Carriers in Chemical Looping Conversions: A Review. *Carbon Resources Conversion* **2019**, *2*, 23–34, doi:10.1016/j.crcon.2018.11.004.

143. Gu, Z.; Zhang, L.; Lu, C.; Qing, S.; Li, K. Enhanced Performance of Copper Ore Oxygen Carrier by Red Mud Modification for Chemical Looping Combustion. *Applied Energy* **2020**, *277*, doi:10.1016/j.apenergy.2020.115590.

144. Liu, F.; Chen, L.; Neathery, J.K.; Saito, K.; Liu, K. Cerium Oxide Promoted Iron-Based Oxygen Carrier for Chemical Looping Combustion. *Industrial and Engineering Chemistry Research* **2014**, *53*, 16341–16348, doi:10.1021/ie503160b.

145. Soleimanisalim, A.H.; Hildor, F.; Mei, D.; Gogolev, I. Selection of Oxygen Carrier for Chemical Looping Gasification of Biomass.; Fluidized Bed Conversion Conference 2022, 2022.

146. Ahmaruzzaman, M. A Review on the Utilization of Fly Ash. **2009**, doi:10.1016/j.pecs.2009.11.003.

147. Moon, H.Y.; Yoo, J.H.; Kim, S.S. A Fundamental Study on the Steel Slag Aggregate for Concrete. *Geosystem Engineering* **2002**, *5*, 38–45, doi:10.1080/12269328.2002.10541186.

148. van der Laan, S.R.; van Hoek, C.J.G.; van Zomeren, A.; Comans, R.N.J.; Kobesen, J.B.A.; Broersen, P.G.J. Chemical Reduction of CO2 to Carbon at Ambient Conditions during Artificial Weathering of Converter Steel Slag. In Proceedings of the ACEME08, 2nd International Conference on Accelerated Carbonation for Environmental and Materials Engineering, Rome (IT) 1-3 October 2008; 2008; pp. 229–237.

149. Eloneva, S.; Teir, S.; Salminen, J.; Fogelholm, C.J.; Zevenhoven, R. Steel Converter Slag as a Raw Material for Precipitation of Pure Calcium Carbonate. *Industrial and Engineering Chemistry Research* **2008**, *47*, 7104–7111, doi:10.1021/ie8004034.

150. Kassman, H.; Andersson, C.; Carlsson, J.; Björklund, U.; Strömberg, B. *Minskade Utsläpp Av CO Och NOx Genom Dosering Av Ammoniumsulfat i Förbränningsrummet*; 2005;

151. Roshan Kumar, T.; Mattisson, T.; Rydén, M.; Stenberg, V. Process Analysis of Chemical Looping Gasification of Biomass for Fischer-Tropsch Crude Production with Net-Negative CO2Emissions: Part 1. *Energy and Fuels* **2022**, doi:10.1021/ACS.ENERGYFUELS.2C00819/ASSET/IMAGES/LARGE/EF2C00819_0014.JPEG.

152. Abad, A. Chemical Looping for Hydrogen Production. In *Calcium and Chemical Looping Technology for Power Generation and Carbon Dioxide (CO2) Capture*; Woodhead Publishing, 2015; pp. 327–374 ISBN 9780857097606.

153. Mendiara, T.; García-Labiano, F.; Abad, A.; Gayán, P.; de Diego, L.F.; Izquierdo, M.T.; Adánez, J. Negative CO2 Emissions through the Use of Biofuels in Chemical Looping Technology: A Review. *Applied Energy* **2018**, *232*, 657–684, doi:10.1016/j.apenergy.2018.09.201.

154. Purnomo, V.; Yilmaz, D.; Leion, H.; Mattisson, T. Study of Defluidization of Iron- and Manganese-Based Oxygen Carriers under Highly Reducing Conditions in a Lab-Scale Fluidized-Bed Batch Reactor. *Fuel Processing Technology* **2021**, *219*, 106874, doi:10.1016/j.fuproc.2021.106874.

155. Lindström, E.; Sandström, M.; Boström, D.; Öhman, M. Slagging Characteristics during Combustion of Cereal Grains Rich in Phosphorus. *Energy and Fuels* **2007**, *21*, 710–717, doi:10.1021/ef060429x.

156. Störner, F.; Hildor, F.; Leion, H.; Zevenhoven, M.; Hupa, L.; Rydén, M. Potassium Ash Interactions with Oxygen Carriers Steel Converter Slag and Iron Mill Scale in Chemical-Looping Combustion of Biomass-Experimental Evaluation Using Model Compounds. *Energy and Fuels* **2020**, *34*, 2304–2314, doi:10.1021/acs.energyfuels.9b03616.

157. Öhman, A.; Karakaya, E.; Urban, F. Enabling the Transition to a Fossil-Free Steel Sector: The Conditions for Technology Transfer for Hydrogen-Based Steelmaking in Europe. *Energy Research and Social Science* **2022**, *84*, 102384, doi:10.1016/j.erss.2021.102384.

158. Holappa, L. A General Vision for Reduction of Energy Consumption and CO2 Emissions from the Steel Industry. *Metals* **2020**, *10*, 1–20, doi:10.3390/met10091117.

159. Stanger, R.; Wall, T.; Spörl, R.; Paneru, M.; Grathwohl, S.; Weidmann, M.; Scheffknecht, G.; McDonald, D.; Myöhänen, K.; Ritvanen, J.; et al. Oxyfuel Combustion for CO2 Capture in Power Plants. *International Journal of Greenhouse Gas Control* **2015**, *40*, 55–125, doi:10.1016/j.ijggc.2015.06.010.